# Réseaux de Transport WDM: Planification de Réseaux Translucides et Economie d'Energie

Mayssa Youssef

ParisTech
INSTITUT DES SCIENCES ET TECHNOLOGIES
PARIS INSTITUTE OF TECHNOLOGY

TELECOM ParisTech

2012-ENST-00xx

EDITE - ED 130

**Doctorat ParisTech**

# T H È S E

**pour obtenir le grade de docteur délivré par**

## TELECOM ParisTech

**Spécialité « Informatique et Réseaux »**

*présentée et soutenue publiquement par*

**Mayssa Youssef**

le 16 Décembre 2011

# Réseaux de Transport WDM :

# Planification de Réseaux Translucides et Economie d'Energie

Directeur de thèse : **Maurice Gagnaire**

THÈSE

**Jury**

| | |
|---|---|
| **M. Bernard Cousin**, Professeur, Université de Rennes-I | Président |
| **M. Bijan Jabbari**, Professeur, George Mason University | Rapporteur |
| **M. Josep Prat**, Professeur, University of Catalunya | Rapporteur |
| **Mme Catherine Lepers**, Professeur, Telecom SudParis | Examinateur |
| **M. Dominique Verchère**, Docteur, Alcatel-Lucent Bell Labs | Examinateur |
| **M. Maurice Gagnaire**, Professeur, Télécom ParisTech | Directeur de thèse |

**TELECOM ParisTech**
école de l'Institut Télécom - membre de ParisTech

# WDM CORE NETWORKS:
# REGENERATOR PLACEMENT AND GREEN NETWORKING

By
Mayssa Youssef

SUBMITTED IN PARTIAL FULFILLMENT OF THE
REQUIREMENTS FOR THE DEGREE OF
DOCTOR OF PHILOSOPHY
AT
TÉLÉCOM PARISTECH
PARIS, FRANCE
NOVEMBER 2011

**Supervisor**
Maurice Gagnaire

**Examining Committee**
Bijan Jabbari
Josep Prat
Catherine Lepers
Bernard Cousin
Dominique Verchère

**Defended on the $16^{th}$ of December, 2011**

*To Lili, and her everlasting innocence...*

*To my loving parents...*

# Résumé

## 0.1 Contexte et motivations

Le dimensionnement de réseaux-coeurs WDM est fortement lié à la disponibilité des ressources et la qualité de transmission. De nos jours, le coût écologique s'ajoute, de ce fait, à ces deux aspects, comme il est devenu un indicateur important de l'efficacité des réseaux.

Etant donné la forte croissance du débit de données, trois paramètres sont étudiés au niveau des réseaux afin de présenter une bonne qualité de service aux clients:

- Qualité de transmission (QoT[1]): Afin de pouvoir assumer les débits demandés, un spectre optique dense en longueurs d'onde et un haut débit par canal sont primordiaux. Cela induit deux sortes d'interaction: $(i)$ une interaction entre les canaux optiques, et $(ii)$ une interaction entre les signaux optiques et la silice. Par conséquent, une estimation précise de la QoT du signal est nécessaire.

- Dynamicité: Jusqu'à présent, les réseaux opèrent des requêtes statiques, c-à-d, des demandes de connection permanentes. Avec l'émergence des services à flux et temps d'activation variables tels les applications cloud et les réseaux privés virtuels, il est devenu nécessaire d'envisager une reconfiguration automatique des circuits optiques sous-jacents.

- Utilisation des ressources électriques: Il est primordial d'optimiser l'utilisation des équipements électriques tels les régénérateurs électriques et les transceivers[2]. Cette optimisation doit trouver le juste compromis entre le coût d'utilisation de ces équipements et leur nécessité pour la surveillance des canaux optiques.

Les réseaux WDM déployés actuellement peuvent être qualifiés d'*opaques*; tout passage par un noeud implique systématiquement une conversion optique-électrique-optique

[1] Quality of Transmission.
[2] Transmitter/receiver.

(OEO) du signal. Il est impossible de déployer un réseau de transport longue distance tout-optique (*transparent*). Ainsi, un troisième type de réseau est proposé: le réseau *translucide*, ou hybride. Dans ce dernier type, l'utilisation d'équipements opto-électroniques est optimisée tenant compte du troisième paramètre cité ci-haut. Il est à noter que les systèmes de transmission utilisés de nos jours dans les réseaux de transport favorisent la transmission longue-distance en compensant à un certain degré les dégradations du signal dues aux effets physiques, linéaires et non-linéaires, liés à la transmission sur fibre.

Dans la première partie de cette thèse, nous proposons une approche de dimensionnement de réseau translucide en minimisant non seulement le nombre total de régénérateurs, mais aussi le nombre de sites de régénération dans le réseau. Cette approche repose sur une optimisation croisée entre les coûts CapEx et OpEx de la régénération.

Dans la deuxième partie de cette thèse, nous nous intéressons au dimensionnement de réseau en tenant compte des aspects énergétiques. Avec une bonne connaissance des flux à pourvoir dans le réseau, un opérateur peut optimiser l'utilisation de ses équipements afin de réduire sa consommation énergétique.

## 0.2 Optimisation du placement de régénérateurs

Le signal optique subit des dégradations pendant son parcours dans le réseau. Ces dégradations sont dues aux effets linéaires et non-linéaires inhérents à la transmission sur fibre, et fortement liés aux caractéristiques du signal, tels le débit par canal et l'espacement entre les canaux juxtaposés. Les systèmes de transmission utilisés de nos jours étendent la distance que le signal peut parcourir dans la silice avant que le besoin de régénération ne se manifeste. Ces systèmes compensent des effets de dégradations tels l'atténuation et la dispersion chromatique. L'accumulation des effets linéaires et non-linéaires sur une longue distance de transmission impose le besoin de régénérer le signal en réinitialisant sa cadence, sa forme et son amplitude. Cette régénération tripartite est appelée régénération 3R pour: (*i*) Re-amplifying, (*ii*) Re-shaping et (*iii*) Re-timing. La régénération 3R déployée de nos jours est exclusivement électrique, son équivalente tout-optique étant toujours une technologie immature. Un régénérateur 3R remet à neuf un canal optique et est formé de deux transpondeurs dos-à-dos (Cf. Figure 1). Un transpondeur est le dispositif en charge de transformer un signal optique courte distance (short reach) en un signal optique longue distance (long reach) moyennant une conversion OEO. La transformation inverse est aussi desservie par un transpondeur.

Un transpondeur, constituant une technologie fiable, est pourtant un équipement coûteux et consomme beaucoup de puissance électrique en comparaison avec les équipements

de transmission déployés au niveau WDM. De plus, un transpondeur a un débit défini par construction, et ne peut de ce fait, desservir que des signaux optiques ayant son débit nominal. Par conséquent, un régénérateur 3R a un débit fixe. Il est aussi important de noter que cette disposition en deux transpondeurs permet la conversion en longueur d'onde ce qui peut être efficace sous une lourde charge de trafic.

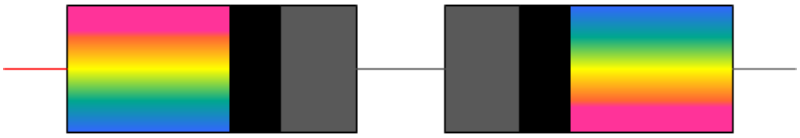

Figure 1: Régénérateur 3R formé de deux transpondeurs dos-à-dos.

Parmi les différentes approches pour la planification de réseau translucide, nous adoptons la régénération éparpillée (sparse regeneration). Cette approche considère un réseau constitué de noeuds tout-optiques à base de switchs optiques (OXC[3]) où quelques uns sont équipés d'une banque de régénérateurs 3R. La Figure 2 est une présentation simplifiée de cette approche, les noeuds C, D et E étant les noeuds translucides du réseau. Une demande de connection ayant pour source et destination les noeuds A et B, respectivement, est illustrée sur son chemin de routage. Elle est régénérée au niveau du noeud C alors qu'elle traverse les noeuds translucides D et E de façon transparente. Ainsi, la régénération n'est pas systématique dans les noeuds translucides traversés.

### 0.2.1 Planification de réseau translucide

Planifier un réseau translucide est choisir les noeuds stratégiques du réseau qui seront dotés de banques de régénérateurs 3R, afin de mener à bien l'établissement d'une charge de trafic donnée. La topology du réseau, ainsi que sa capacité et les exigences de qualité de service ont un fort impact sur le processus de planification.

Dans cette étude, les coûts additionnels inhérents au placement de régénérateurs sont considérés. En effet, rajouter une banque de régénérateurs à un noeud transparent implique deux sortes de coûts:

- Coûts de déploiement: comprenant le prix intrinsèque des régénérateurs et le coût de leur installation (rajout d'armoires, équipe d'installation...).

- Coûts d'opération: inhérents à l'usage des régénérateurs (alimentation électrique et refroidissement, supervision et maintenance).

[3]Optical Cross-Connect

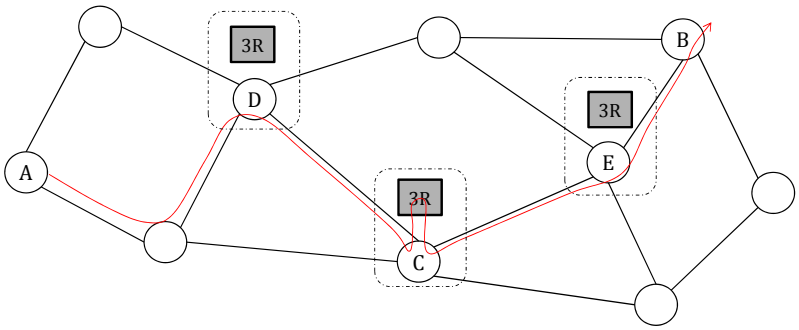


Figure 2: Réseau translucide.

Ainsi, nous résumons le problème de planification de réseau translucide par les spécifications suivantes:

***Données du problème***

*Caractéristiques du réseau*:

- Une topologie de réseau où les noeuds sont considérés transparents *a-priori*;
- Un ensemble de longueurs d'onde disponibles par lien physique;

*Charge de trafic*:

- Un ensemble de demandes de connections permanentes (PLDs[4]), nécessitant chacune un canal optique;

***Objectif du problème***

L'objectif de la planification de réseau est d'offrir une qualité de service (QoS[5]) garantie aux clients de l'opérateur, tout en minimisant les coûts réseau:

- Taux de rejet maximal: il s'agit d'établir le maximum posible de PLDs en garantissant assez de ressources et une bonne QoT à la destination. Cet objectif joue aussi le rôle de contrainte.
- Coûts additionnels: il s'agit de minimiser les coûts correspondant au déploiement des régénérateurs 3R. Cela n'est possible qu'en minimisant le nombre de sites de régénérations et le nombre de régénérateurs activés dans chaque site, simultanément.

***Contraintes du problème***

*Qualité de transmission:*

[4]Permanent Lightpath Demands.
[5]Quality of Service.

L'opérateur de réseau exige un seuil admissible pour la QoT. Ce seuil représente une valeur du BER à la destination qui ne doit pas être dépassée afin de mener à bien l'établissement d'une PLD.

*Contrainte de la continuité de longueur d'onde:*

Un chemin optique est routé moyennant une longueur d'onde unique sur tous les liens qu'il traverse si aucune conversion de longueur d'onde n'est envisagée au niveau d'un noeud intermédiaire. Une relaxation de cette contrainte est possible au niveau d'un régénérateur.

*Capacité de régénération par site:*

Le nombre de régénérateurs dans une banque de régénération est limité pour des raisons de consommation énergétique ou d'espace.

### 0.2.2 Modèle de coût

Dans cette thèse, deux types de ressources réseaux sont considérés: les ressources optiques et les ressources électriques. D'une part, les ressources optiques peuvent être exprimées en longueurs d'onde étant donné qu'une longueur d'onde par lien physique est exigée pour l'établissement d'une requête. Ainsi, les ressources optiques sont limitées par la capacité du réseau, et plus finement, par le nombre de longueurs d'onde déployées par lien. D'autre part, les ressources électriques comprennent les cartes clients (transceivers) et les régénérateurs 3R utilisés. Le nombre de cartes clients n'est pas sujet d'optimisation puisqu'une PLD a besoin d'un transmetteur et d'un récepteur comme condition de départ pour son établissement, et constitue par suite une part fixe non négociable. Quant aux régénérateurs, leur nombre dépend étroitement du routage adopté et donc peut être optimisé. Par conséquent, nous représentons les ressources électriques par les régénérateurs nécessaires pour garantir une QoT admissible.

Le coût relatif à l'établissement d'une PLD est représenté par une pondération des ressources électriques et des ressources optiques:

$$\text{Coût}_{(\text{connection})} = \alpha \times \text{Coût}_{(\text{ressources optiques})} + (1-\alpha) \times \text{Coût}_{(\text{ressources électriques})} \quad (0.2.1)$$

Les ressources optiques peuvent être représentées par le nombre de liens (hops) traversés par le chemin optique. Les longueurs d'onde utilisés sur ces hops ne sont, en elles-mêmes, pas importantes dans le décompte de leur nombre.

Quant aux ressources électriques, leur coût dépend de la configuration des sites où la régénération 3R de la connection se fait.

$$\text{Coût}_{(\text{ressources électriques})} = \text{Coût}_{(\text{régénération})} = \text{Coût}_{CapEx} + \text{Coût}_{OpEx} \tag{0.2.2}$$

Différents scénarios de régénération sont envisagés, et leurs coûts correspondants sont considérés:

- Si le noeud où l'on envisage de régénérer un signal est transparent, l'investissement nécessaire en banque de régénérateurs est à considérer. Le signal aura besoin d'activer un seul régénérateur 3R dans cette banque. Ainsi, le coût correspondant à une telle situation est bipartite; une partie de ce coût revient au CapEx d'installation de l'équipement ainsi que de son unité d'alimentation et de refroidissement. La deuxième partie consiste en l'OpEx relatif à l'activation du premier régénérateur.

- Si le noeud choisi pour la régénération a déjà une banque de régénérateurs, et que ces derniers ne sont pas tous activés, il est juste question d'activer un régénérateur pour la PLD considérée. Ainsi, le coût additionnel est un coût OpEx relatif à l'activation d'un régénérateur.

- Si le noeud choisi pour la régénération a déjà une banque de régénérateurs, et que ces derniers sont tous activés, deux possibilités sont envisagées:

  ($i$) l'opérateur s'investit dans l'installation d'une nouvelle banque de régénérateurs, ou bien ($ii$) le noeud considéré n'est plus éligible à régénérer des PLDs.

Pour éliminer toute indécision, nous considérons que la banque de régénérateurs a une taille suffisamment grande pour accepter toutes les régénérations requises, et dimensionnons les banques en conséquence.

#### 0.2.2.1 Coût OpEx d'un régénérateur

Quand un premier régénérateur est activé au niveau d'un noeud donné du réseau, une équipe est dédiée pour mener à bien son opération, superviser sa performance et intervenir au cas de disfonctionnement. Quand un second régénérateur est activé, la même équipe se charge de son fonctionnement, mais superviser deux régénérateurs n'est pas pareil à en superviser un seul. De même, superviser '$x$' régénérateurs n'est pas pareil à n'en superviser qu'un seul.

Etant donné que le coût OpEx ne peut pas, à la différence du coût CapEx, être déduit par du nombre d'équipements déployés surtout la partie du coût OpEx relative

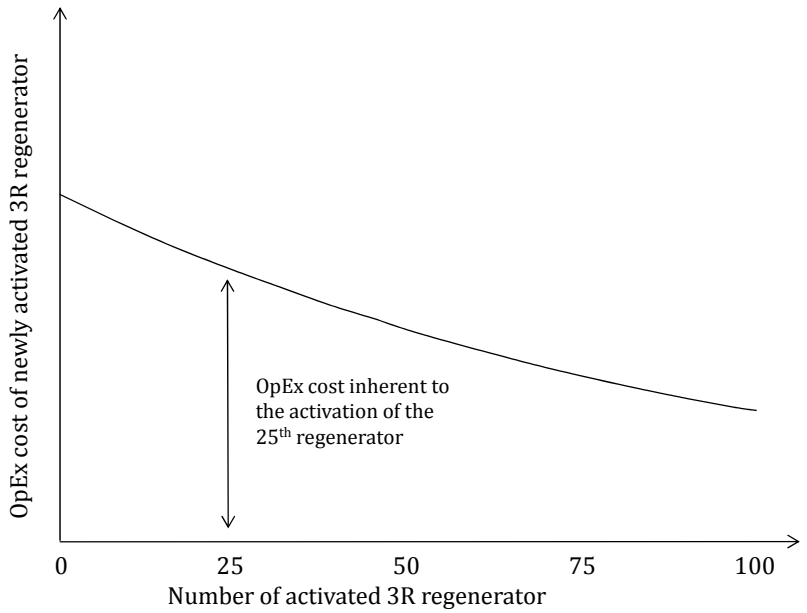


Figure 3: Coût OpEx d'un régénérateur selon son ordre d'activation dans le noeud.

à l'intervention humaine, nous considérons que ce coût est une fonction décroissante du nombre de régénérateurs activés dans un site.

La Figure 3 illustre notre approche pour le coût additionnel OpEx par régénérateur activé, étant donné son ordre d'activation dans le noeud.

#### 0.2.2.2 Coûts CapEx et OpEx d'un noeud translucide

Se basant sur les considérations précédentes, le coût d'un noeud translucide (*i.e.*, d'installation d'un site de régénération dans un noeud) est constitué d'un coût fixe CapEx et d'un coût variable OpEx. Le coût OpEx total au niveau d'un noeud translucide est donné par le cumul de tous les coûts OpEx des régénérateurs activés au niveau de ce noeud. La Figure 4 illustre le coût total d'un noeud translucide en fonction du nombre de régénérateurs activés.

#### 0.2.2.3 Coût total d'un chemin optique

Le coût total de régénération d'un chemin optique dépend à la fois du nombre de régénérations nécessaires depuis sa source jusqu'à sa destination, et du scénario de régénération au niveau des sites considérés. Par conséquent, nous exprimons le coût de régénération d'un chemin optique par l'équation suivante:

$$\text{Coût}_{\text{régénération}} = \sum_{i=1}^{\mathcal{H}-1} \mathcal{C}_{\mathcal{R}}\left(v_i\right) \tag{0.2.3}$$

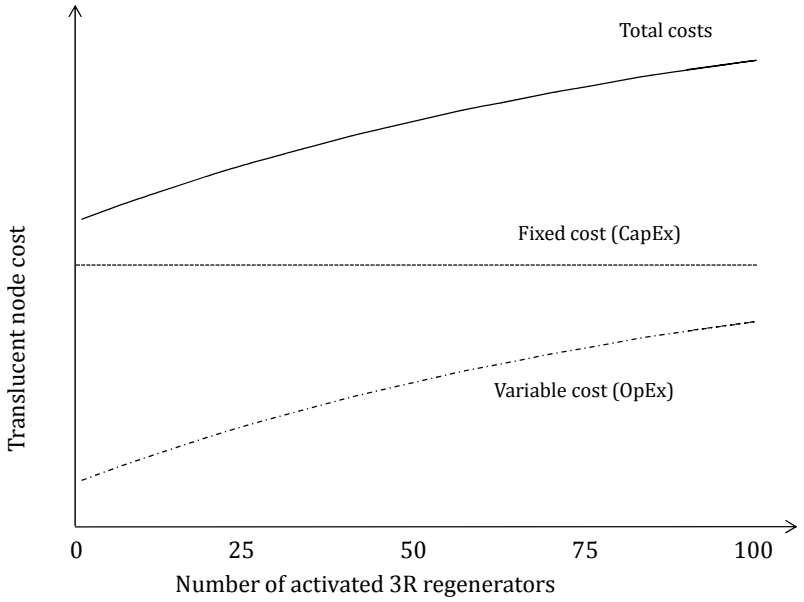


Figure 4: Coût total d'un noeud translucide.

où "$\mathcal{H}-1$" est le nombre de noeuds intermédiaires ($v_i$) entre la source et la destination de la route donnée ($\mathcal{H}$ étant le nombre de hops de cette route).

$\mathcal{C}_{\mathcal{R}}(v_i)$ est le coût de régénération au noeud $v_i$. Ce dernier coût peut être exprimé selon les explications antérieures comme suit:

$$\mathcal{C}_{\mathcal{R}}(v_i) = \begin{cases} 0 & \text{si } v_i \text{ n'est pas utilisé pour régénérer le chemin optique,} \\ \mathcal{C}_C + \mathcal{C}_O \cdot e^{-\frac{1}{\mathcal{X}}} & \text{si } v_i \text{ est considéré comme un site de régénération pour la première fois,} \\ \mathcal{C}_O \cdot e^{-\frac{x_0+1}{\mathcal{X}}} & \text{si } v_i \text{ contient déjà } x_0 (< \mathcal{X}) \text{ régénérateurs actifs,} \\ \infty & \text{si } x_0 = \mathcal{X} \text{ c-à-d, Tous les régénérateurs de } v_i \text{ sont activés.} \end{cases} \tag{0.2.4}$$

Dans cette équation, $\mathcal{C}_C$ et $\mathcal{C}_O$ sont des facteurs de pondération dépendant des prix de constructeur ainsi que de la stratégie de déploiement adoptée par l'opérateur (refroidissement, gestion de personnel). $\mathcal{X}$ est la taille de la banque de régénérateurs. Nous avons considéré cette forme exponentielle afin d'obtenir une fonction convexe pour l'OpEx additionnel par régénérateur activé. Une connaissance plus fine de la politique de gestion de l'opérateur peut aboutir à d'autres fonctions convexes.

Selon nos suppositions, le coût total d'une connection peut être exprimé par l'équation suivante:

$$\text{Coût}_{(connection)} = \alpha \times \frac{\mathcal{H}}{\overline{\mathcal{H}}} + (1-\alpha) \times \sum_{i=1}^{\mathcal{H}-1} \mathcal{C}_{\mathcal{R}}(v_i) \tag{0.2.5}$$

Dans cette équation, $\mathcal{H}$ et $\overline{\mathcal{H}}$ représentent respectivement le nombre de hops dont est formée la route, et le nombre de hops moyen sur toutes les routes possibles entre la source et la destination (par exemple, sur les $\mathcal{K}$ plus courts chemins). La variable $\overline{\mathcal{H}}$ est nécessaire afin que les deux parties de l'équation 0.2.2.3 deviennent d'ordres comparables.

## 0.3 COR2P

Dans cette partie, nous présentons notre solution pour le dimensionnement de réseau translucide COR2P. COR2P étant le sigle de "***Cross-Optimization for RWA and Regenerator Placement***", est une heuristique qui établit une charge de trafic donnée tenant compte de la qualité de transmission; son but est de planifier un réseau translucide à partir d'un réseau transparent.

COR2P est formé de trois étapes successives et repose sur une considération de coûts CapEx et OpEx qui fait que les régénérateurs sont concentrés dans quelques sites du réseau, et non pas éparpillés sur la quasi-totalité des noeuds.

Il est à noter que, pour l'estimation de la qualité de transmission, COR2P fait appel à un outil appelé BER-Predictor qui a pour fonction de fournir les valeurs du BER[6] à la destination d'un chemin optique donné (route + longueur d'onde).

### 0.3.1 Notations

Considérons les notations et conventions typographiques suivantes:

- $\mathcal{G} = (\mathcal{V}, \mathcal{E}, \xi)$ est un graphe représentant la topologie du réseau. $\mathcal{V}$ représente l'ensemble des noeuds et $\mathcal{E}$ représente l'ensemble des liens. $\xi$ est une fonction de poids $\xi : \mathcal{E} \rightarrow \mathbb{R}^+$ représentant la longueur physique des liens. Les liens dans l'ensemble $\mathcal{E}$ sont unidirectionels, mais il est impératif que si $\xi$ contient un lien allant du noeud $v_a$ jusqu'au noeud $v_b$, un lien allant de $v_b$ jusqu'au noeud $v_a$ appartient à $\xi$.
- $N = |\mathcal{V}|$ représente le nombre de noeuds dans le réseau.
- $W$ représente le nombre de longueurs d'onde disponbiles sur un lien physique.
- $\mathcal{D}$ représente l'ensemble de PLDs à établir dans le réseau.
- Une PLD $d_i (1 \leq i \leq |\mathcal{D}|)$, est une demande de connection entre deux noeuds $S_i$ et $D_i$ de $\mathcal{V}$.

[6] Bit Error Rate.

- $\mathcal{P}_i$ représente l'ensemble de chemins disponibles entre $S_i$ and $D_i$. Ces chemins (les $\mathcal{K}$ plus courts chemins, s'il y a lieu) sont générés à l'avance selon l'algorithme d'Eppstein [1] pour toutes les PLDs.
- $p_{ik}$ représente le $k^{\text{ème}}$ plus court chemin, $1 \leq k \leq \mathcal{K}$ dans $\mathcal{P}_i$ entre $S_i$ et $D_i$.
- $\mathcal{H}_{ik}$ représente le nombre de hops relatifs au chemin $p_{ik}$.
- $\mathcal{R}$ représente le nombre initial de sites de régénération dans le réseau. Parallèlement, $\mathcal{R}^*$ représente le nombre de sites de régénération effectivement déployés à la fin d'exécution de COR2P.
- $\mathcal{X}$ représente la taille de la banque de régénérateurs.

### 0.3.2 Synopsis de COR2P

COR2P est formé de trois étapes consécutives:

#### 0.3.2.1 Etape 1 - Routage préliminaire

Dans cette étape, COR2P procède au routage des PLDs en considérant que le réseau est transparent. Par conséquent, la contrainte de continuité de longueur d'onde s'impose dans ce contexte.

Au début, les valeurs de BER ($BER_{ik}$) sont calculées pour tous les $\mathcal{K}$ plus courts chemins ($p_{ik}$) des PLDs $d_i$, par l'intermédiaire de BER-Predictor. Dans cette première étape, les éléments du réseau sont considérés à réponse spectrale plate (flat systems), c-à-d, le BER à la destination ne dépend pas de la longueur d'onde.

Ensuite, les PLDs sont ordonnées dans l'ordre décroissant de leur BER ($BER_i^*$ sur leur meilleure route). Ainsi, la première PLD dans la liste a la pire QoT.

Respectant cet ordre, les PLDs sont traitées chacune à part, et sont affectées un chemin et une longueur d'onde. Au cas où le réseau est tellement chargé qu'aucune solution de routage et d'affectation de longueur d'onde n'est possible, la demande est mise à part pour la traiter dans l'étape 3 de COR2P. De telles PLDs auront plus de chance pour s'établir avec la relaxation de la contrainte de continuité de longueur d'onde fournie par l'ajout de régénérateurs dans l'étape 3.

#### 0.3.2.2 Etape 2 - Placement potentiel de régénérateurs

Dans cette étape, COR2P détermine les noeuds candidats les plus probables pour la régénération. Chaque noeud "$v_i$" est donc affecté un compteur "$c_i$" représentant le besoin en régénération à son niveau.

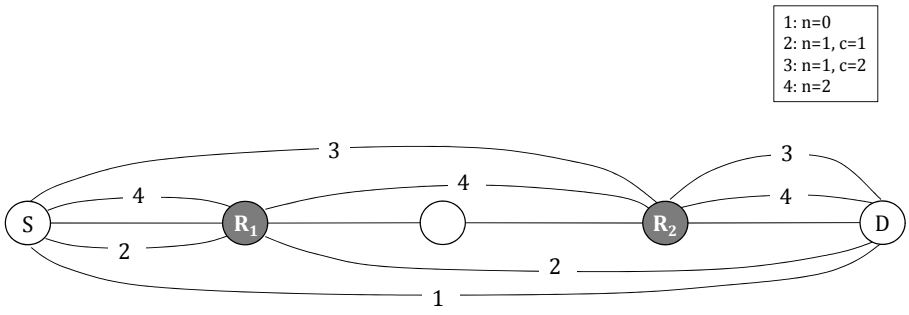


Figure 5: Possibilités de régénération.

Les PLDs réussies dans l'étape précédente sont considérées. Un suivi de QoT est effectué pour chaque chemin optique, au niveau de tous les noeuds intermédiaires. Toutes les fois que la QoT échoue, le compteur du noeud précédent sa chute (au-dessous d'un seuil exigé par l'opérateur) est incrémenté. De façon récursive, ce suivi est effectué depuis le noeud dont le compteur a été incrémenté jusqu'à la destination.

Une fois tous les chemins optiques sont traités, les noeuds du réseau sont triés dans l'ordre décroissant de leurs compteurs. Les premiers $\mathcal{R}$ noeuds de la liste triée sont considérés les sites de régénération que l'étape 3 doit respecter, sans y restreindre la régénération des chemins optiques faibles.

#### 0.3.2.3 Etape 3 - RWA et placement de régénérateurs effectifs

Dans cette étape, les systèmes de transmission ne sont plus considérés à réponse spectrale plate; la QoT du signal en sa destination dépend de sa longueur d'onde (non-flat system).

Au début, les chemins optiques réussis dans l'Etape 1 sont considérées. La stratégie adoptée pour l'affectation de longueur d'onde est la Best-BER-Fit (BBF). Sous cette stratégie, la longueur d'onde, disponible et permettant la QoT la plus proche du seuil d'admissibilité est choisie [3]. Ensuite, les PLDs échouées sont traitées.

Les PLDs n'ayant pas réussi à obtenir une solution de RWA[7] sans recours à la régénération sont traitées en essayant toutes les combinaisons de régénération possible sur leur $\mathcal{K}$ plus courts chemins, à condition qu'il existe des longueurs d'onde disponibles sur les sous-chemins optiques délimités par les sites de régénérations. Si plusieurs possibilités existent, COR2P choisit celle qui fournit le moindre coût calculé selon Equation 0.2.2.3.

Afin de gérer des contentions en longueur d'onde qui peuvent avoir lieu sous une lourde charge de trafic, COR2P permet l'ajout d'un site de régénération, quand c'est nécessaire,

[7]Routage et affectation de longueur d'onde (Routing and Wavelength Assignment).

**Pseudo-Code 1** Synopsis de l'Etape 3 de COR2P

Let $\Theta$ be the set of demands to be regenerated.
Let $\Delta$ be the set of demands rejected in Step 1.
**Initialization**
$\Theta = \Delta$
$\mathcal{R}$ nodes are considered regeneration sites
**Processing**
**for all** $d_i \in \mathcal{D} \backslash \Delta$ **do**
  $\lambda^*$=Get_BBF[1]$(p_{ik^*})$ {$p_{ik^*}$ *is the path assigned to* $d_i$ *in Step 1*}
  **if** $(\lambda^* \neq -1)$ **then**
    Assign $\lambda^*$ to $d_i$
    Update network resources
  **else**
    $\Theta = \Theta \cup \{d_i\}$
  **end if**
**end for**
**for all** $(d_i \in \Theta)$ **do**
  $cost_i = \infty$
  **for** $(k = 1$ to $k = \mathcal{K})$ **do**
    $cost_{ik} = Get\_Cost^2(p_{ik})$
    $cost_i = min(cost_i, cost_{ik})$
  **end for**
  **if** $(cost_i = \infty)$ **then**
    **if** ($p_{i1}$ supports no regeneration site) **then**
      **if** (one or more links on $p_{i1}$ present full spectrum usage) **then**
        $d_i$ is blocked
      **else**
        $h = 2$
        **while** $(h \neq \mathcal{H}_{i1})$ **do**
          Estimate $BER_1$ and $BER_2$, BERs relative to the BBF wavelengths at the end of subpaths $(v_1 - ... - v_{h^*})$ and $(v_{h^*} - ... - v_{(\mathcal{H}_{i1}+1)})$
          **if** $((BER_1 \geq BER_{th})$ & $(BER_2 \geq BER_{th}))$ **then**
            $d_i$ is blocked
          **else**
            **if** $((BER_1 \geq BER_{th})$ || $(BER_2 \geq BER_{th}))$ **then**
              $h^{*}++$
            **else**
              $v_h$ is considered a regeneration site
              A regenerator is deployed in $v_h$
              $d_i$ is established
              $h = \mathcal{H}_{i1}$
            **end if**
          **end if**
        **end while**
      **end if**
    **else**
      $d_i$ is blocked
    **end if**
  **else**
    Solution of the Get_Cost($p_{i1}$) function provides places to add regenerators along with an RWA solution
  **end if**
**end for**

[1] Get_BBF(*path*) is a function that returns the Best-BER-Fit wavelength, available over the parameter *path*. Get_BBF(*path*) returns $-1$ if no available wavelength guarantees the quality of transmission requirements.
[2] Pseudo-code of the Get_Cost(*path*) function is provided in Pseudo-code **??**.

sur le plus court chemin d'une PLD. Le synopsis de cette étape est donné dans Pseudo-Code 1. La fonction GET_COST(*path*) détaillée dans Pseudo-Code 2, essaie différents placements de régénérateurs sur le chemin *path* et calcule les coûts correspondants. Enfin, elle choisit la *solution* présentant le moindre coût.

La Figure 5 présente un exemple des différentes possibilités de régénération sur un chemin allant du noeud source $S$ au noeud destination $D$. Les sous-chemins relatifs à chaque possibilité de régénérations sont aussi illustrés.

**Pseudo-Code 2** Synopsis of Get_Cost (*path*)

**Initialization**
Let $\mathcal{H}$ be the number of hops of "*path*"
Let $s$ and $d$ be the source and destination of "*path*"
Let $\mathcal{N}_R$ be the number of regeneration sites over "*path*"
$minCost = \infty$
**for** ($n = 1$ to $n = \mathcal{N}_R$) **do**
  Consider the $n$-combinations from the set of $\mathcal{N}_R$ sites
  **for** ($c = 1$ to $c = C(n, \mathcal{N}_R)$ **do**
    $v_1, v_2, \ldots v_n$ are used as regeneration sites over "*path*", according to combination '$c$'
    Find a set of BBF free wavelengths $\{\lambda_p : p = 1...n+1\}$ over the subpaths of "*path*" delimited by $v_i$, $1 \leq i \leq n$. These wavelengths should provide good QoT.
    **if** (Such set exists) **then**
      Compute the cost $Cost_c$ relative to the use of "*path*" with the combination '$c$' of regeneration sites, using the *Cost Function* { *Equation* (**??**) }
    **end if**
    **if** ($Cost_c < minCost$) **then**
      $minCost = Cost_c$
      Store this "*solution*"("*path*", '$c$', $\{\lambda_p : p = 1...n+1\}$)
    **end if**
  **end for**
**end for**
Return "*solution*"

Les résultats obtenus avec COR2P montrent que les noeuds ayant les degrés physiques les plus élevés sont les plus favorisés pour la régénération. Une fraction des noeuds du réseau, considérés translucides, peut offrir une bonne performance vis-à-vis du taux de rejet et du coût relatif à la régénération. En effet, 17 % des noeuds du réseau NSFNet-18 est un pourcentage suffisant pour établir des charges de trafic moyennes à lourdes.

## 0.4 Green Networking

Afin de subvenir aux besoins en capacité dans les réseaux, des équipement de haute performance sont déployés de plus en plus, tant dans l'accès que dans le réseau de transport. Par conséquent, l'évolution de la consommation énergétique dans les réseaux est devenue un sujet de haute priorité. Les statistiques montrent une augmentation notable dans la consommation énergétique des réseaux. Ce qui étaye sur le fait que la capacité des réseaux du futur ne va pas être limitée par celle des équipements à déployer, mais par les contraintes

énergétiques.

La Figure 6 illustre des estimations typiques dans un réseau opérateur. Bien que 6% seulement des équipements réseau sont déployés aux parties métro et coeur, leur consommation énergétique constitue 30% de la consommation totale du réseau. Ceci revient au fait que le besoin énergétique dépend étroitement de la capacité traitée dans les équipements.

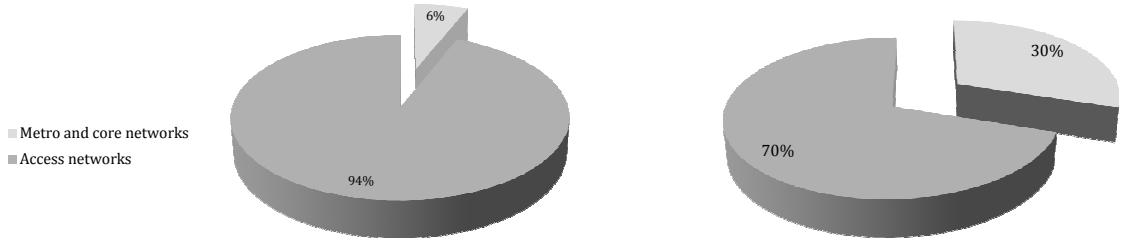


(a) Pourcentages d'équipements utilisés. (b) Besoin en énergie.

Figure 6: Besoins énergétiques dans un réseau d'opérateurs.

Dans notre étude, nous considérons la consommation énergétique dans les réseaux de transport WDM. En général, économiser de l'énergie peut compenser une part des coûts CapEx et OpEx d'un opérateur. De plus, l'introduction d'équipements tout-optiques permet non seulement d'obtenir une capacité de transmission plus élevée, mais aussi de réduire le nombre de conversions OEO consommant beaucoup d'énergie. Mais il est à noter que les équipements jouant le rôle d'interface entre les routeurs électriques et les switchs optiques (Add/Drop transponders, ou transceivers) sont des équipements électriques. Ainsi, dans cette partie de la thèse, nous focalisons sur ces transceivers en essayant d'optimiser leur utilisation.

Typiquement, une fois les canaux optiques sont provisionnés, aucune reconfiguration n'est effectuée jusqu'à leur fin de vie [5]. Récemment, de nouveaux services ayant des durées, des dates d'incidence et des débits aléatoires émergent. En effet, la charge de trafic à laquelle est assujetti le réseau n'est pas constante, comme le montre la Figure 7. Le profile de charge illustré est relatif au réseau coeur des pays-bas observé pendant 48 heures.

Les réseaux traditionnels sont surdimensionnés pour subvenir aux besoin de la charge maximale. Les routeurs et les cartes clients sont toujours opérationnels même aux heures creuses, ce qui favorise la consommation inutile d'énergie. Pour le moment, avec les équipements mis sur le marché, il n'est pas possible de passer à des modes de faible consommation, sans oublier le fait qu'une telle possibilité rajoute de la complexité au niveau contrôle de réseau, chose qui n'est pas réalisable actuellement.

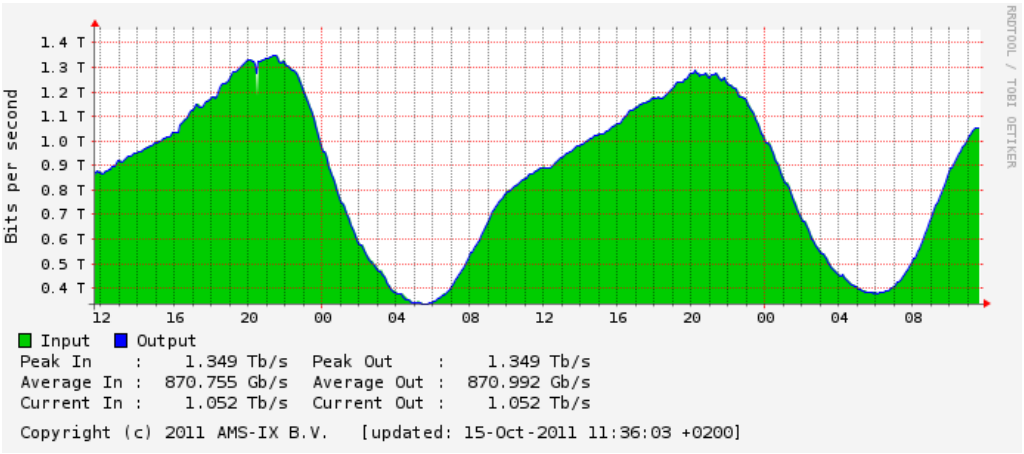


Figure 7: Profile du trafic aux Pays Bas.

En général, un réseau dynamique doit être capable d'offrir à ses clients la capacité qu'ils requièrent avec un temps de réponse minimal, et sans dépenser inutilement la capacité du réseau. Jusqu'à présent, des débits fixes ont été utilisés (2.5, 10, 40 Gbps). Si la capacité d'un canal n'est pas suffisante, plusieurs canaux sont nécessaires pour l'établissement d'un service. Et quand la capacité des canaux est suffisante, il y a une chance que le canal comprenne une capacité inutilisée (le surplus de capacité par rapport à celle de la requête considérée). Dans les deux cas, il existe un décalage entre la capacité offerte et celle demandée, ce qui amène l'opérateur à favoriser l'optimisation de ses ressources, pour effectuer un maximum de retour sur investissement. Des travaux de recherche portant sur des transceivers à débit flexible sont en cours [4, 2]. De tels transceivers pourront basculer d'un débit à un autre sous commande. Mais pour le moment, la reconfigurabilité en termes de requêtes est déjà employée, c-à-d, un canal peut servir différentes requêtes dans différents instants, et même, multiples requêtes simultanément, moyennant l'agrégation de trafic.

Il est maintenant possible d'envoyer différents débits sur un même brin de fibre. Cela a pour avantage de permettre une utilisation meilleure de la capacité du réseau. Avec une connaissance du profile de charge, les opérateurs peuvent dimensionner leur réseau en optimisant les ressources nécessaires à déployer. L'ingénieurie de trafic joue aussi un rôle primordial dans le choix des équipements.

Considérant un trafic variable dans le temps, les procédures de RWA peuvent tenir compte de la corrélation spatio-temporelle entre les chemins optiques. L'agrégation de trafic peut servir pour optimiser la capacité utilisée des transceivers. Le passage transparent par un noeud (optical bypass) est aussi important, étant donné qu'il aide à minimiser

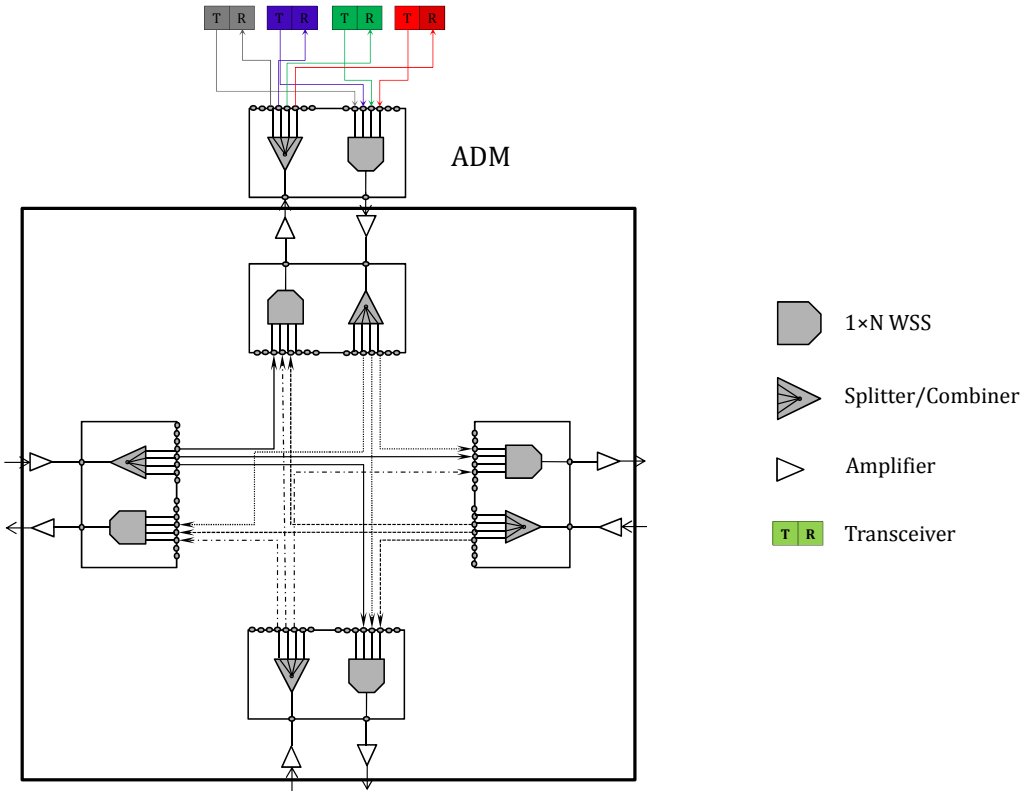


Figure 8: Bloc diagram d'un noeud de degré 3.

le nombre de transceivers intermédiaires. Malgré que le bypass optique et l'agrégation de trafic sont opposés, ils peuvent, ensemble, fournir le juste nécessaire en ressources et garantir une utilisation plus juste de la capacité du réseau.

### 0.4.1 Contraintes liées à l'architecture de noeud

Dans cette partie de la thèse, nous ne considérons pas la QoT des chemins optiques, les régénérateurs 3R sont donc négligés de l'architecture de noeud.

Dans les OXCs basés sur la technologie WSS[8], les interfaces d'insertion/extraction peuvent être considérées comme un degré physique de noeud, s'ajoutant aux autres degrés relatifs à la connectivité physique. La Figure 8 montre l'architecture de noeud de degré 3. Le module d'insertion/extraction (ADM[9]) est formé d'un seul WSS et d'un splitter. Les signaux d'entrée et de sortie des WSSs et splitters relatifs aux différents degrés (y compris celui du ADM) sont des signaux composites. La façon dont le ADM est disposé rajoute une contrainte à la transmission/réception; en effet, une longueur d'onde ne peut être insérée (respectivement extraite) qu'une seule fois à un instant donné. Par conséquent,

[8]Wavelength-Selective Switch.
[9]Add/Drop Multiplexer.

l'affectation de longueur d'onde doit tenir compte de cette contrainte afin que tous les signaux à insérer/extraire au niveau d'un noeud donné, soient affectés différentes longueurs d'onde.

Les transceivers, à leur tour, présentent des contraintes. En effet, le transmetteur et le récepteur du même transceiver sont utilisés en duo (dual-channel transceiver). De plus, même si la reconfigurabilité des transceivers en longueur d'onde est possible, les deux parties de l'équipement sont employées à la même longueur d'onde en même temps. La reconfigurabilité en débit des transceivers n'est pas encore déployée, leurs débits sont donc fixes. Etant donné tout le précédent, il devient obligatoire que deux signaux corrélés dans le temps (un inséré et un extrait au niveau du même noeud) ayant la même longueur d'onde soient desservis par le même transceiver, et doivent ainsi avoir le même débit.

### 0.4.2 Optimisation des ressources réseaux

Dans cette partie, nous expliquons notre méthodologie pour le dimensionnement optimisé de transceivers. Il est important de préciser que nous offrons la possibilité de diviser les requêtes en plusieurs fractions de débit moindre. Ces fractions sont routées dans le réseau de façon indépendante; chacune est affectée une solution de RWA ainsi qu'un plan d'agrégation avec d'autres requêtes au niveau de noeuds intermédiaires.

Le trafic considéré est composé de requêtes pré-planifiées (scheduled demands (SD)), c-à-d, leurs dates d'arrivée et leurs périodes d'activation sont connues d'avances. Moyennant leur corrélation temporelle, le plan de contrôle peut leur fournir des solutions de routage qui peuvent aussi introduire la notion de corrélation spatiale afin de profiter de l'agrégation aux noeuds. Les transceivers à déployer dans le réseaux seront utilisés de deux façons sous l'égide du partage de ressources:

- *Partage simultané de ressources*: un transceiver peut être utilisé par différentes SDs corrélées temporellement moyennant l'agrégation.
- *Partage de ressources en différentes périodes de temps*: un transceiver peut être utilisé par différents ensembles de SDs à différentes périodes, pourvu que leurs périodes d'activation sont disjointes.

Ce partage de ressources a été labélisé sous "Grooming". Dans notre contexte, nous en profitons pour planifier un plan de trasceiver (nombre et types au niveau de chaque noeud) procurant la moindre consommation énergétique sous une charge de trafic donnée. En général, pour fournir une solution de grooming, une topologie virtuelle est affectée à la topologie physique du réseau. Des liens virtuels relient les noeuds du réseau et peuvent correspondre à un ou plusieurs liens physiques successifs. La Figure 9 illustre un exemple

de topologie virtuelle adoptée pour une topologie de réseau formée de 10 noeuds. Les chemins optiques virtuels sont représentés par des courbes grises. Des noeuds du réseau ont été court-circuités (bypassed) dans cette topologie virtuelle (noeuds 2, 3, 8, et 10). Après la construction de la topologie virtuelle, les SDs sont affectées une succession de chemins optiques depuis leurs sources jusqu'à leurs destinations. Ensuite, les ressources nécessaires sont choisies en l'occurence des capacités cumulatives sur les chemins optiques virtuels. L'affectation de longueurs d'onde devient plus facile une fois le routage et le grooming sont effectués.

Notre problème diffère des problèmes de grooming classiques par le fait que nous considérons des débits multiples de transmission.

Se basant sur les explications précédente, nous pouvons décrire le problème de planification de réseau tenant compte de la consommation énergétique comme suit:

***Données du problème***

*Spécifications du réseau*:

- un réseau où tous les OXCs sont basés sur la technologie WSS;
- un ensemble de longueurs d'onde, disponibles par lien physique;
- un ensemble de types de transceivers, charactérisés par leurs débits et leurs consommations respectives;

*Charge de trafic*:

- un ensemble de requêtes de trafic. Nous considérons des SDs, sachant que les demandes permanentes (Permanent Demands (PDs)) peuvent être considérées comme un cas particulier de SDs, activées sur toute la période d'observation.

***Objectif du problème***

Notre objectif est d'établir un ensemble de requêtes (SDs ou PDs) en minimisant le taux de rejet et la consommation énergétique du réseau.

***Contraintes du problème***

*Contraintes en rapport avec les architectures des OXCs et des transceivers:*

- une longueur d'onde '$\lambda$' peut être extraite une seule fois à un temps donné;
- '$\lambda$' peut être insérée une seule fois à un temps donné;
- si '$\lambda$' est insérée et extraite à la fois, les deux canaux doivent avoir le même débit de données;

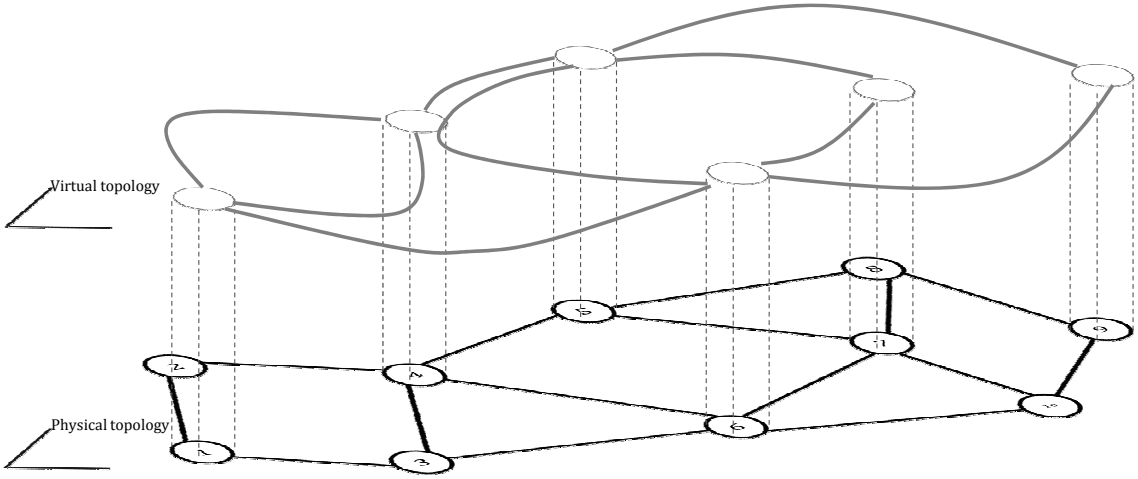


Figure 9: A virtual topology example.

*Contrainte de continuité de la longueur d'onde:*

Les chemins optiques routés sur la topologie virtuelle court-circuitent des noeuds intermédiaires de la topologie physique. Chacun est donc affecté la même longueur d'onde sur tous les liens physiques sous-jacents. Une SD (ou PD), routée sur plusieurs chemins optiques de la topologie virtuelle peuvent être affectées différentes longueurs d'onde sur ces chemins optiques.

### 0.4.3 Optimisation de la consommation énergétique dans un contexte de transmission multi-débit

Comme mentionné ci-dessus, nous considérons la possibilité de diviser le volume d'une SD en différents flux pouvant avoir n'importe quelle granularité. Cette approximation fluide au niveau électrique résulte en des SDs partielles (p-SD) traitées indépendamment. Ainsi, un routage bifurqué est effectué. Dans la Figure 10, nous illustrons un exemple d'une SD (du noeud 1 au noeud 7, et de capacité $\gamma_i$) décomposée en 3 p-SDs: p-SD$_{i1}$ (points), p-SD$_{i2}$ (tirets et points), and p-SD$_{i3}$ (tirets), où $\sum_{k=1}^{k=3} \gamma_{ik} = \gamma_i$. La figure montre les différents chemins virtuels choisis pour chaque p-SD, et les longueurs d'onde affectées sur chaque brin. p-SD$_1$ et p-SD$_2$ suivent le même chemin après le passage par le noeud 4. Sur le chemin optique liant les noeuds 4 et 5, elles sont affectés différentes longueurs d'onde ($\lambda_1$, $\lambda_2$), et ont parsuite été servies par différents transceivers aux noeuds 4 et 5. Sur le chemin optique liant les noeuds 5 et 7, elles sont affectés la même longueur d'onde $\lambda_1$. Cela implique que le même canal les dessert, moyennant les mêmes transceivers. Par conséquent $\gamma_{i1} + \gamma_{i2}$ ne doit pas excéder le débit nominal du transceiver choisi.

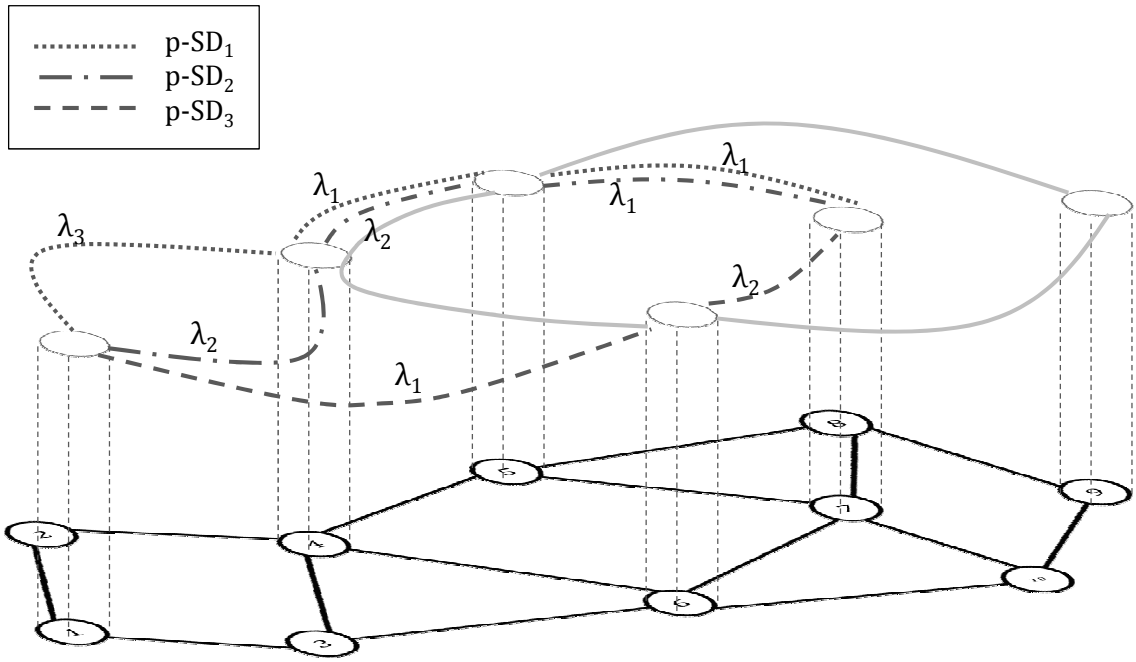


Figure 10: Example of p-SD establishment under bifurcated routing assumption.

L'ensemble de tous les chemins optiques obtenus définit une topologie virtuelle pour le réseau et le problème global est divisé en quatre sous-problèmes inter-dépendants:

- *Routage des SDs sur la topologie virtuelle*:

  Les p-SDs sont routées sur la topologie virtuelle sur un ou plusieurs chemins optiques consécutifs depuis la source jusqu'à la destination.

- *Routage des chemins optiques virtuels sur la topologie physique*:

  Cela concerne le processus d'affecter à chaque chemin virtuel une route continue de la source jusqu'à la destination en court-circuitant les noeuds intermédiaires.

- *Affectation de Transceivers aux chemins optiques*: Un chemin optique est desservi par une paire de transceivers aux extrémités. Seuls le transmetteur du transceiver de la source et le récepteur du transceiver de la destination sont utilisés. Les deux transceivers sont accordés à la même longueur d'onde et doivent avoir le même type (même débit).

- *Affectation de longueurs d'onde aux chemins optiques*: Une longueur d'onde et une seule est choisie pour acheminer un chemin optique sur tous les liens pendant sa durée d'activation. Les contraintes citées ci-haut sont à respecter impérativement.

Dans cette partie de la thèse, nous avons formulé notre approche sous forme exacte

par l'intermédiaire d'un ILP[10]. Les résultats sur un petit réseau montrent que l'utilisation d'un mélange de différents types de transceivers est intéressante pour la minimisation de la puissance globale consommée dans le réseau. Les différences en puissance consommée entre des trafics pré-planifiés et statiques sont aussi investiguées. En effet, une réduction de 40 % peut être atteinte en considérant les dates exactes d'activation et d'extinction des requêtes. Ce qui montre que le sur-dimensionnement des réseau, effectué jusqu'à présent aboutit à une perte de puissance inutile.

## 0.5 Conclusion

La thèse présente est focalisée sur la planification de réseaux de transports WDM, sous différents contextes d'optimisation. Dans la première partie, le coût économique de l'utilisation de régénérateurs est discuté alors que dans la deuxième partie, la consommation en puissance était mise en relief. Considérant les deux parties simultanément, il est possible de proposer une solution de planification de réseaux de transport tenant compte de la transmission multi-débit, et des trafics pré-planifiés. Cela requiert avant tout, un outil d'estimation de la QoT qui peut fournir des valeurs dans un tel contexte. Il est aussi important d'introduire la notion de transceivers à débit flexible, ce qui permet de réduire la consommation inutile pendant les temps d'inactivité. Ce type de transceivers ne constitue pas encore une technologie mâture.

[10]Integer Linear Program.

# Contents

# List of Tables

# List of Figures

# Acknowledgements

This dissertation would not have been possible without the guidance and the help of several individuals who in one way or another contributed and extended their valuable assistance in the preparation and completion of this study.

First and foremost, I would like to express my gratitude to my supervisor, Prof. Maurice Gagnaire not only for his support throughout my Ph.D. research work, but also because he was a great influence on my attitude towards my career and life.

I am also grateful to Prof. Bijan Jabbari and Prof. Josep Prat for their time and effort reviewing the present work and convey my thanks to Prof. Catherine Lepers, Prof. Bernard Cousin and D. Dominique Verchère for their contribution in the final examination of my research.

I heartily acknowledge D. Sawsan Al Zahr and D. Elias Doumith for the good advice, scientific guidance and friendship. I wish you both a happy life ahead and a continued success in your career.

It is also important for me to acknowledge the kindness of Mrs. Florence Besnard and Mrs. Fabienne Lassausaie, it has always been delightful to see your beautiful and joyful faces.

My friends Paty, Wissam, Rosy, Farhan, Azin, Shivam, Ali, Ahmed, Paul, Mario, Felipe, Rachad, Amy, and many, many others... have always been a source of energy. Thank you for the chats, the walks, and the laughs.

My family has always been there for me spiritually, emotionally, and psychologically. Nothing can really express my feelings and gratitude towards my parents Ahmad and Ghada for the values they have given me. They have taught me to never be afraid of the truth and openly express my thoughts and feelings. I thank my brother Karim for his support and friendship, I have always considered you as an older brother. I also thank Fares for being such a lovely younger brother, I adore your one-of-a-kind attitude! I would also like to express my hearty feelings to my sister Lili, you have been a source of inspiration at all times... And of course, Dima and Sara, you don't know how helpful you were during my good and bad times!

Finally, my deepest thanks are dedicated to my dearest Dhia for putting up with me and guiding me in each step. You have taught me what life really means. I feel so proud and fortunate to have you near me...

*"You have been told also life is darkness,*
*And in your weariness you echo what was said by the weary.*
*And I say that life is indeed darkness save when there is urge,*
*And all urge is blind save when there is knowledge,*
*And all knowledge is vain save when there is work,*
*And all work is empty save when there is love,*
*And when you work with love you bind yourself to yourself,*
*Aand to one another, and to God..."*

*– Gibran Khalil Gibran, The prophet.*

# Abstract

As operators strive today to optimize their networks, considerations of cost, availability, eco-sustainability, and quality of service are beginning to converge. Solutions that reduce capital and operational expenditures (CapEx and OpEx) not only save money, but also tend to reduce the environmental impact. Classically, two approaches are considered for network planning and management. On one hand, network design considering permanent traffic is investigated by means of offline optimization techniques. On the other hand, traffic engineering addressing random traffic is investigated by means of online optimization techniques. Recently, a third approach considering predictable dynamic connections has been introduced. This latter is investigated by offline optimization techniques. The purpose of this thesis is twofold. First, we have addressed translucent WDM network design to provide a compromise between actual opaque networks and idealistic transparent networks. The second part of this thesis addresses energy efficiency in WDM networks.

In opaque networks, optical signals undergo expensive electrical regeneration systematically at each node, regardless of their quality. In transparent (*i.e.*, all-optical) networks, on the other hand, signal quality deteriorates due to the accumulation of physical impairments from source to destination. Translucent networks constitute a tradeoff between opaque and transparent networks. Indeed, in such networks, sparsely chosen nodes are equipped with electrical regenerators while the others are transparent to the optical signal. In this thesis, we have proposed an innovative optimization technique for translucent network design. Our approach, assuming a finite network capacity, aims at satisfying, at the lowest cost, the largest number of permanent connection requests while respecting their end-to-end Quality of Transmission (QoT). For this purpose, we have developed an algorithm called COR2P for Cross-Optimization for Routing and Wavelength Assignement (RWA) and Regenerator Placement consisting in a cross-optimization between CapEx and OpEx costs. This cross-optimization is implemented by means of an original cost function, resulting in reducing the total number of regenerators as well as centralizing them in the minimum number of nodes. Both linear and non-linear effects are considered in the degradation of QoT. The performance of COR2P has been compared with other

Impairement-Aware-RWA (IA-RWA) algorithms from the literature. This first objective has been carried out as a contribution within the European DICONET project, and the BONE European network of excellence.

The second part of this thesis focuses on energy-aware WDM network design applied to scheduled traffic. We have first identified the network elements presenting an opportunity to minimize power consumption in the network. The client cards interfacing the IP router and the optical cross-connect represent the key elements which deployment is to be addressed. Actually, such components are powered-on permanently even in the absence of traffic. To prevent this power waste, we propose to optimize the number and usage of these components. For that purpose, the time-space correlation between traffic connections has been closely considered in order to determine potential client card utilization in time by means of traffic grooming. In current networks, client cards operating at different standardized data rates (10Gbps, 40Gbps, ...) can transmit simultaneously on the same fiber. Operators plan to exploit multi-rate transmission to provide more dynamic services. Our objective in this context is then to find an ideal mapping between a set of scheduled connection requests onto a Wavelength-Selective-Switch-based (WSS-based) infrastructure. Both an exact approach and a heuristic-based algorithm have been proposed to solve the routing, grooming, wavelength assignment, and client card assignment problems.

# Chapter 1

# Introduction

## 1.1 Context and motivations

Three main domains are considered in carriers' networks: access networks, metropolitan area networks and core networks. This thesis deals with optical core network design. In the context of core networks, two major aspects are to be taken into account: network availability, and quality of transmission. More recently, a third aspect has been introduced, addressing the ecological footprint of large-size networks. Wavelength Division Multiplexing (WDM) technique has driven a huge capacity growth, the theoretical limit being around 1 Pbps per fiber [82]. In current networks, transmission line equipment operate at standardized data rates: 1 Gbps, 2.5 Gbps, 10 Gbps and 40 Gbps. The 100 Gbps equipment are about to be deployed. In this context, three parameters need to be investigated:

1. *Quality of transmission (QoT)*: the increase in traffic loads induces a higher density of optical channels per fiber, as well as a higher modulation rate per channel. In this context, the interaction between the different optical carriers as well as the interaction with the optical medium cannot be neglected. The quality of transmission of the signal is altered and an accurate quality management is thus necessary.

2. *Dynamicity*: to date, carriers' networks operation is mainly based on permanent traffic requests. With the emergence of services such as cloud applications and virtual private networks, dynamic lightpath establishment is required. Depending on the traffic granularity and connections durations, various optical switching technologies have been developed: optical circuit-switching (OCS), optical packet-switching (OPS) and optical burst-switching (OBS). This thesis focuses on the automatic reconfigurability of optical circuit switches. Reducing optical-electrical-optical conversions in OCS networks enables a reduction of manual service provisioning, not to mention the inherent capital and operational costs.

3. *Electrical resources utilization*: on one hand, since electrical devices (*e.g.*, electrical regenerators and transceivers based on electrical transponders) are costly, power

hungry, and data-rate-dependent, it is desirable to optimize their utilization throughout the network. On the other hand, the lower the amount of electrical devices, the more difficult the monitoring of the optical channels. In other terms, the ideal usage of electrical devices is subject to a tradeoff.

The three points listed above, are, in fact, strongly dependent and will be investigated along this thesis. However, optical monitoring is out of the scope of our work.

The transition from an *opaque* network to an all-optical (*transparent*) network is only achievable via an intermediate step: *translucent* networks. In translucent networks, the needs in opto-electronic equipment are optimized, the quality of service and cost reduction being simultaneously considered. Optical transmission systems currently deployed in WDM networks extend the achievable reach of optical signals by compensating partially some of the physical layer impairments such as chromatic dispersion or attenuation. Meanwhile, considering only linear impairments does not guarantee an admissible bit error rate (BER) at destination [63, 80]. Recent research in the field of optical network planning take into account the different limitations of physical layer in the routing and wavelength assignment operation (RWA). The Impairment-Aware RWA (IA-RWA) approaches define rules and strategies for lightpath establishment in a transparent network, in order to minimize the number of rejected demands due to either capacity or QoT limitations. Besides combating transmission impairments in all-optical transparent networks, some related studies focus on electrical regenerator placement using electrical regeneration to extend the reach of the transported signal. Different possible implementations of electrical regeneration for translucent networks are considered in the literature [18, 60, 85]. Most research works in the domain of translucent network design consider either the determination of regeneration sites according to topology-driven strategies, or the insertion of regenerators in the network nodes in accordance with the IA-RWA solutions for a certain set of static traffic requests. Minimizing the needed number of regenerators has been the essential objective of such solutions. In the first part of this thesis, we propose to jointly minimize the number of regenerators and the number of regeneration sites in the network, besides providing a solution to the IA-RWA problem. Our approach considers a CapEx/OpEx-oriented cost, related to electrical regeneration. A cost function is implemented within the original network planning tool called COR2P[1]. This cost function urges the concentration of the regenerators in a few network nodes.

With more focus on energy-aware network solutions, operators have yet to introduce green technologies and equipment. Network design and management are practically based on deploying and maintaining extremely reliable infrastructure that can handle roughly all types of services. With good knowledge of today's traffic needs at the core network, operators can save their networks' energy consumption and reduce their equipment environmental footprints. Wavelength-Selective-Switch-based Optical Cross-Connects (WSS-based OXCs) can dynamically route wavelengths in a colorless and directionless way [41].

[1]Cross-Optimization for Regenerator placement and RWA.

At the interface of the OXC and the core router, router client cards performing OEO conversion are deployed. These transponder-based cards constitute the unavoidable most energy-consuming equipment at the WDM layer. In order to save energy at this layer, it is best to optimize the deployment and usage of transponder cards so their operation matches the exact need of the network. In the second part of this thesis, we address energy-aware network design, targeting the choice of client cards under scheduled traffic and multi-data-rate transmission. In this part, the QoT is neglected. Traffic grooming and optical bypass under power constraints introduce flexibility in the routing and wavelength assignment process, with regard to the time-space-correlation of traffic requests.

The first part of this thesis was granted by the DICONET European project. Our contribution within this project was to provide the COR2P design tool, which was at the heart of one of the project's deliverables. Beyond the DICONET project, we have collaborated with the ADVA core networking team [1] that provided a clear vision of typical OXC architectures. Few parameters dealing with energy consumption of transponder cards, have been provided by engineers from Huawei equipment supplier [3].

## 1.2 Thesis outline

Chapter 2 describes in detail the different approaches for future WDM core network design along with their advantages and disadvantages. We also delve in corporate objectives of network operators in order to define our strategy addressing network cost and power-consumption minimization. We identify two main investigation fields that correspond to the two parts of this thesis: Part I, entitled "Cross-Optimization for Translucent WDM Network Design" and Part II, entitled "Energy-Aware WDM Network Design".

Part I includes three chapters. In chapter 3, we provide a description of a point-to-point WDM transmission line, as deployed in today's mesh networks. We then provide an overview of linear and non-linear physical impairments at the optical layer. Finally, we describe a QoT tool called BER-Predictor, that we use in our investigation to estimate the QoT of optical lightpaths at their destination nodes. This QoT tool has been developed by Alcatel Lucent (Bell Labs) [67] during a national project called RYTHM, in which our lab has contributed before the DICONET project. Chapter 4 assesses relevant state-of-the-art research in the field of translucent network design. Chapter 5 describes in details our approach for translucent network design. We first explain our cost model regarding regenerator deployment in network nodes. We then provide detailed description of our heuristic, COR2P, incorporating our cost model. Results including comparisons with two other approaches from the literature are discussed at the end of this chapter.

Part II includes chapters 6 and 7. Chapter 6 describes the essential drivers for introducing power-awareness in core networks and identifies candidate components enabling power-aware RWA on the basis of existing devices. Related work is also commented. Chapter 7 describes our approach for client cards choice at the core network nodes, targeting power-consumption minimization. An exact approach based on an ILP formulation

is presented and its results are discussed. In addition, a heuristic approach based on a genetic algorithm is provided.

Finally, Chapter 8 concludes this thesis and provides perspectives for future work.

# Chapter 2

# Problem Statement

## 2.1 WDM core networks

Wavelength-division multiplexing (WDM) technologies have been deployed for building high bandwidth optical communications networks. Large-scale core networks are currently undergoing an evolution towards higher capacity at lower costs. At one hand, higher capacity can be obtained via denser WDM transmission systems and/or higher line rates; both these solutions emphasize the need for more flexibility and reconfigurability in order to operate while large-scale optical networks are currently being manually provisioned. At the other hand, when aiming to reduce corporate costs, network operators are first faced with the need for more scalable switching systems that can afford low energy consumption while optimizing squared meters. In addition, manual configuration needs to be reduced, as much as possible, in order to provide a more manageable backbone network to operate not only with equipment from different vendors, but also with networks belonging to different operators. Real-time service provisioning and faults management are also major requirements for future networks, regardless of the used switching/routing technologies.

WDM technique consists in injecting several optical channels onto the same fiber.

In current optical transmission systems, data can be sent over a few tens of optical channels on a single fiber thanks to dense wavelength division multiplexing (DWDM), reaching bit rates of Gigabits per second over each channel. Terabits per second per fiber are achievable on the most loaded optical fiber-links of existing core networks.

Transmission distance plays a critical role in determining optical network cost. Indeed, as the transmission distance and line rates increase, transmission is progressively corrupted by physical impairments due to the underlying physics of the optical layer. Therefore, carriers' optical networks are based on three main architectures corresponding to the different geographical regions and distances, namely, access, metro and core networks [11].

### 2.1.1 Access networks

Access networks reach the end user (corporations or individuals) directly from the central office, and span a few kilometers up to several tens of kilometers in urban areas. The

essential purpose of access networks is to aggregate traffic destined in majority to the long-haul (core) network or to another access network in the neighborhood. WDM systems are not yet used for accessing individual end users because of their cost and the low level of mutualization. Indeed, the equipment located close to the end users must be inexpensive and simple and do not need to provide high capacity or high performance, due to modest individual traffic demands. As illustrated in Figure 2.1, optical access networks are based on two possible architectures: Point-to-Point (P2P), and Point-to-Multipoint (P2MP) as in Passive Optical Networks (PON).

### 2.1.2 Metro networks

Metropolitan area networks (MAN) are used to interconnect several access networks in the same neighborhood. They are also used to bridge traffic from access to long-haul networks. MANs span metropolitan areas and range between a few kilometers to a few hundreds of kilometers. MANs are generally based on SONET/SDH [1] rings where Reconfigurable Optical Add/Drop Multiplexers (ROADM) provide flexible operation and processing of traffic, being adapted to degree-2 network nodes.

### 2.1.3 Core networks

Core networks are typically regional, continental or even intercontinental networks. They can span from several hundreds up to a few thousands of kilometers, and therefore, are severely impaired by physical degradations increased with distance and high data rates, such as attenuation, dispersion, and nonlinearities due to interaction between different channels on the same fiber. Optical amplifiers such as Erbium-Doped Fiber Amplifiers (EDFA) (every 80 km) and Raman amplifiers (every 100 km) have been deployed in order to facilitate long-reach transmission. Sophisticated dispersion compensation and channel equalization techniques have participated in extending the optical reach to 2000 km.

Typically, core networks are mesh networks. Therefore, the nodal connectivity degree is generally higher than 2, which drives the need to deploy OXCs.

Figure 2.1 illustrates the three different classes of networks described in this section.

In this thesis, we focalize on quality of transmission and network planning issues in the context of WDM core networks.

## 2.2 Actual and future data plane: IP-over-WDM

Data traffic has already surpassed voice traffic in volume. The question of a converged transport network capable of handling both circuit-based and packet-based services has arisen and solutions have been proposed. IP [2] will form a basis for new services and

[1] Synchronous Optical Networking (SONET) and Synchronous Digital Hierarchy (SDH) are standardized multiplexing protocols that transfer multiple digital bit streams over optical fiber. SONET is used in the United States and Canada while SDH is used in the rest of the world.

[2] Internet Protocol.

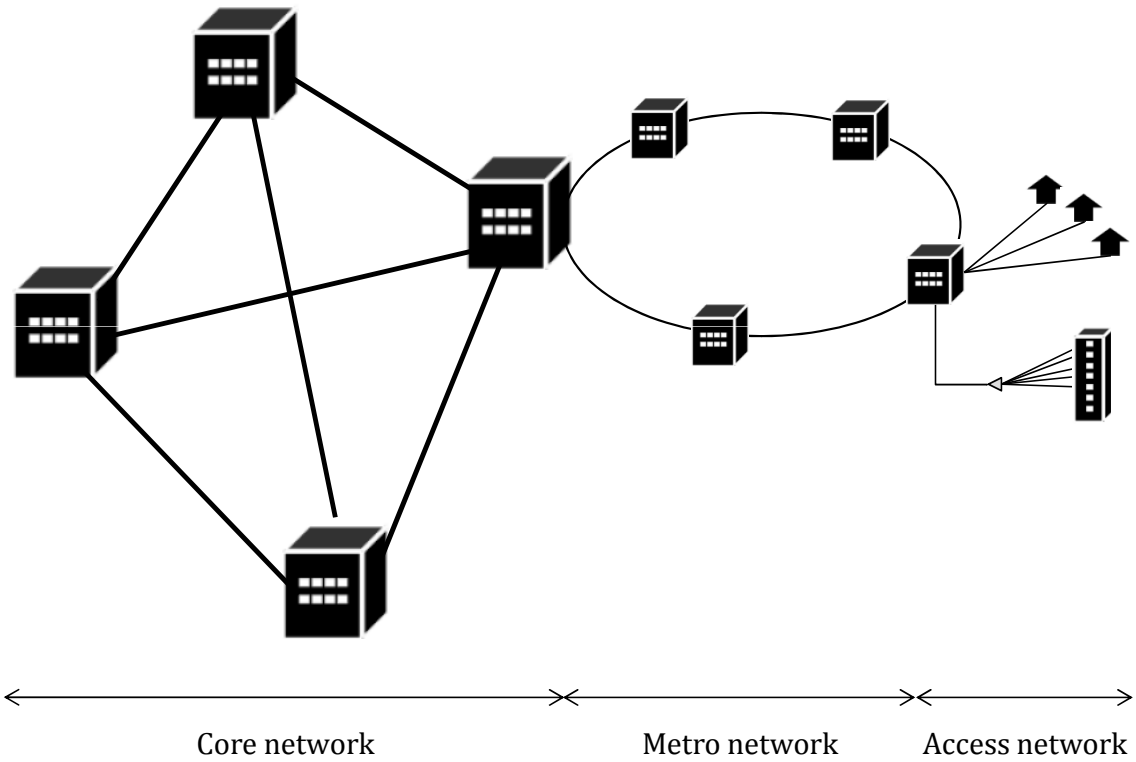


Figure 2.1: Hierarchical network.

insure the transition from circuit-based to packet-based services as voice and video over IP. Different approaches for IP-over-WDM are proposed for future data plane. A first approach consists in transporting IP over Asynchronous Transfer Mode (ATM) in order to carry different types of traffic onto the same pipe with different Quality of Service (QoS) requirements. Data is then sent over SONET/SDH, and finally over WDM fiber. ATM also has the advantage of traffic engineering capability that complements IP's best effort traffic routing, although this approach is very complex to manage.

The second approach consists in transmitting IP-over-MPLS [3] over SONET/SDH and then WDM. The first and second solutions are implemented in today's networks.

The third approach employs IP-over-MPLS directly over WDM. This latter solution, although being the most efficient solution for IP-over-WDM, requires that the IP/MPLS layer looks up for path protection and restoration, which is not as simple as in the second approach where IP-over-MPLS is responsible for restoration. In addition, suppressing *de facto* SONET/SDH adds the constraint inherent to the lack of clock referencing in carrier networks to this third approach.

Protocol stacks within the dashed line of Figure 2.2 summarize these three approaches for IP-over-WDM [58].

As 95 % of data traffic are Ethernet frames at the end users, and since Ethernet is

[3]Multi-Protocol Label Switching (MPLS) is a mechanism which directs and carries data from one network node to the next with the help of labels. MPLS creates virtual links between distant nodes. It can encapsulate packets of various network protocols including Internet Protocol (IP).

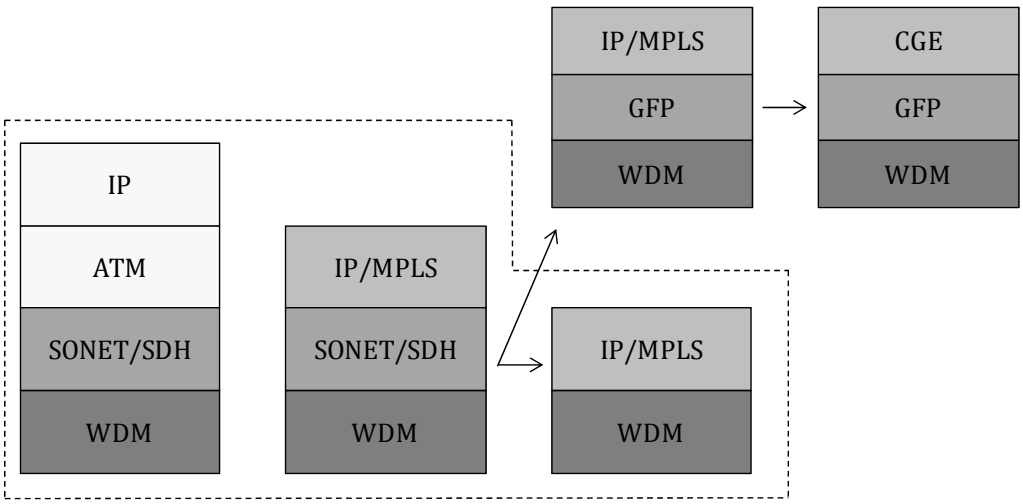


Figure 2.2: Approaches for IP-over-WDM

capable of supporting IP services, Ethernet has become the potential convergence solution for Next Generation Networks (NGN). Carrier-Grade Ethernet (CGE) is proposed to offer a transport solution for IP-over-WDM [14].

The Generic Frame Protocol (GFP) also seems an interesting approach to replace SONET/SDH in future [46]. These approaches are also illustrated in Figure 2.2.

## 2.3 Translucent networks: bringing transparency to the core network

### 2.3.1 Opaque networks

Most of the transport networks deployed nowadays, can be qualified as *opaque* networks. In such networks, the optical signal is transmitted over point-to-point links from source to destination, each intermediate node between two successive links converts it to an electrical signal for routing purposes. This conversion is performed thanks to an electrical component called a *transponder*. By definition, a transponder is a device that allows access to WDM channels. Transponders can be tunable or fixed in terms of wavelengths. A transponder receives an optical signal, detects its carrier wavelength by means of a photodetector and a filter then converts it into an electrical signal. This operation is called Optical-to-Electrical conversion (OE). A laser, performing intensity modulation over the electrical signal, emits an optical signal with a specific wavelength. In case of a tunable transponder, an array of pretuned lasers is deployed [11]. This operation is called Electrical-to-Optical conversion (EO). In its simplest form, a transponder receives a signal carried by a short-reach (SR) carrier wavelength (*grey light*), converts it to an electrical signal and then to an optical long-reach (LR) signal (*colored* signal) carried by a WDM wavelength according to the ITU grid recommendations [54]. The reverse operation (*i.e.*, transforming a LR signal into a SR signal) is also possible through a transponder. Figure 2.3 depicts a transponder

operating in two fashions: LR-to-SR and SR-to-LR. Figure 2.4 illustrates an opaque node.

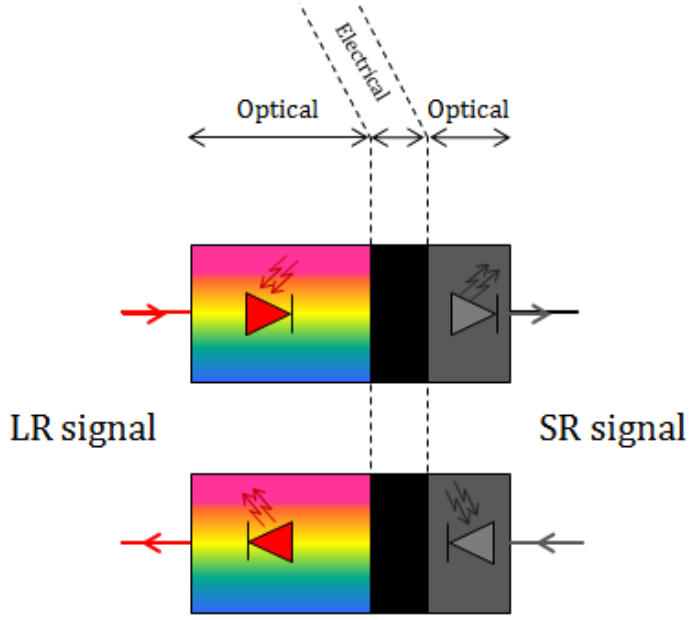


Figure 2.3: An overview of a transponder.

At the input of the node, WDM signals are first demultiplexed into elementary colored signals. Each of these signals is converted into a short-reach grey signal by means of a transponder. The SR signal is then fed to an opaque port attached to the Electrical Cross-Connect[4] (EXC). This port transforms the SR signal into an electrical signal to be processed in the EXC. If the data signal has reached its destination at the current node, the EXC routes it towards an output port at to the upper SONET/SDH or MPLS layer interface. If the current node is only a transit node on the signal's route, the EXC redirects it towards an opaque port corresponding to the convenient direction (*i.e.*, the corresponding output fiber). The signal is then transformed into a SR optical signal at the opaque port, then to a LR signal carried by a certain wavelength, within the transponder. Optionally, the EXC can groom other small granularity electrical signals to the considered signal before transmission. All outgoing colored signals are multiplexed into one WDM composite signal before transmission over the fiber.

During its migration into a network node, a signal undergoes multiple OE and EO conversions. Thus, the operating expenses of opaque networks are quite high, and opto-electric conversions constitute a major fraction of network equipment cost. Macroscopically, the network's cost is proportional to the number of hops spanned by optical signals [18].

Collaterally, optic-electric-optic (OEO) conversion at the nodes performs the so-called 3R regeneration (Reamplification, Reshaping and Retiming) of the signal. By doing so, the signal is *cleaned up* from degradations due to the physical impairments affecting signal's quality through transmission systems and links. Currently, 3R regeneration can only be

[4]Electrical switching core, responsible for switching at the SONET/SDH layer

realized through OEO conversion.

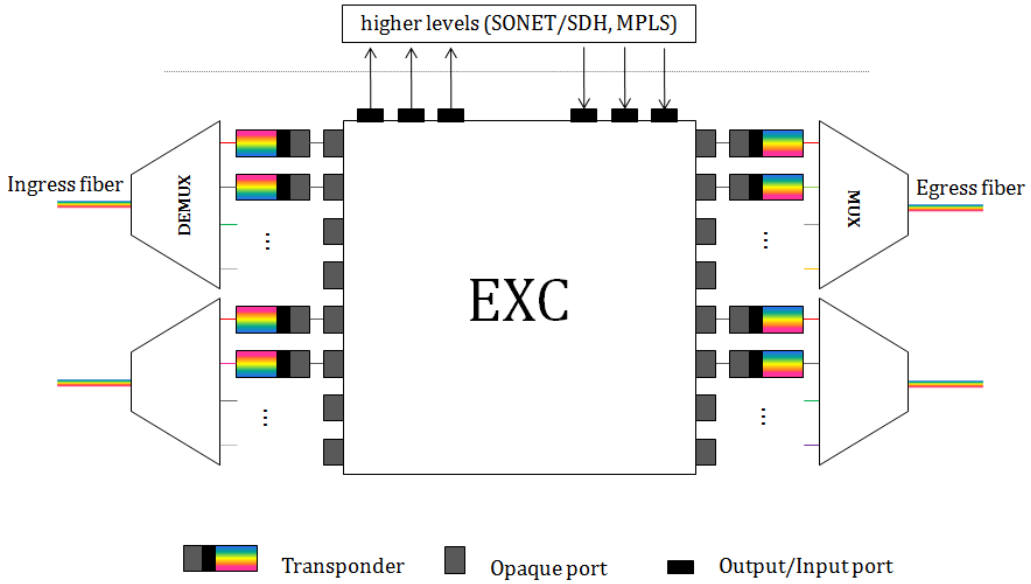


Figure 2.4: Simplified opaque node architecture.

### 2.3.2 Introduction of optics in the switching core

The demand for bandwidth in the internet has been the subject of a tremendous growth in the past decade. One reason for this explosive growth is the advent of network applications such as triple-play[5], and the externalization of the private data centers (*Cloud computing*).

Up to now, WDM technique has enabled to upgrade the capacity of optical networks according to the traffic growth. Recently, the necessity to deploy sparse all-optical switching nodes has emerged, due to the congestion at the opaque nodes.

In the past decade, new optical switching node architectures have emerged, mainly based on two photonic technologies, namely: Micro-Electro-Mechanical Systems (MEMS) mirrors, and Wavelength-Selective Switches (WSS) for nodes of connectivity degrees higher than two[6] [84, 8, 17]. Using such switching fabrics, an optical signal may pass through a network node without systematically undergoing OEO conversion at intermediate nodes [9]. OXCs made of either switching technologies, along with long-haul transmission systems, allow the emergence of all-optical (*transparent*) networks.

### 2.3.3 Transparent Networks: *pros and cons*

In transparent networks, OE and EO conversions occur only when signals need to be added (*resp.* dropped) to (*resp.* from) the optical layer. Transparency in this concern, is not only

[5]Voice, data and video.

[6]Reconfigurable Optical Add/Drop Multiplexters (ROADMs) mainly based on Wavelength Blockers (WB) and Planar Lightwave Circuits (PLC), are used for add, drop and cut-through operations in network nodes of connectivity degree equal to 2.

related to the absence of electrical processing of signals while routed through the network; it also reflects the transparency of network components to (*i*) the digital signal format (SONET/SDH, IP, ...), (*ii*) the signal's bitrate, and (*iii*) the modulation format of optical signals (RZ, NRZ, ...) [15]. In this regard, if protocols or bit rates change in future, the network is still likely to be able to support changes without requiring a complete overhaul.

Figure 2.5 depicts a 4-degree transparent node architecture, regardless of the optical switching technology adopted in the OXC. An incoming signal is processed at the OXC, its different wavelengths[7] are directed, each to its convenient output direction:

- A Pass-through wavelength is sent to the OXC part belonging to the corresponding fiber on the wavelength's next hop[8].
- A wavelength that had reached its destination node in the core network is processed at the Add/Drop Multiplexer (ADM) that feeds it into a vacant Drop transponder in order to process its data at the EXC.

A signal originating at a node's EXC is first modulated on a WDM wavelength by an Add transponder, sent by the ADM to the convenient direction of the OXC, that incorporates it in the composite WDM signal to finally, be transmitted over the output fiber. Add/Drop transponder usage is detailed in Section 2.4.1.

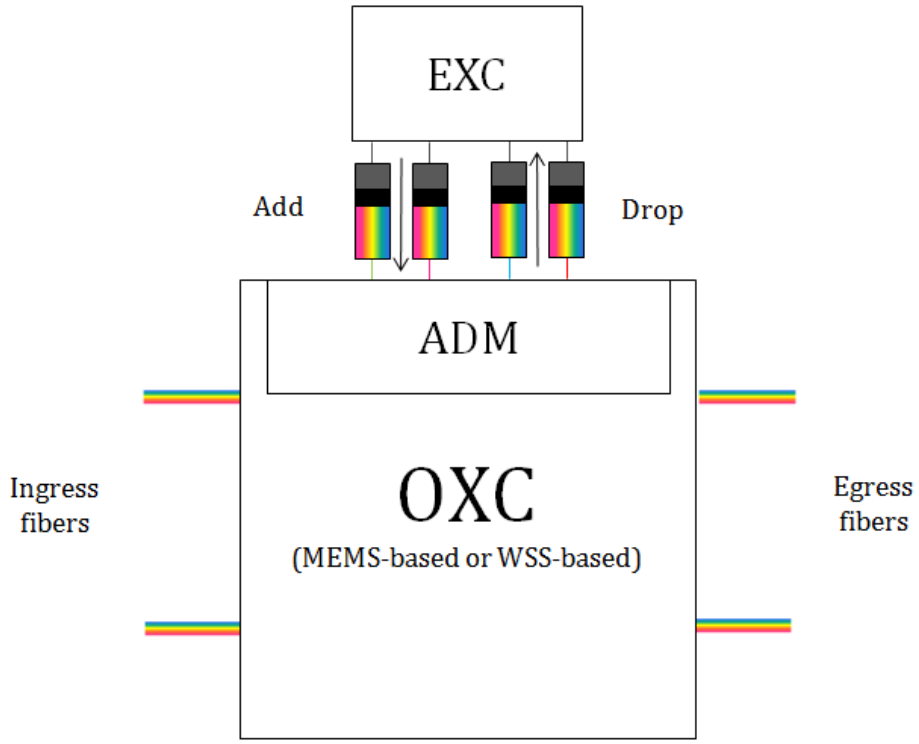


Figure 2.5: Simplified transparent node architecture.

[7] In the rest of this thesis, a colored signal may be expressed by its wavelength.
[8] A hop represents a transition from a network node to a neighboring node, via a single link.

Even though transparent networks constitute an attractive solution at different levels, they are faced with technical difficulties related to cumulative performance degradations. The causes of these degradations are the physical impairments introduced by long-haul transmission and the cascading of optical transmission components such as OXCs and optical amplifiers. Physical impairments not only depend on the transmission systems' characteristics (*e.g.*, attenuation, dispersion...), but also on signal's characteristics (*e.g.*, modulation format and data rate). Due to signal degradation scaling with the network size, the reach distance of signals in WDM optical networks becomes limited under the current state of technology. In consequence, due to the absence of 3R regeneration, transparent networks cannot exceed 200 km of maximum transmission distance.

Node bypassing in transparent networks forbids wavelength conversion at the nodes. A colored signal keeps its color (wavelength) from its insertion at the source node until its extraction at the destination node. On one hand, this fact reduces flexibility in terms of wavelength assignment, and then in terms of network's capacity. On the other hand, and in order to avoid wavelength conflict over links, some signals can not benefit from their shortest path in order to reach their destination, implying the passage through more network components and fibers.

To sum up, as long as the network's scale is not too large, transparency is effective. The main constraint inherent to transparency is, meanwhile, the wavelength continuity constraint [37].

### 2.3.4 Translucent networks

Opaque and transparent networks have each their advantages and drawbacks. While an opaque network remains relatively simple and flexible at the operation level, a transparent network offers the reduction of OEO conversions, and in result, that of network cost due to the use of less active components. It is also less energy-consuming than an opaque network. A third concept of core networks has been introduced in the last decade, namely: *the translucent networks*. Translucent (or hybrid) networks stand half-way between the latter concepts of networks, providing a compromise between cost reduction and performance while guaranteeing routing flexibility of signals.

Translucency in WDM networks implies that the optical signal travels as far as possible through the network until its quality degrades requiring, thereby, regeneration at intermediate nodes along its path.

Translucent networks use a set of sparsely but strategically placed 3R regenerators at the nodes [18]. Thus, they constitute a compromise between all-electronic switching and all-optical switching, seeking a certain balance between network design cost and performance. It is shown that translucent networks can achieve performance comparable to that of opaque networks in terms of service provisioning at a much lower network cost, if 3R regenerators are judiciously placed [96, 35].

Three approaches for translucent networks are defined in the literature:

- Translucent networks made of transparent islands: The border between two adjacent islands corresponds to a 3R regeneration site [12, 35].

- Translucent networks made of sparse electrical and transparent nodes [43].

- Translucent networks made of transparent nodes, some of them being equipped with 3R regenerators [12]. This third category for translucent network design is the most adopted in the literature since it is the most flexible and cost-effective [35].

In this thesis, we adopt the third approach when dealing with translucent network issues, this approach is often called "*sparse regeneration*" in the literature [96]. The choice and management of translucent nodes has been the subject of many studies during the last decade. In figure 2.6, a translucent network is illustrated. Translucent nodes are equipped with 3R regenerators while the rest are transparent nodes. A connection request from node 'A' to node 'B' is routed as depicted. It undergoes regeneration at translucent node 'C' while transiting transparently through translucent nodes 'D' and 'E'. This example aims to insure that regeneration is not systematic at each intermediate translucent node.

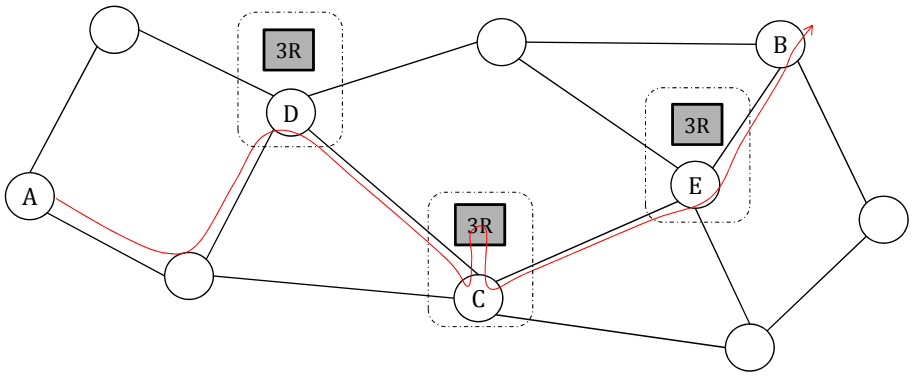


Figure 2.6: Translucent network.

In this thesis, a translucent node (also called a *hybrid* node) is considered made of an optical switching core, an electric switching core, and a bank (pool) of 3R regenerators. Figure 2.7 shows the different parts of a translucent node. In comparison to a transparent node architecture, translucent node architecture adds a bank of 3R regenerators that receives impaired colored signals from the ADM, regenerates them, then sends them back to the ADM to be inserted to the OXC.

Bringing in OEO facility alleviates the constraints on transparent core networks. On one hand, a translucent network is much flexible than a transparent network due to the possibility of wavelength conversion at the translucent nodes. In a transparent network and under high loads, it is probable that a connection request gets blocked, for the reason that the network does not present any vacant wavelength over all intermediate links from source to destination. Translucent networks presents a smooth solution for the wavelength

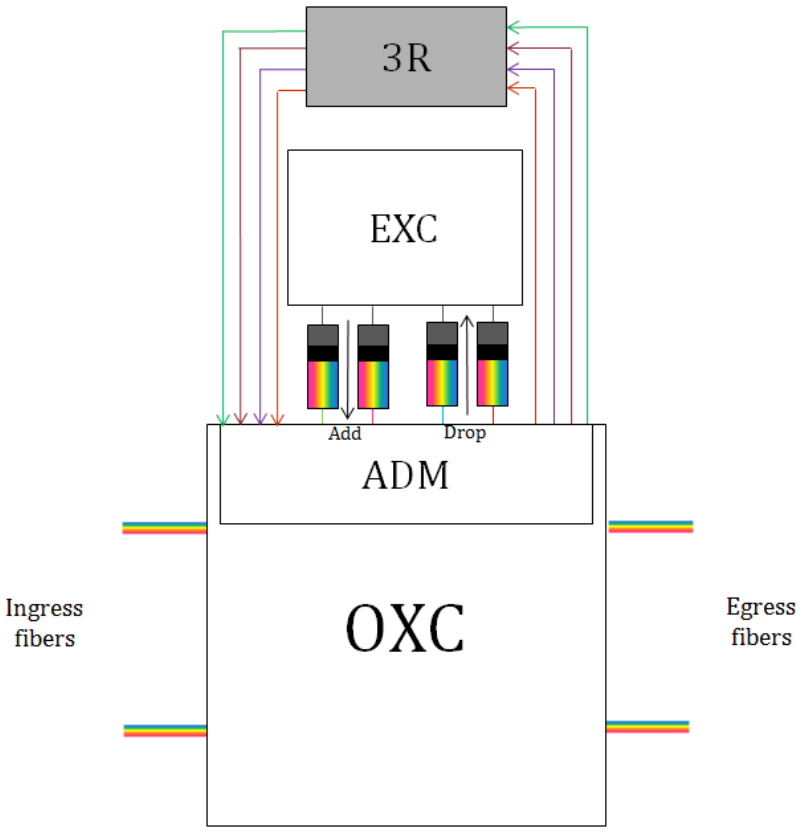


Figure 2.7: Translucent node architecture.

continuity constraint where a signal can be extracted from the optical domain at a translucent node on its route, and have its wavelength changed into a vacant wavelength over the next transparent path to follow (Cf. Section 2.4).

On the other hand, 3R regeneration's purpose is to "*clean-up*" noisy and distorted signals due to physical impairments. As mentioned previously, physical impairments accumulate over the signal along its route, making it hard to reach hundreds of kilometers under all-optical transmission. Translucent networks, on the contrary, can reach a continental size due to the possibility to renew noisy signals at one or more intermediate network nodes [15, 72].

## 2.4 Transponders in translucent networks

Transponders constitute a mature and reliable technology. Meanwhile, they are bit-rate-dependent and power-greedy. 3R transponders are the most complex and costly category of transponders. Transponders are used for three major functionalities in the core network, namely: Add/Drop functionality, signal regeneration and wavelength conversion.

### 2.4.1 Add/Drop functionality

Add/Drop functionality serves not only the traffic terminating at the node, but also a part of the pass-through traffic, as it will be explained in the following.

IP traffic nowadays circulates through the core networks over WDM or DWDM wavelengths. Without getting into the details of transmission inside the OXC of a network node, a colored signal is subject to optical demultiplexing at the reception. Three kinds of signals can be distinguished at this level:

- *Signals to be ignored by the EXC of the node*: These colored signals pass *transparently* through the OXC towards the required egress direction. They are multiplexed with other wavelengths at the output of the OXC.
- *Signals to be terminated at the EXC of the node*: When some wavelengths have reached their destination in the core network, each one of them is forwarded to a transponder (fixed or tuned). Each resulting grey signal is then sent to an opaque port of the SONET/SDH EXC. The individual clock corresponding to each optical carrier is recovered. Erroneous bits are detected and eventually corrected. The SONET/SDH EXC eventually proceeds to restoration, if needed.
- *Signals driven to the EXC only to be groomed with other signals on the same wavelength*: Multiple lower-speed signals can be aggregated in order to better use the optical channel capacity. The resulting output optical channel is then injected into the core transport network.

In the two latter cases, colored signals are said *dropped* when *extracted* from the optical level to be processed by the EXC and *added* to the optical level if originating (or resulting of a grooming process) at the EXC. Added wavelengths are directed each to its convenient egress degree, multiplexed with other wavelengths to form a WDM composite signal that will be transmitted on the corresponding fiber-link. The add/drop functionalities necessitate transponders to operate successful WDM to SONET/SDH conversion.

### 2.4.2 Signal's Regeneration

Due to physical limitations on fiber, signals' quality is altered, not only in terms of power amplitude, but also in shape. Regeneration consists in re-amplifying, and/or reshaping, and/or re-timing a degraded signal. In order to maintain a comprehensible signal at destination, its QoT is monitored at intermediate nodes along its route. In opaque networks, monitoring is performed at each intermediate node. Add/Drop signals as well as pass-through traffic to be aggregated to other sub-wavelength traffic, undergo 3R regeneration systematically through transponders at the Add/Drop level. Traffic destined to pass transparently through a certain OXC might also have been impaired while passing through previous links and OXCs. In case no regeneration occurs at the considered node, losses inherent to filtering, multiplexing/demultiplexing at the OXC (regardless of the underlying technology) are added to the losses inherent to the previous impairments.

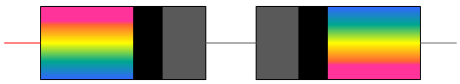

Figure 2.8: 3R regenerator made of two back-to-back transponders.

When an unacceptable QoT level is monitored at a certain node, 3R regeneration must be performed over the affected wavelengths. Add/Drop transponders perform 3R regeneration and deteriorated signals are transferred to the EXC then reinserted into the OXC before being sent to the next node.

Classically, 3R regeneration is obtained through two back-to-back transponders as illustrated in Figure 2.8. It is worth noting that 3R regenerators can be fixed or flexible in terms of wavelengths depending on their transponders. On one hand, input and output wavelengths in fixed regenerators are predefined. Such regenerators are used for *permanent* traffic connections that are to remain for a long time period in the network. It is worth noting that the input and output wavelengths can be different. In the other hand, tunable regenerators are more flexible for being able to serve different traffic connections at different times. This type of regenerators is profitable for medium to short duration traffic [15].

### 2.4.3 Wavelength conversion

Thanks to WDM technology, multiple single carrier (wavelength) signals are multiplexed into one WDM composite signal sent over fiber-links. In this respect, a single wavelength is allowed to be transmitted only once in a composite signal. Consider Figure 2.4.3, two lightpaths carrying traffic over wavelength $\lambda_1$ jointly arrive to node N from different fiber-links $L_1$ and $L_2$. These signals are then to be routed over fiber-link $L_3$. In order to avoid wavelength conflict and the loss of one of the two single carrier signals, one of them should switch to another wavelength, at the level of node N, such that this wavelength is free over $L_3$. This mechanism is called *wavelength conversion* (WC). Wavelength conversion not only adds flexibility to lightpath establishment, but also provides efficiency of wavelength utilization.

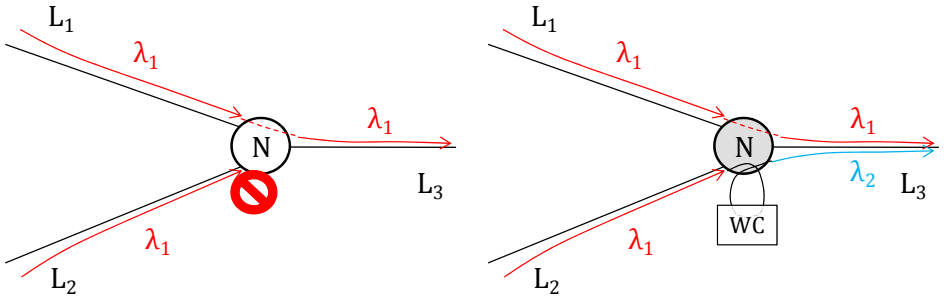


Figure 2.9: Wavelength conflict at network nodes: transparent node 2.9(a) vs. translucent node 2.9(b)

In general, there are two approaches to realize wavelength conversion, namely OEO-based wavelength conversion and all-optical wavelength conversion.

OEO-based WC employs two transponders to process the single carrier signal, the same way a 3R regenerator does. As mentioned in section 2.4.2, input and output wavelengths of an OEO device can be different. Wavelength converters can be either fixed or tunable. Specifically, the optical signal is first converted into electronic format, then the electronic signal is used to modulate a tunable laser to convert to an optical signal. Here, the tunable laser will be tuned to the wavelength that we want to convert to. OEO wavelength conversion is a quite mature technique.

On the second hand, all-optical wavelength conversion is a more advanced conversion technique. It does not need to convert a signal into electronic format then to optical format. All optical conversion in general utilizes some optical effects in optical components to realize wavelength conversion. These effects include Four-Wave Mixing (FWM), Semiconductor Optical Amplifier (SOA) saturation, cross-phase modulation (XPM), etc. All-optical wavelength conversion, are still immature and unavailable commercially in the meantime.

## 2.5 Corporate objectives of network operators

The strong competition in the telecommunication market is a great driver that triggers network operators to control network costs, and update used networking technologies in order to provide a guaranteed QoS to the end-users. Network operators strive today to find a fair compromise between minimizing the network's total cost of ownership and offering good QoS services at competitive prices. Offering customers more bandwidth for less money erodes profit margins. It also requires increasingly higher electrical power consumption and technology updates in order to maintain service quality. In this context, three inter-dependant drivers rule operators' network architecture and management policies.

### 2.5.1 QoS

An operator needs to keep up with the QoS required by its clients. In the remaining of this thesis, QoS provided to the end users by the carriers corresponds to both the availability of infrastructure (electrical and optical resources) and the QoT as observed at destination. We define below our perspective for availability and QoT:

- *Availability*: availability in core networks relies on Add/Drop electrical resources (a pair of Add/Drop transceivers and a pair of opaque interfaces at the EXC) and eventual 3R regenerators as well as on optical channels over the considered path's links.

- $QoT$: we define by QoT-admissible signals at destination, noisy optical signal whose

erroneous bits can be recovered by post-processing. In transparent networks, Forward Error Correction (FEC) is the most efficient technique in this purpose. Non-QoT-admissible signals, unfortunately, can not benefit from post-processing alone, in order to become recognizable. 3R regeneration at intermediate nodes is necessary in this case.

In summary, a connection request is rejected for either lack of optical and/or optical resources, or non-QoT-admissibility at destination. The higher the network resources' availability, the higher the potential income of the carrier. In this respect, an opaque network is the category of network that provides the best QoS, as long as traffic does not exceed the total capacity of the network given by the number of ports at the EXC and the number of wavelengths over each link. Transparent networks are unreliable, when QoS is concerned, for both availability and QoT issues, except under lower traffic loads and small networks *scenarii*.

### 2.5.2 Cost reduction

Network operators require not only lowest cost network components, but also lowest cost networks. As bandwidth demand increases, more equipment are purchased and more costs are added to the initial network cost. Figure 2.10 shows the relative growth of revenues and incremented costs with respect to bandwidth growth from year 2004 to year 2010 of British Telecom [7]. While revenues are slowly rising, incremental costs' growth is relatively fast which erodes profit margins. The first concern operators address in order to minimize networks' cost is choosing cost-effective networking technologies. Today's network cost is driven by huge increase in demand for bandwidth. At the core network, operators are trying to keep traffic at the lowest cost layer, *i.e.*, the optical layer. Indeed, the cost per transmitted bit is much lower using optical components than when using electrical devices. As we already mentioned, this is a main reason that urges operators and vendors to drive more and more transparency in networks.

Network cost includes capital and operational expenditures (CapEx and OpEx):

- CapEx cost is related to the operator's investment in equipment and software. Avoiding unnecessary network elements is an important issue in the design process of a network, in order to minimize CapEx costs. Also, replacing electrical equipment with equivalent optical equipment alleviates network's cost in terms of equipment price. Extending the optical reach would also reduce the need for OEO regeneration, and therefore, less costly 3R regenerators would be needed in the network.

- OpEx costs, on the other hand, include space expenses (equipment room rental) and power expenses (equipment feeding and cooling) as well as human intervention for supervision and maintenance. A part of the OpEx costs is proportional to the CapEx cost of equipment, such as a part of the power consumption and the maintenance of the equipment. Eliminating extra-expenses, *i.e.*, expenses relative to unnecessary

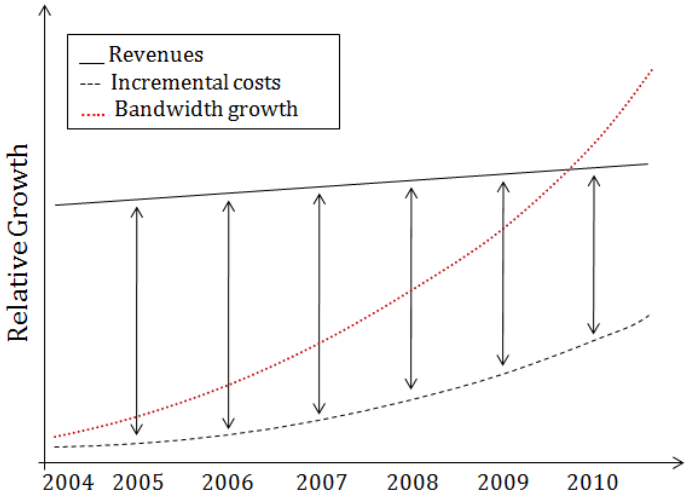


Figure 2.10: Network revenues vs. incremental costs of British Telecom network [7].

equipment also reduces OpEx. It is also essential to eliminate as much as possible manual configuration of the equipment. This requires an intelligent core network with flexible (dynamic) network equipment in order to present automatic network operation exploration and fast decision making (*e.g.*, fault detection, accurate failure localization and fast re-routing decisions, ...).

### 2.5.3 Eco-sustainability

The global focus on greenhouse gas (GHG) reductions aims to fight climate change. Bandwidth demand explosion resulted in more investment in network equipment which increased carbon footprint mainly at the access network. Operators and equipment vendors nowadays address these problems. Research teams are redefining network architectures in order to reduce power consumption. Technologies and operational solutions that reduce power requirements not only reduce the environmental impact, but also, network expenses. Extending the optical reach reduces the number of 3R regenerators as already mentioned in the previous section. By doing so, power consumption inherent to 3R regeneration will be reduced.

Globally, automated and dynamic resource allocation in optical networks enable to reduce the power consumption, where equipment are only activated when needed. Totally automated networks can switch on and off networking equipment according to the traffic load variation. sleeping modes are investigated for that purpose.

## 2.6 Reduction of EO and OE conversions

In this thesis, we propose solutions helping network operators attain their corporate objectives. Our research is focalized on the optical transport layer at the core network. We

propose to follow up the optical signal through its transmission over fiber and through network components while providing cost reduction, an acceptable QoS as well as ecological footprint reduction. Figure 2.11 depicts the network elements to be considered in the remaining of this thesis. Links between nodes are bidirectional (*i.e.*, made of two fiber links). The optical layer in our perspective includes fiber, optical components (amplifiers, optical switching core) as well as electrical components which perform OEO conversion.In the remaining of this thesis, we consider transponder-based components such as transceivers[9] and 3R regenerators to be part of the optical layer. In our study, we do not take into account dedicated wavelength conversion arrays, considering that 3R regenerators also provide this facility.

Figure 2.11 shows two established connection requests; the first one, from node $N_1$ to node $N_2$, is represented by a green dashed curve (considering that its lightpath has been assigned the green color), the second one (blue continuous curve) is from node $N_4$ to node $N_1$ and its lightpath has been assigned the blue color. We can distinguish the following statements:

- Each of these lightpaths begins at an add transponder at its source nodes, and terminates in a drop transponder at its destination nodes.
- The green lightpath's route is direct from $N_1$ to $N_2$. Network links shouldn't exceed the optical reach of the used optical components, this how, lightpaths are, at least, of guaranteed QoT at one-link paths.
- The blue lightpath's route is $N_4$-$N_3$-$N_1$. At its establishment over this route, the quality of this lightpath is estimated at destination. If QoT is inadmissible, then the lightpath should undergo 3R regeneration on an intermediate node (here: $N_3$). Therefore, at $N_3$, the signal is directed by the OXC towards the ADM that sends it, on its turn, to the 3R regenerator bank where it is renewed. In this illustration, the lightpath conserved its wavelength, which is not mendatory.

Even though EXCs feed the optical layer with its signals, we do not include it in the optical layer. We only consider modulated signals and their operation.

Table 2.1 summarizes relative price and Mean Time Before Failure (MTBP), as well as power consumption of components used at the optical layer [33]. From component costs and power consumption, the CapEx cost can be deduced. A part of the OpEx cost, on the other hand, can be deduced from MTBF, while the rest is proportional to the number of components to deploy (physical footprint of equipment in equipment rooms). Indeed, the lower the MTBF, the higher the inherent OpEx cost. What is important to mention here, is that comparison should take into consideration the relative number of transceivers and

[9]In this thesis, we consider the EXC having only grey interfaces to which are connected transponders for WDM adaptation. Historically, network components are bi-directional, an Add transponder is coupled to a Drop transponder, even if they serve different connections. We call a Drop transponder a *transmitter*, and an Add transponder a *receiver*. A transceiver contains both a transmitter and a receiver.

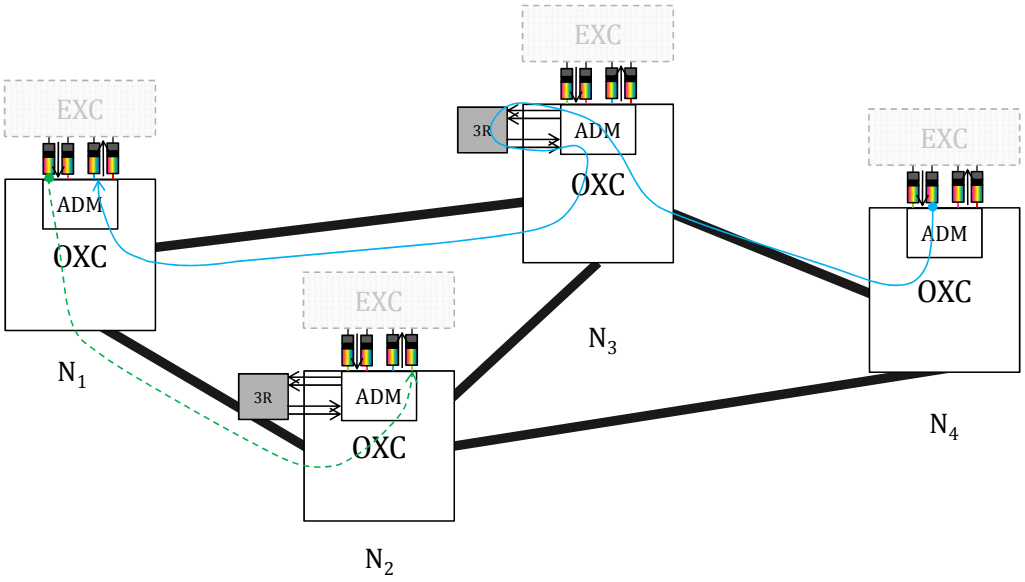


Figure 2.11: Optical transport layer.

regenerators that should be used at each node. Indeed, tens of transceivers (as well as 3R regenerators) can be used while only two WSS are used for Add/Drop. In this respect, the transponders are the most costly components in a WDM optical network, in terms of price and power consumption, whereas the rest of components are all-optical. The operator should seek reducing transponder usage. This concerns 3R regeneration (OEO conversion) and lightpath Add/Drop (OE and EO conversions). The first issue can be alleviated by intelligent routing and LH (ULH) systems deployment. Current optical networks employ transmission systems providing maximum transmission distance (MTD) of thousands of kilometers. Translucent networks, as aforementioned are designed to maximize all-optical switching and minimize transponder usage. Still, it is important to optimize regeneration at the translucent network. Inherently to the translucent node choice, the number of regenerators per node is also an important parameter to be considered.

Table 2.1: Cost of optical layer components

| Equipment | Relative Cost | Power consumption [W] | Relative MTBF[1] |
|---|---|---|---|
| Long reach 10G Transceiver | 1 | 30 | 1 |
| Double-stage EDFA[2] | 1.33 | 25 | 2 |
| $1 \times 4$ WSS | 2.35 | 30 | 1.2 |
| 3R regenerator | 1 | 30 | 1 |

[1] Mean Time Before Failure.
[2]Erbium-Doped Fiber Amplifier.

As for the second issue, only intelligent routing and signal grooming at the EXC can minimize the number of Add/Drop transponders to be deployed. Grooming, as mentioned earlier, multiplexes electrical signals (at current SONET/SDH layer) together to form a unique signal. The purpose of this operation is to optimize the usage of wavelength bandwidth. For example, let us consider the example illustrated in Figure 2.12 where three SONET/SDH signals having a data rate of less than a third of the optical channel capacity, each. Instead of sending them in three separate channels, using three Add transponders at the source node, it is preferable to groom them over one channel using just one transponder. The same operation also takes place at intermediate nodes.

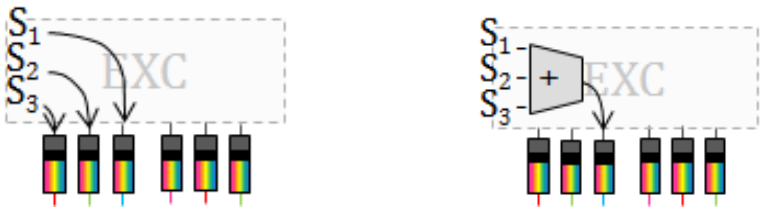


(a) Electrical signals transmitted without grooming.

(b) Electrical signals groomed together before transmission.

Figure 2.12: Grooming at the EXC

### 2.6.1 Grooming vs. 3R regeneration: the reason behind separate operation

Figure 2.13 illustrates a grooming operation of two signals at an intermediate node along their route. The green and blue lightpaths carry sub-wavelength capacity signals and pursue the same route after passage through the illustrated node. They are first dropped at the ADM, and their corresponding electrical signals are groomed at the EXC. The resulting signal is then added to the OXC after EO conversion (red signal). Finally, the red lightpath pursues the path pre-defined for the green and blue lightpaths. It is important to notice that once the blue and green lightpaths have passed the Drop transponders, the resulting SR signals are a clean replica of the carried data, all noise carried on the LR signals being eliminated. Extracting a signal to be groomed then reinserted to the optical layer restores its quality as if it were processed by 3R regeneration.

Indeed, grooming has a strong impact on QoT and power consumption. In this thesis, two subjects are discussed. In the first subject, only full-channel-capacity connection requests are considered. The establishment of such requests is concerned with the number of optical channels and the QoT. In the second subject, sub-channel-capacity connection requests are addressed. We only consider the possibility for grooming in their establishment.

This organization is encouraged by the fact that, given an observation period, real-network traffic is made of ($i$) a set of static connection requests which stay active over

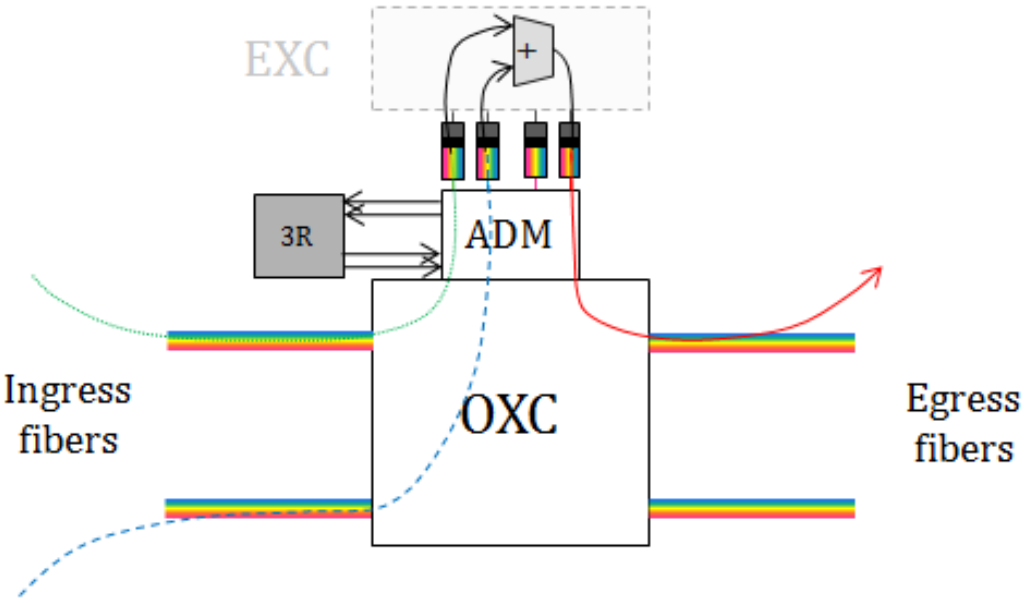


Figure 2.13: Grooming operation at an intermediate node.

the whole observation period, (*ii*) a set of scheduled connection requests which set-up and tear-down dates are known in advance, and (*iii*) a set of random connection requests. This latter traffic pattern includes bursty requests with dynamic and unpredictable start-up dates and activation periods. We do not consider random requests in this thesis. Under a given traffic load, the control plane proceeds to grooming before defining two separate connection establishment schemes. The grooming operation is essentially provided at the source/destination nodes of connection requests [104]. The resulting requests at the source nodes can be classified as: (*i*) requests with full (or almost) channel capacity use over the observation period (considered as static connection requests) and (*ii*) residual requests, having fine granularities (sub-channel capacity) and shorter active periods (considered as scheduled connection requests). An example of such traffic separation can be found in the next paragraph. Two procedures can then be exploited. On one hand, the first set of lightpaths can be transmitted in the network from source to destination without the need of intermediate grooming. Their corresponding Add/Drop transponders are unavoidable, thus, neglected in our study. Through their transmission, lightpaths undergo QoT follow-up over intermediate nodes in order to seek 3R regeneration needs (if any). The optimization of 3R regenerator placement (RP) in the network is commonly defined in the literature as *translucent network design*. Many research groups have proposed exact and heuristic-based solutions to this problem.

On the other hand, residual lightpaths at the source nodes need a centralized management at the control plane in order to provide an optimized RWA solution along with grooming at intermediate nodes. The number of necessary Add/Drop transponders to

add at these nodes can be optimized, especially under scheduled traffic schemes that allow for transceiver re-use at nodes (*resource sharing*). Resulting lightpaths can then be followed-up for QoT. Figure 2.15 distinguishes the two procedures.

**2.6.1.0.1 Illustrative example** The following example illustrates a traffic matrix in a 4-node mesh-network. We consider a symmetrical traffic matrix $\Delta$ in order to simplify the illustration. The observation period is divided into 5 time periods that have equal (or unequal) durations. Traffic requests between any two nodes are represented as a tuple made of the activation time (one or more successive periods) and of the requested capacity. Capacities are expressed in fractions of a full-channel capacity. In the following, only the upper triangle of the matrix is shown.

$$\Delta = \begin{pmatrix} & N_1 & N_2 & N_3 & N_4 \\ N_1 & \emptyset & \begin{pmatrix}(T_1-T_2,0.25)\\(T_2\dots T_4,0.5)\\(T_5,0.5)\\(T_3-T_4,0.5)\\(T_5,0.75)\end{pmatrix} & \begin{pmatrix}(T_1\dots T_3,0.25)\\(T_2,0.5)\\(T_2,0.5)\\(T_3\dots T_5,0.75)\\(T_4-T_5,0.5)\end{pmatrix} & \begin{pmatrix}(T_1-T_2,0.5)\\(T_2-T_3,0.25)\\(T_4,0.75)\\(T_3-T_4,0.5)\\(T_5,1)\end{pmatrix} \\ N_2 & \vdots & \emptyset & \begin{pmatrix}(T_5,0.75)\\(T_5,0.5)\\(T_1-T_2,0.5)\\(T_3-T_4,1)\\(T_3-T_4,0.25)\end{pmatrix} & \begin{pmatrix}(T_1,0.5)\\(T_2\dots T_4,0.5)\\(T_5,0.75)\end{pmatrix} \\ N_3 & \vdots & \vdots & \emptyset & \begin{pmatrix}(T_1,1)\\(T_4,0.5)\\(T_2-T_3,0.75)\\(T_4-T_5,0.5)\end{pmatrix} \\ N_4 & \vdots & \vdots & \vdots & \emptyset \end{pmatrix}$$

Figure 2.14 depicts the incremental capacity request over the observation period for traffic that needs to be established from node 1 to node 2. Different colors are given for each traffic request represented in matrix $\Delta$. It is clear that all requests except one (represented by a white stripe) can fit into a single channel over the whole observation period by means of electrical grooming. In this respect, the traffic from node 1 to node 2 can macroscopically be represented by two traffic requests: (*i*) a static (permanent) traffic request with a full-channel capacity, and (*ii*) a scheduled traffic request active in time period $T_5$ and requiring 75 % of a channel capacity.

Traffic grooming at the nodes allows us to simply represent $\Delta$ as the sum of a permanent

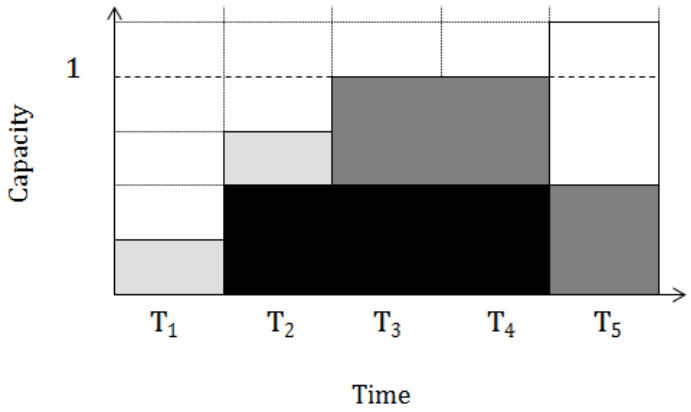


Figure 2.14: Incremental traffic from node 1 to node 2.

lightpath demands[10] (PLDs) matrix, and a scheduled demand[11] matrix as follows:

$$\Delta = \begin{pmatrix} - & N_1 & N_2 & N_3 & N_4 \\ N_1 & \emptyset & 1 & 1 & 1 \\ N_2 & \vdots & \emptyset & 1 & 1 \\ N_3 & \vdots & \vdots & \emptyset & 1 \\ N_4 & \vdots & \vdots & \vdots & \emptyset \end{pmatrix} + \begin{pmatrix} - & N_1 & N_2 & N_3 & N_4 \\ N_1 & \emptyset & \Big((T_5, 0.25)\Big) & \begin{pmatrix}(T_2, 0.25)\\(T_4 - T_5, 0.25)\end{pmatrix} & \Big((T_4, 0.25)\Big) \\ N_2 & \vdots & \emptyset & \Big((T_3 \dots T_5, 0.25)\Big) & \emptyset \\ N_3 & \vdots & \vdots & \emptyset & \emptyset \\ N_4 & \vdots & \vdots & \vdots & \emptyset \end{pmatrix}$$

The PLD matrix represents only the number of lightpaths to be established between each node pair, because the time notion is useless in this context.

## 2.7 Research *scenarii*

In this thesis, we first propose a translucent network design solution, offering 3R regenerator optimized placement with respect to corporate CapEx and OpEx costs, and QoS constraints. In this first part, we consider permanent traffic requests. These requests are supposed resulting of *pre*-grooming at the sources. Therefore, they are of full-channel capacity.

Our aim is to establish convenient lightpaths to carry these requests, with minimum rejection ratio, while minimizing inherent CapEx and OpEx costs. Optimizing QoT necessitates to invest in 3R regenerators that contribute to CapEx and OpEx. The QoS constraint urges operation to insert 3R regenerators in order to provide flexible network capacity (allowing WC) and interpretable data at reception (renewing impaired signals).

[10] A full channel is required for the establishment of a lightpath. A permanent request (demand) is active the whole observation period.

[11] We do not call them "scheduled lightpath demands" because they can have granularities that are not necessarily equal to a channel capacity.

This tends to add more equipment to deploy and operate, while cost reduction aims to reduce them. The compromise between the two constraints results in optimum placement (in node choice and in number) of 3R regenerators. The effect on power consumption is also of a certain importance in comparison to opaque networks.

In its second part, this thesis focalizes on Add/Drop transponders (transceivers), their number, their types and their usage. Networks are converging to a more dynamic and flexible infrastructure. Cost and power consumption constraints have urged the minimum investment in network components in order to maximize network capacity use in minimum fees and ecological effects. According to the latest equipment on the shelves, it is possible to transmit on the same fiber different optical signals operating at different data rates (1, 10, 40 Gbps...). Transceivers with different data rates require, of course, different power consumptions. Traffic requests can be of different characteristics (schedule, capacity demand, ...). A dynamic network is adaptable to the offered load. Multiple data rate transceivers allow minimizing misused capacity that can be caused by the usage of unified data rates transceivers, where higher data rates transceivers are often under-used and low data rates transceivers are used in great numbers. In this part, we consider the case of scheduled traffic, where traffic requests are characterized with their set-up (start) and tear-down (end) dates. This type of requests is common in nowadays' network services (Optical Virtual Private Network (OVPN), HDTV services, and services accessing storage and calculation in a grid network environment, ...). Another characteristic is added to the time schedules of requests: multiple data rate requirements. In other terms, time and bit rate granularities are considered in this second part of the thesis. These characteristics widen the complexity degree of designing an optical network with multiple data rate transceivers.

This part of the thesis considers a transparent network, and proposes to provide the numbers, types and activity periods of transceivers at each node of the network, under a given scheduled traffic load. The main purpose of this part is to minimize the total power consumption of the optical network. A permanent traffic load with multiple capacity requirements can also be treated by the proposed method.

This thesis, distinguishing the two procedures stated in the previous section, can be considered as a step towards considering the two procedures together. Future studies can rely on the second part's results in order to introduce QoS to guarantee the establishment of routed requests.

Figure 2.15: Separate operation of traffic requests at the control plane.

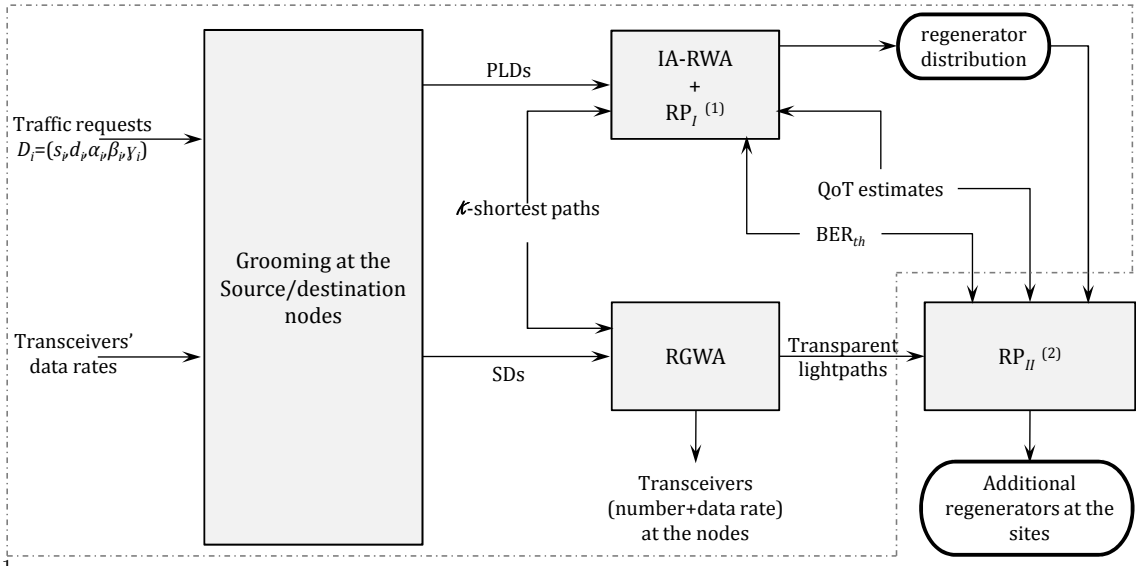


[1] RP$_I$ stands for the operation of regenerator placement starting from a transparent network. It provides the choice of regeneration sites and the number of regenerators in each.
[2] RP$_{II}$, inserts regenerators respecting the regeneration sites of the output network of RP$_I$.

# Part I

# Cross-Optimization for Translucent WDM Network Design

# Chapter 3

# Quality of transmission in core networks

## 3.1 Introduction

The optical fiber is not an ideal transmission medium. Signals propagating through fiber-links undergo various degradations affecting their power intensity and their time and frequency properties. Noise also tends to accumulate on the signal during its propagation. There are network components dedicated to cope with the losses and distortions applied to the signal. These components are not idealistic, but help extend the optical reach.

The Quality of Transmission (QoT) of a signal at its destination is of very high importance, because it conditions the acceptability of the signal at the receiver. A minimum QoT is required in order to recover the transmitted signal. QoT depends on the impairment effects present on the transmission line. In order to be able of affecting a lightpath to a data stream, QoT should be estimated at destination with respect to the line impairments. In the following, we first present the different equipment constituting a line transmission. Afterwards, we summarize the different linear and non-linear effects affecting the signal's QoT. Finally, we present a QoT tool called BER-Predictor that we use in this thesis to estimate the QoT of lightpaths.

## 3.2 A point-to-point WDM transmission system: taxonomy

In the following, we present the key elements enabling optical networking.

### 3.2.1 Optical cross-connects

OXCs are deployed at the nodes to ensure the routing of a wavelength from one direction (fiber-link) to another. The functionality of an OXC can be summarized by three essential tasks, regardless of the underlying technology:

- Demultiplexing (demux) of composite signals arriving from ingress links to the node. Indeed, we can consider that all composite signals arriving to a node are demultiplexed into individual signals (wavelengths) that are directed to the optical switch.

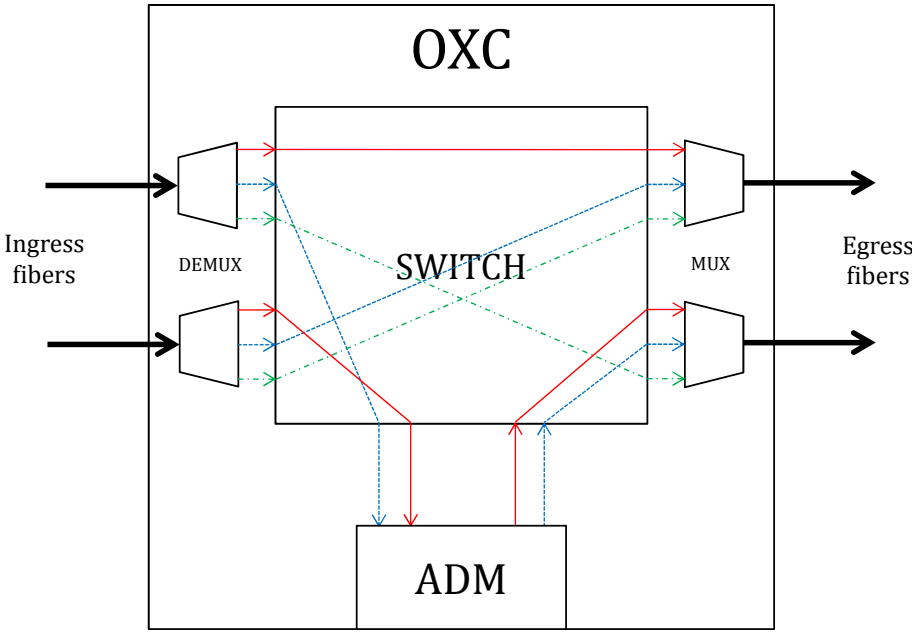


Figure 3.1: Block representation of an OXC.

- Multiplexing (mux) of individual signals to form a composite signal, in order to be transmitted over an egress link.

- Optical switching of wavelengths, where each wavelength (originating at the ADM (Add mode), or from an ingress link, after demux) is routed towards its convenient direction (*i.e.*, the mux related to the next link on the wavelength's path, or to the ADM in order to be dropped to the upper electric layer).

It is worth mentioning that, in MEMS-based OXCs, demux and mux functionalities are external to the switch itself, while they are implicitly incorporated in WSS-based OXCs. Since it is most encouraged to deploy this latter type of OXCs [41], and because it does not create a major difference, we consider these functionalities intrinsic to the OXC. Figure 3.1 shows a simplified illustration of the demux, switching and mux functionalities in an OXC.

Considering transmission over fiber-links, certain in-line components attached to the fiber are necessary to help the signal resist to losses inherent to the fiber medium. We consider Standard Single Mode Fiber (S-SMF) in all this thesis, since it is the most commonly used in today's networks.

In core mesh networks, nodes have generally a connectivity degree superior to 2. Under transparent or translucent network assumptions, the optical switching fabric needs to present a cross-connect-like architecture in order to provide switching from/to any direction. Two main technologies are used for this purpose, namely, Optical-Cross-Connect based on Micro-Electro-Mechanical Mirrors Systems (MEMS-based OXC) and OXC based on wavelength-selective switches (WSS-based OXC).

#### 3.2.1.1 MEMS-based OXC

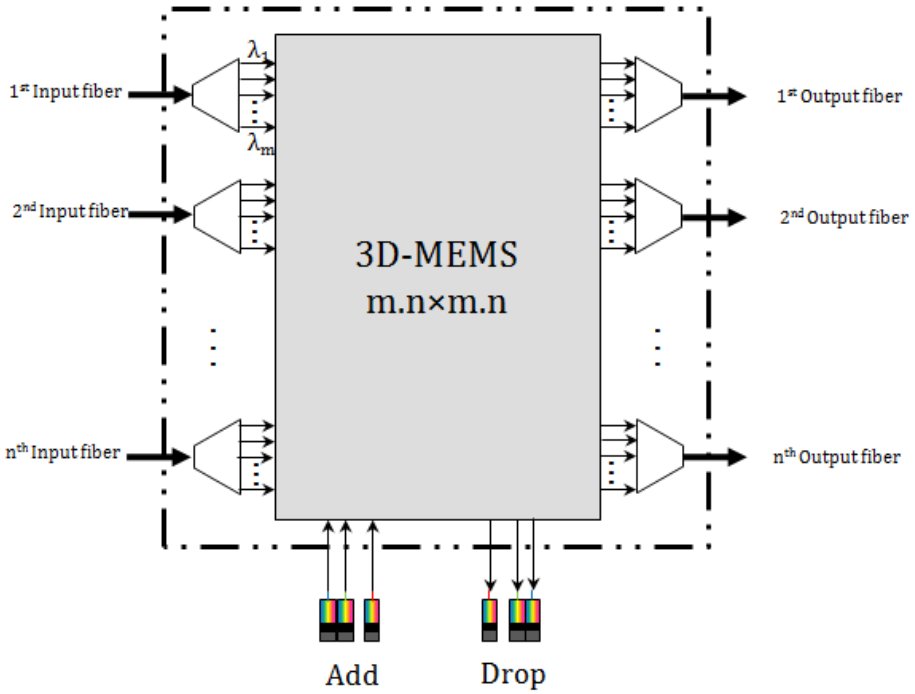


Figure 3.2: 3D MEMS-based OXC.

MEMS technoloy has emerged as a major candidate for building switches able to handle a large number of wavelengths ($> 100$). MEMS technology is based on high-precision components (micro-mirrors) providing reliable high-speed switching of optical signals. OXCs [30, 66]. Figures 3.2 and 3.3 illustrate two OXC architectures based on MEMS technology. 2D and 3D MEMs-based architectures first demultiplex incoming composite signals, then operate the convenient switching before proceeding to multiplexing output signals. Mux and Demux are independent modules in this architecture. While the 2D-MEMS-based OXC seems to offer a modular architecture, the 3D-MEMS-based OXC, although very promising and simple to implement, acts like a single point of failure. needed before the two switching cores, as well as $m \cdot n$ $1 \times 2$ couplers after the switching cores, not to mention the number of fibers to connect the couplers/splitters to the switching cores.

#### 3.2.1.2 WSS-based OXC

In our consideration, node architecture is colorless and directionless, *i.e.*, allows for routing any wavelength in any direction [77]. Node directions include bidirectional links as well as the Add/Drop module at the node. Figure 3.4 illustrates a bloc diagram of a WSS-based OXC. A WSS is a subsystem that acts in two steps. First, it acts like a tunable Demux that selects a set of wavelength from each incoming signal, then it acts like a Mux multiplexing the selected sets into one composite signal at its output. Using WSS devices, the structure and implementation of the OXC can be greatly simplified. A major feature provided by

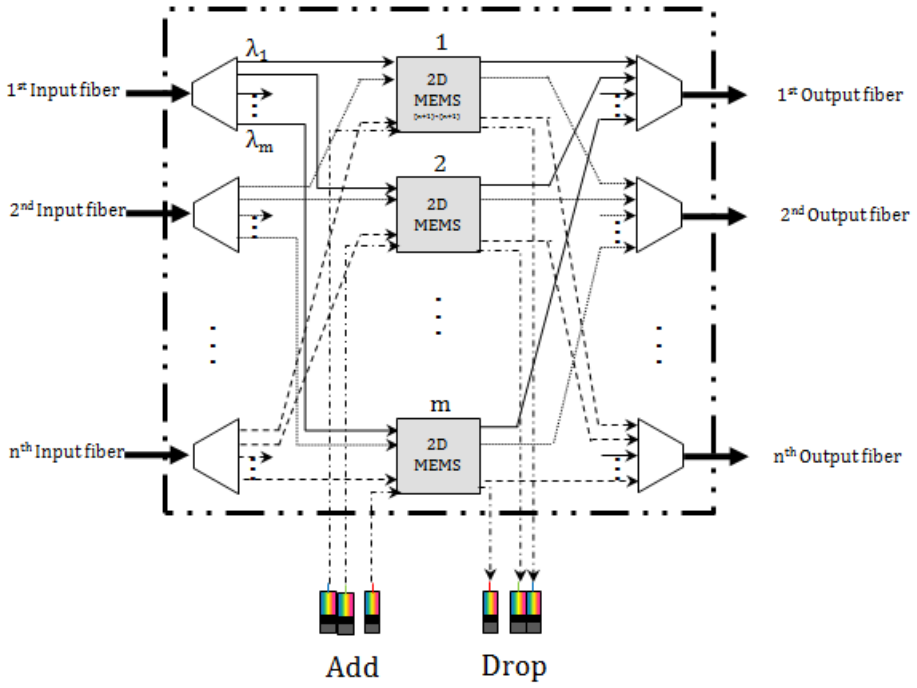


Figure 3.3: 2D MEMS-based OXC.

this architecture is multicasting. In fact, this architecture relies on a broadcast (at the splitters) and select (at the WSS) scheme.

In the three figures, we outlined our definition of OXC presented in the simplified presentations of transparent and translucent nodes architecture, provided in Figures 2.5 and 2.7.

### 3.2.2 Optical amplifiers

The passage of an optical signal through the fiber or/and other network elements such as OXCs, induces power loss which weakens the signal. Because of the accumulation of losses over the propagating signal, amplification is needed in order to maintain a detectable power level. In this respect, optical amplifiers are deployed at given locations over the fiber links, as well as at the output of the nodes. Three types of optical amplifiers have been deployed for optical transmission.

Semiconductor Optical Amplifiers (SOAs) are laser diodes having fiber attached to both ends. They amplify any optical signal that comes from either fiber and transmit the amplified signal out of the second fiber. The main drawbacks of this type of amplifiers are the inherent high-coupling losses and high noise figure.

Erbium-Doped Fiber Amplifiers (EDFA) are the common type of amplifiers used in the networks. EDFAs are segments of fiber, doped with Erbium which atoms are excited by a pump signal into a higher energy level. The ingress data signal is then amplified by stimulating the excited atoms that release photons. In-line amplifiers of this type are made of two EDFA stages (Cf. Figure 3.5). At the inter-stage of such amplifiers,

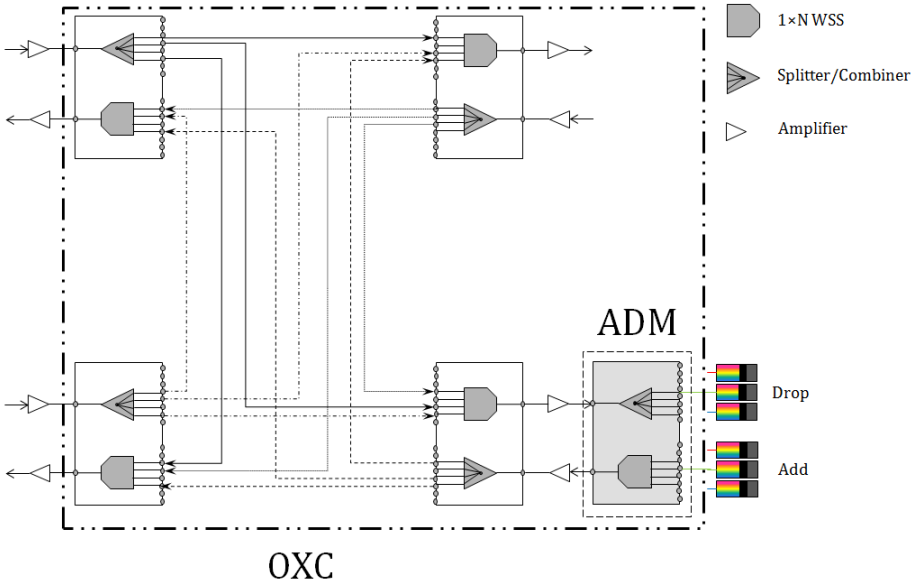


Figure 3.4: WSS-based OXC.

a Dispersion Compensating Module (DCM) is used to cope with dispersion induced by transmission (Cf. Section A.1.3.0.3). A fiber-link bears a number of double-stage in-line amplifiers. This number is related to the physical length of the link. A *span* is a fiber section delimited by two amplification sites. Spans' lengths are given by a compromise between the signal's degradation, the type of amplifier and the total cost inherent to the deployment of in-line amplifiers [94]. In average, a span's length is generally around 80 km. Certain physical limitations inherent to amplification through EDFAs are to be considered

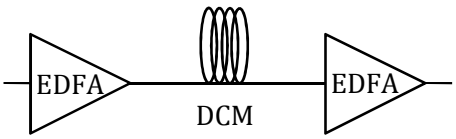


Figure 3.5: Double-stage in-line amplifier including a DCM.

in network operation:

- Unequal gain spectrum of EDFAs: Figure 3.6 depicts the gain spectrum of an EDFA [20]. Indeed, EDFAs amplify signals carried by the different wavelengths unequally. In addition, the more spans a composite signal traverses, the more uneven wavelengths' powers become. The difference in power levels between the different channels (wavelengths) of a composite signal has many consequences. On one hand, channels presenting weak powers at the output of an EDFA amplifier will become even weaker (low values of the Optical Signal-to-Noise Ratio (OSNR)) due to transmission impairments. Weak channels are much sensible to Cross-talk than channels having higher values of OSNR (Cf. Section A.2.5). On the second hand, channels presenting higher powers are subject to non-linear impairments over the transmission

line.

- Amplification of noise: EDFAs do not distinguish noisy signals from *clean* signals. Hence, noise is amplified along with the signal that carries it.

- Amplified Spontaneous Emission (ASE): Erbium doping is an active field inside the EDFA. It spontaneously emits photons in all directions causing noise added to the proper signal. When the signal passes through cascaded EDFAs, the noise caused by spontaneous emission is amplified resulting in an ASE noise. ASE is a serious transmission impairment causing the OSNR at destination to be severely degraded.

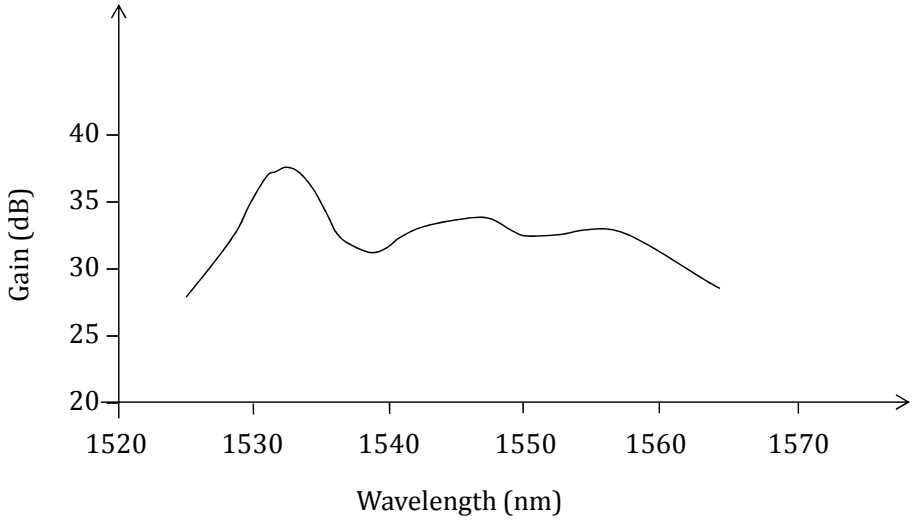


Figure 3.6: Gain spectrum of an EDFA for an input power of -40dBm [20].

Pre-line amplifiers (booster) and post-line amplifiers are also EDFA amplifiers deployed at the nodes. Boosters are deployed at the egress directions of the nodes for reach extension, while post-line amplifiers are deployed to compensate for losses in the demux.

Raman amplifiers are also used in networks but much less frequently than EDFA, *i.e.*, over longer spans. They have lower noise figure and Raman amplifiers are used to complement EDFA performance in LH and ULH networks. Raman amplifiers have lower noise figure and handle wider bands than EDFAs.

### 3.2.3 Gain equalization

Due to the infeasibility of flat gain spectrum amplifiers[1], Dynamic Gain Equalizers (DGE) are deployed in order to minimize the power difference between channels. DGEs are employed every $N$ in-line amplifiers, where $N$ depends on the transmission line's performance with respect to channels' power levels. A DGE placed after the post-line amplifier is important to alleviate cross-talk effect at the node. At the egress directions of a node,

[1] 100% flat gain spectrum amplifiers are not feasible. For ULH transmission, amplifiers providing gain flatness to the limit of 0.5 dB are deployed.

channel powers are equalized beforehand inside the node, since each optical channel has its own transmission history; not all channels are originating at the considered node. Being dynamic, gain equalizers can adapt to changing in the transmission system (aging of components, use of more channels...). Optical Performance Monitoring (OPM) deployed after the DGE device, controls the optical power of channels at the output of the amplifiers.

Figure 3.7 shows an overview of a point-to-point WDM transmission line. DGE devices are deployed each (N-1) spans.

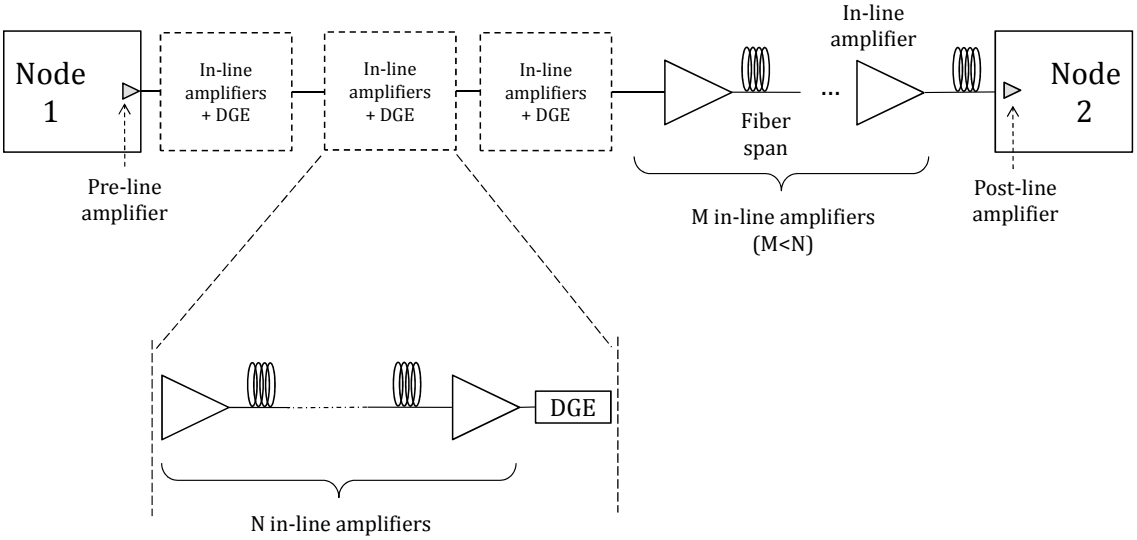


Figure 3.7: A schematic diagram of transmission components over a single link.

## 3.3 Physical Impairments

As the optical signal propagates through the optical fiber links and passive or active optical components, it encounters many impairments that affect its intensity level not to mention its temporal, spectral and polarization properties.

There are different factors behind physical layer impairments and their amplitude. Among these factors, we mention: (*i*) equipment and fiber characteristics, (*ii*) network size and (*iii*) network's management and operation.

Physical layer impairments can be classified into linear and non-linear effects. Linear impairments are independent of the signal power and affect each of the wavelengths individually, whereas non-linear impairments not only affect each optical channel individually, but also cause disturbance and interference between all channels.

Impairments are discussed in Appendix A.

## 3.4 Signal Regeneration

As aforementioned in Chapter 2, after an optical signal is transmitted for a long distance, its quality of transmission (QoT) is affected by all the physical impairments cited in the

previous section. There are three signal properties that can be "renewed" via regeneration: power level, shape and clock. According to these properties, we can state three regeneration types: 1R regeneration, 2R regeneration and 3R regeneration.

1R regeneration includes pre-line amplifiers, in-line amplifiers and post-line amplifiers. It provides Re-amplification of signal power. As mentioned earlier in Section 3.2.2, the amplifier introduces spontaneous emission noise, and amplify the noise already carried by the optical signal. 2R regeneration, in its turn, provides not only Re-amplification of the signal's power, but also Re-shaping (suppression of noise and fluctuation). Finally, 3R regeneration includes Re-amplification, Re-shaping and Re-timing of signals. Re-timing synchronizes the signal to its original bit timing pattern or bit rate.

3R regeneration essentially produces a "fresh" copy of the signal at each regeneration step, allowing the signal to go through a very large number of regenerators. However, it eliminates transparency to bit rates and the framing protocols, since acquiring the clock usually requires knowledge of both of these. Some limited form of bit rate transparency is possible by making use of programmable clock recovery chips that can work at a set of bit rates that are multiple of one another. So far, OEO conversion is the most popular and mature technique for accurate 3R regeneration. The fundamental principle of OEO regeneration is to convert an optical signal into electronic format first so that the time and shape are restored, and then to use the electronic signal to modulate an optical laser that generates a new optical signal (Cf. Section 2.4.2).

OEO 3R regeneration is based on transponders. The input carrier can be converted to another wavelength of the spectrum. We distinguish two kinds of regenerators: (*i*) fixed regenerators, where input and output carriers are fixed before deployment[2] and (*ii*) tunable regenerators. In the latter type, the regenerator is adaptable to the input carrier, it detects its carrier wavelength thanks to an array of pre-tuned photo-detectors. When the signal is recovered, it's either modulated (by means of a tunable laser) at its input carrier (without WC), or at another carrier (by means of an array of pre-tuned lasers) before retransmission.

A regenerator sends feedback to the control and management module of the network. It helps the network monitor faults and failures by sending control sequences and checksums, although it can not explore the useful data carried by the signal. In this respect, a regenerator has no access to the finest granularities of groomed signals that constitute the signal going through it.

There are two types of 3R regeneration from a placement point of view: (*i*) *in-line* 3R regeneration, used on links of ULH networks exceeding the optical reach provided by deployed systems and (*ii*) *in-node* 3R regeneration, used in network nodes. In our study, we do not consider in-line 3R regeneration. In in-node 3R regeneration, regenerators are deployed by pools (banks) at nodes presenting regeneration facility, *i.e.*, translucent nodes in a translucent network architecture.

[2]The input and output wavelengths can be different.

## 3.5 Optical 3R regeneration

Beside the OEO technique, it is also possible to carry out 3R regeneration in all-optical domain without converting optical signal into electronic signal. The advantage of all-optical 3R regeneration is its bit-rate transparency, and the absence of the bottleneck inherent to electronic modulation. However, the all-optical 3R regeneration technique is currently not mature, not to mention that it is still very expensive.

State-of-the-art all-optical 3R regeneration rely on many non-linear effects in order to re-amplify, re-shape and re-time the optical signals.

SPM in a highly non-linear fiber, results in channel spectrum broadening. An optical filter selects a dominant spectral peak, where noise in '0'-bits is removed and reduced considerably in '1'-bits. Adding a modulator insures the recovery of the signal's clock [76, 65].

XPM is also used for 3R regeneration. An optical signal (on $\lambda_1$) impaired by transmission, and an extracted optical clock (on $\lambda_2$) having a narrower pulse width than that of the signal are incident to a highly non-linear fiber. A polarization controller (PC) helps maximize the XPM effect between the two kinds of pulse. A bandpass filter (BPF) placed behind the fiber has a narrower bandwidth than the spectral width of the clock pulse, and its center wavelength is fixed to $\lambda_2$. This system results in a reverse bit pattern and a wavelength conversion [91].

Other all-optical 3R regenerators based on semi-conductor devices are also proposed in literature [105]. All-optical 3R regeneration, is emerging, but has yet to become commercial.

## 3.6 BER estimation

### 3.6.1 $\mathcal{Q}$ factor

We define by *lightpath* an optical signal carried by a given wavelength and following a given route from source to destination. Lightpath establishment is ruled by two conditions:

- Resource availability: indeed, not only the availability of a transmitter at the source node and of a receiver at the destination node providing the same wavelength is important, the vacancy of this wavelength over the links of the physical path is also of same importance.
- QoT at destination: in order to recover the signal at destination, the QoT of the lightpath should meet the receiver's sensitivity.

The QoT in digital networks is represented by the Bit Error Rate (BER) at destination. It reflects the number of erroneous bits found in the recovered binary sequence, as a result of misinterpretation of bits affected by too many noise and distortion. The higher the QoT, the lower the BER. Usually, a transmission system is characterized by a given threshold

for BER (or QoT). A signal is said of acceptable QoT (*resp.*, BER) if the measured QoT (*resp.*, BER) at destination is higher (*resp.*, less) than the corresponding threshold.

The typical values of the BER threshold are comprised between $10^{-15}$ and $10^{-9}$.

Forward Error Correction (FEC) codes are used to control errors over non-idealistic transmission systems. Their use provides a certain margin for the QoT threshold.

Usually, a quality factor ($\mathcal{Q}$ factor) is used to estimate the BER. The $\mathcal{Q}$ factor provides the quality of the bit stream at the reception regardless of its quality at the transmission. Consider that $I_1$ (*resp.* $I_0$) is the average photocurrent measured at the destination. It is given by averaging the photocurrents relative to the decisions where the corresponding bit is considered '1' (*resp.* '0') according to a given threshold photocurrent $I_{th}$[3]. $\sigma_1$ and $\sigma_0$ are their standard deviations. The $\mathcal{Q}$ factor can be expressed by the following equation:

$$Q = \frac{I_{th} - I_0}{\sigma_0} = \frac{I_1 - I_{th}}{\sigma_1} \tag{3.6.1}$$

'0' bits and '1' bits are equiprobable, the BER can hence be expressed by the following equation:

$$BER = \frac{1}{2}[P(0,1) + P(1,0)] \tag{3.6.2}$$

where P(0,1) (*resp.*(1,0)) is the probability that a '1' bit (*resp.* '0' bit) is mistakenly identified as a '0' bit (*resp.* '1' bit).

Noise is considered having a Gaussian probability density function, the above conditional probabilities can then be expressed by Equations (3.6.3) and (3.6.4), where $erfc$ stands for the complementary error function (Cf. Equation (3.6.5)).

$$P(0,1) = \frac{1}{\sigma_1\sqrt{(2\pi)}} \int_{-\infty}^{I_{th}} exp\left(-\frac{(I-I_1)^2}{2\sigma_1^2}\right) \mathrm{d}I = \frac{1}{2} erfc\left(\frac{I_1 - I_{th}}{\sigma_1\sqrt{(2)}}\right) \tag{3.6.3}$$

$$P(1,0) = \frac{1}{\sigma_0\sqrt{(2\pi)}} \int_{I_{th}}^{\infty} exp\left(-\frac{(I-I_0)^2}{2\sigma_0^2}\right) \mathrm{d}I = \frac{1}{2} erfc\left(\frac{I_{th} - I_0}{\sigma_0\sqrt{(2)}}\right) \tag{3.6.4}$$

$$erfc(x) = \frac{2}{\sqrt{\pi}} \int_x^{\infty} exp(-y^2)\mathrm{d}y \tag{3.6.5}$$

From Equations (3.6.2), (3.6.3) and (3.6.4), we can deduce the BER depending on $I_{th}$:

$$BER = \frac{1}{4}\left[erfc\left(\frac{I_1 - I_{th}}{\sigma_1\sqrt{2}}\right) + erfc\left(\frac{I_{th} - I_0}{\sigma_0\sqrt{2}}\right)\right] \tag{3.6.6}$$

The optimal value of $I_{th}$ minimizing the BER can be approximated by Equation (3.6.7) [40].

$$I_{th} = \frac{\sigma_0 I_1 + \sigma_1 I_0}{\sigma_0 + \sigma_1} \tag{3.6.7}$$

From Equations (3.6.1) and (3.6.7), we deduce:

$$\mathcal{Q} = \frac{I_1 - I_0}{\sigma_1 + \sigma_0} \tag{3.6.8}$$

[3]If $I \geq I_{th}$ then the bit is a '1' bit, otherwise, it is a '0' bit.

and from Equations (3.6.6) and (3.6.1), the BER can be expressed in terms of $\mathcal{Q}$ factor:

$$BER = \frac{1}{2} erfc\left(\frac{\mathcal{Q}}{\sqrt{2}}\right) \tag{3.6.9}$$

The $\mathcal{Q}$ factor is also related to the OSNR according to Equation:

$$\mathcal{Q} = \sqrt{\frac{B_o}{B_e}} \cdot \frac{2 \cdot OSNR}{1 + \sqrt{1 + 4 \cdot OSNR}} \tag{3.6.10}$$

where $B_o$ and $B_e$ are the optical and electrical bandwidths of the receiver [97].

In a first approximation, $\mathcal{Q}$ factor depends linearly on the OSNR (both expressed in dB) within a reference bandwidth such as 0.1 nm for common OSNR values (10 to 23 dB) [67]. The condition for a bit stream to be comprehensible at destination is to have an OSNR value equal to or higher than the threshold OSNR ($OSNR_{th}$).

The physical impairments cited in Section 3.3 induce penalties on the OSNR of the signal at the reception. Hence, the OSNR at destination takes into account, not only the ASE of cascaded EDFA amplifiers at the transmission line, but also penalties relative to linear and non-linear impairments, present on the fiber-links and at the traversed nodes (Cf. Equation (3.6.11)). The analytical relation between the OSNR and the penalties caused by the physical impairments has been derived from physical equations and experimental measurements, through interpolation [80, 67, 68].

$$OSNR = OSNR_{ASE} - OSNR_{pen,l} - OSNR_{pen,nl} \tag{3.6.11}$$

### 3.6.2 BER-Predictor

In our research work, we have used a tool called "BER-Predictor" for the estimation of the QoT of lightpaths [88]. BER-Predictor provides an estimate of the BER (OSNR, and $\mathcal{Q}$ factor) corresponding to a given lightpath, at its destination. BER-Predictor considers the simultaneous impact of four main impairments: ASE, CD, PMD and Kerr effect, represented by its resulting non-linear phase-shift ($\Phi_{nl}$).

BER-Predictor considers a network topology wherein each link respects the bloc-diagram given in Figure 3.7. The estimation of the QoT considers the path upon which the signal propagates as a succession of network components (OXC, fiber, amplifier...). According to this, the impairments accumulate through their passage by each component, and finally, at the destination, OSNR penalties corresponding to the impairment values are calculated and added to the main OSNR of the lightpath. The values of the BER and the $\mathcal{Q}$ factor can then be deduced.

The input of BER-Predictor are first, the network topology, providing detailed component succession on the links, their lengths and their spans' lengths, their type (SSMF, LEAF[4], ...), as well as the technology used at the switching fabrics (WSS, MEMS). The second input of BER-Predictor is the lightpath (wavelength + physical path) that needs

[4]LEAF is a Non-Zero Dispersion-Shifted Fiber (NZ-DSF) where the non-zero dispersion point is outside the spectral range used for communication.

a QoT estimation at its end. The lightpath input of BER-Predictor are all-optical lightpaths, they by-pass intermediate nodes by transiting only through their OXC.

**3.6.2.0.1 Penalties over the links** BER-Predictor considers two different modes of the fiber: flat mode and non-flat mode. In the flat mode, impairments are independent of the wavelength, same as the amplifier's spectral gain. In this case, BER-Predictor consider the impairments values at the central wavelength (1550 nm).

In the non-flat mode, CD, $\Phi_{nl}$ and attenuation over the fibers (transmission fiber and DCF) are wavelength-dependent, and respect the fibers' specifications. At the amplifier level, the spectral gain is also wavelength-dependent, not to mention ASE noise.

For each span of the fiber, CD, PMD, $\Phi_{nl}$, and the attenuation are calculated at its end. Table 3.1 presents the values of physical impairment SMF and DCF fibers at the central 1550 nm wavelength [15].

| | Loss (dB/km) | CD (ps/nm.km) | PMD (ps/$\sqrt{\text{km}}$) |
|---|---|---|---|
| SMF | 0.23 | 17.1 | 0.1 |
| DCF | 0.6 | -92 | 0.19 |

Table 3.1: Physical impairments over SMF and DCF.

As for amplifiers, we distinguish two modes of impairment calculation. If the amplifier is a booster, or a post-line amplifier, then the power of the signal is calculated at the output of the amplifier (with respect to the flatness or non-flatness of the system). The power of ASE is also calculated, in order to update the OSNR after the passage through the amplifier.

In the case of in-line amplifiers, two EDFA amplifiers are considered in two stages, separated by a DCF. For each of the two EDFAs, power calculation is the same as in the last mode. And the gain of EDFA, is chosen so as to compensate for losses (in the OXC for the booster, in the fiber for the first stage EDFA and the post-line amplifier, and in the DCF for the second stage EDFA). Table 3.2 presents the noise figure in booster and in-line amplifiers [88].

| | NF (dB) |
|---|---|
| Booster | 6 |
| In-line amplifier | 5.25 |

Table 3.2: Noise Figures of booster and in-line amplifiers.

**3.6.2.0.2 Penalties through the switch** BER-Predictor considers the OXC as an attenuator where the impairments are due to the migration in the node. The inherent impairments closely dependent on the deployed technology (whether WSS or MEMS-based OXC).

Three modes of impairment-prediction exist at the OXC, depending on whether the considered node is the source node of the lightpath (Add mode), an intermediate node over

the lightpath (transit mode) or the destination node of the lightpath (Drop mode) [88, 15]. Tables 3.3 and 3.4 show the values of impairments in MEMS-based OXCs and WSS-based OXCs, respectively.

| | Loss (dB) | CD (ps/nm) | PMD (ps) |
|---|---|---|---|
| Transit | 18 | ±20.25 | 0.43 |
| Add/Drop | 14 | ± 10.25 | 0.3 |

Table 3.3: Physical impairments in a MEMS-based OXC.

| | Loss (dB) | CD (ps/nm) | PMD (ps) |
|---|---|---|---|
| Transit | 12.8 | ±10 | 0.4 |
| Add | 9.3 | ± 10 | 0.4 |
| Drop | 12.5 | ± 20 | 0.4 |

Table 3.4: Physical impairments in a WSS-based OXC.

## 3.7 Conclusion

In this chapter, we have first illustrated the optical components deployed in carriers' networks. We have closely examined the different successive stages a lightpath undergoes while propagating over the fiber-links. We have also enumerated the linear and non-linear physical impairments that affect the signal's quality during its propagation, limiting the optical reach in optical networks. Their impact has to be alleviated in order to extend the optical reach. Amplifiers are deployed to compensate for power loss. Similarly, dispersion compensating modules compensate for dispersion over the fiber. Loss and dispersion compensating components, alone, do not systematically guarantee an admissible signal quality at destination. Amplifiers necessitate gain equalization because of their wavelength-dependent gain, in order to reduce non-linear effects that can be caused due to optical channel power disparities. Optical amplifiers also add and amplify noise.

In a dedicated section, we have briefly described the relation that exists between the different physical impairments and the optical signal-to-noise ratio. The accumulation of physical impairments on a transmission line adds penalties to the OSNR of each lightpath.

In this chapter, we also described a tool called BER-Predictor, that enables the evaluation of the BER (OSNR/$\mathcal{Q}$ factor) of lightpaths at their destination, with respect to the network topology and the various transmission equipment. BER-Predictor considers the simultaneous effects of four transmission impairments, namely, the chromatic dispersion, the polarization mode dispersion, the amplified spontaneous emission and the non-linear phase-shift.

In Chapter 5, we use BER-Predictor to evaluate the QoT of lightpaths.

# Chapter 4

# Survey on Translucent Network Design

## 4.1 Introduction

As aforementioned in Section of Chapter 2, three approaches for translucent design are proposed in the literature. The first approach for translucent network design propose to divide the core network into islands of transparency, connected via boundary opaque nodes [12, 87, 99]. Each island is a transparent domain. This approach has a major drawback consisting in its low scalability. Any operational change in the network, like upgrade or extension of a certain island, requires a reorganization of all the islands, since a minimum overlapping should be respected between the islands. Consequently, the set of boundary nodes (opaque nodes) is bound to change, entraining a necessary update at the control plane and especially at the routing tables.

The second approach consists in designing translucent networks where nodes are either opaque or transparent [35]. This design approach is more scalable that the first one where the whole network is considered as a single domain, and the lightpaths are routing according to their QoT needs. The drawback of this type of translucent networks is the systematic regeneration of lightpaths passing through the opaque nodes, regardless of their QoT.

In our study, we adopt the third translucent network design approach wherein the network's nodes are either transparent or translucent. This approach introduces the possibility of optically bypassing the translucent nodes if the QoT of the considered lightpath is admissible at the following node on the route.

In this chapter, we survey relevant research work in the translucent network design area. More specifically, we address the third design approach.

## 4.2 Survey on translucent network design

In general, translucent network design solutions proposed in the literature fall under one of the following categories:

1. *Choice of regeneration sites*: in this category, the objective is to choose the network nodes wherein regenerator pools are to be added for regeneration purposes. This category can either be *topology-based*, *i.e.*, its operation relies on the network's topology and/or full-connectivity graph, or *traffic-based*, *i.e.*, its operation relies on an effective traffic load applied to the network.

2. *Regenerator allocation*: the objective here is to place (activate) regenerators in given regenerator sites, the choice of regeneration sites being done *a priori*. Solutions providing regenerator allocation in translucent nodes are basically traffic-based.

3. *Decision on regeneration sites and regenerator allocation*: in this category, design solutions choose regenerator sites among the network nodes and activates regenerators in them, in a whole one-step procedure. In this respect, this category is generally traffic-based.

### 4.2.1 Study of Ramamruthy *et al.*

In [96, 73], Ramamurthy et *al.*, proposed different translucent network design approaches relying on successive procedures of categories 1 and 2 (as described in the previous section). They proposed four solutions for the choice of regeneration sites in the network, and two solutions for RWA and regenerator allocation within the chosen sites:

1. *Solutions for the choice of regeneration sites:*

   (a) *Nodal degree first (NDF)*: This solution is topology-driven, where N regeneration sites are selected among the network nodes according to their physical degree.

   (b) *Centered node first (CNF)*: This solution is also topology-driven. By definition, a node is more *centered* than others if it appears on a greater number of shortest paths, computed according to hop numbers. In this regard, the N most centered nodes are selected to become regeneration sites.

   (c) *Traffic-load-prediction-based (TLP)*: As its name suggests, this solution is traffic-driven. At first, a set of lightpath requests is generated according to a predicted traffic pattern. Afterwards, lightpath requests are assigned routes according to a given routing algorithm (*e.g.*, HD-SPF[1]). Next, nodes are assigned counters

[1]Hop-Distance-based Shortest Path First: This wavelength routing algorithm finds the shortest hop-distance path between two network nodes, according to Dijkstra algorithm, each link of the network being assigned a weight equal to 1.

equal to the numbers of times they appear on the routes followed by the requests. In the end, the N nodes with highest counters are selected to become regeneration sites.

(d) *Signal-quality-prediction-based (SQP)*: This solution is also traffic-driven. Like the previous solution, a set of lightpath requests is generated following a predicted traffic pattern, and requests are also routed according to a given wavelength routing algorithm. This time, nodes are assigned counters that are incremented each time the quality of a lightpath drops following the passage through this node. The transmission quality of lightpaths depends on a maximum reach distance expressed in a maximum hop number $LN_{max}$. Finally, the N nodes with highest counters are selected to become regeneration sites .

In the latter solutions, the selected N nodes are provided a pool of regenerators of size X, each. A regeneration site is capable of regenerating at most X channel at the same time.

2. *Solutions for the regenerator allocation:*

(a) *Fragmentation*: In the routing process of a given set of lightpath requests, if a connection request has a deteriorated quality at destination, regenerators are fetched along its route, respecting the $LN_{max}$ distance. As for wavelength assignment, strategies like Best-BER-Fit (BBF), First-Fit (FF), etc... [79] are chosen to assign wavelengths to the different segments of the request, separated by the used regeneration sites. If no regenerator placement on the connection's route is possible, the connection is rejected. This latter case is envisaged whenever the assigned route does not hold any regeneration site, or the pools in the existing sites on the route are fully used.

(b) *Trace-back*: In this solution, a continuous wavelength is first fetched over the whole route of the connection, the connections being considered one by one. If no wavelength is available, regenerators are needed to draw wavelength conversion over the route. The existing regeneration sites on the route are tested starting from the closest one to the source node and the quality requirements are tested all along the procedure, also according to $LN_{max}$. In the case where all regenerator allocation solutions provide at least a segment with deteriorated quality of transmission at its second end, the connection request is rejected.

Considering different network topologies, the authors investigate the proposed network design solutions. Simulation results show that in medium-sized networks, the topology-based regenerator placement algorithms: NDF and CNF, yield better results followed by SQP and TLP, respectively. However, in the large-sized network, SQP yields the best performance followed by NDF, TLP, and CNF. Most importantly, the signal quality-prediction-based regenerator placement algorithm achieves good performance in all kinds of network topologies.

### 4.2.2 Study of Pan *et al.*

In [69], Pan et *al.*, propose a global optimization technique based on a tabu-search for the choice of regeneration sites in the network. This approach is topology-driven wherein a full connectivity matrix is considered. First of all, arbitrary network nodes are considered as regeneration sites for initialization of the heuristic. The connection establishment criterion is the maximum optical reach (1500, 2000, 2500 km). At each iteration, the establishment of the requests is tested according to the quality of transmission at each subsequent transparent lightpath. If the given set of regeneration sites provides positive returns, the authors suppose that the set includes more than enough sites, and therefore, one site is dropped to the tabu list. Otherwise, the authors suppose that the set includes less than enough sites, and choose a node from the tabu list to become a regeneration site. This test is repeated until a maximum number of iterations has been reached.

Regardless of the fact that this solution only chooses the regeneration sites in the network without providing actual RWA and RP solutions to a real-network traffic set, the authors did not specify whether the translucency of the network adopts the sparse regeneration approach (translucent nodes for regeneration) or the approach wherein the chosen nodes are fully opaque. In this order, checking the establishment of requests may have been happening automatically at all the sites found on the weak requests' paths.

### 4.2.3 Study of Rumley *et al.*

In [78], Rumley et *al.*, propose three algorithms for routing and regenerator placement. The three procedures are topology-driven and do not consider WA in their investigation. The maximum optical reach $L_{max}$ is the criterion for traffic establishment, where $L_{max}$ is expressed in Equation (4.2.1) by means of the physical length $d_{max}$ of the longest link, and the physical length $D_{max}$ of the longest shortest path in the network:

$$L_{max} = d_{max} + CLF \times (D_{max} - d_{max}) \tag{4.2.1}$$

$CLF$ represents the critical length factor, expressing the transparency level of the network. When $CLF$ is set to 1, the network is fully transparent. When it is set to 0, the signal reach is sufficient to guarantee a successful transmission over all the links of the network, considered one by one.

1. MIN_REG aims at minimizing the total number of regenerators. This procedure tries all the possibilities of regeneration for the requests whose paths exceed $L_{max}$. The regeneration option providing the least regenerators is retained. MIN_REG can be considered a category 3 design solution. Let us consider $x_{ij}$ the given number of regenerators for a connection between nodes $i$ and $j$ under this procedure, where the considered traffic matrix is unitary. Under a real-network traffic set, the needed number of regenerators is equal to $\sum_{i,j:i\neq j} x_{ij} \times n_{ij}$, where $n_{ij}$ is the number of lightpath requests between node $i$ and $j$.

2. MIN_SITE aims at minimizing the number of regeneration sites. This procedure checks all the possible node subsets starting from one-element subsets. For each considered subset, the weak connections in terms of QoT are split according to the regeneration sites in the subset. The sub-sequent lightpaths are tested and the operation is finished when a given set of nodes guarantees the establishment of the traffic set.

   This procedure automatically regenerates problematic connection requests at the nodes existing on their shortest path. Which adds more regenerators than needed.

3. MIN_SITE_RR aims at minimizing the number of sites first, then the total number of regenerators. It can be considered as the succession of MIN_SITE and a re-routing procedure that tries to find the best route that minimizes the number of needed regenerators for a given traffic request.

Comparisons between the three procedures show that MIN_SITE_RR provides the least regeneration cost thanks to the flexibility it holds within the re-routing operation.

### 4.2.4 Study of Patel *et al.*

In [71], Patel et *al.*, provide a solution for traffic grooming and regenerator placement in WDM networks. The choice of regenerator sites is considered as done beforehand. The objective is to minimize the network's CapEx cost. A connection's cost is expressed in terms of relative costs of transponders, client cards, line cards and regenerators, used in order to establish the connection. The connection establishment criterion is the maximum optical reach in hop-distance. Although the idea of inserting the grooming possibility into the network allows a better usage of electrical and optical resources, the whole operation has not been treated as a global optimization problem, which can deteriorate the performance provided by the grooming possibility.

The authors considered static traffic requests requiring 1/10 the capacity of an optical channel, each. In this study, simulation results show that joint traffic grooming and IA-RP yield less costs than grooming or RP considered aside.

### 4.2.5 Study of Al Zahr *et al.*

In [63], Al Zahr et *al.*, consider physical impairment in their IA-RWA and RP approach. The quality criterion is a $\mathcal{Q}$ factor threshold ($\mathcal{Q}_{th}$). The $\mathcal{Q}$ factor of the connections at destination is computed by the BER-Predictor tool presented in Chapter 3. The considered impairments are ASE, CD, PMD and non-linear phase-shift due to XPM and SPM. The proposed heuristic called Lightpath Establishment and Regenerator Placement (LERP) addresses static traffic requests of 10 Gbps and seeks the minimization of the rejection ratio as well as the number of required regenerators. This approach has served as a benchmark to validate the approach that we propose, comparisons will next be provided. In this respect, we leave the detailed description of this approach to Section 5.5.4.1.

### 4.2.6 Study of Pachnicke *et al.*

In [85, 86], Pachnicke et *al.*, propose a translucent network design made of two steps (a category 1 procedure followed by a category 2 procedure). First, the choice of regeneration sites is made through a topology-driven strategy, where a full connection matrix is considered. The regeneration sites are chosen iteratively. At each iteration, the node allowing the establishment of the highest number of connections is considered a regeneration site. The established connections are then taken out from investigation. The iterations are done when all connections are successfully established. The quality criterion is a $\mathcal{Q}$ factor threshold, where the ASE, Xtalk, XPM and FWM are taken into account.

Secondly, a constraint-based routing (CBR) solution addressing mainly dynamic traffic requests is described. The requests of 10 Gbps arrive according to a Poisson arrival process. At first, a path (among $\mathcal{K}$-shortest paths) is chosen if at least one wavelength is free over its links from source to destination. If there is no free wavelength on either of the $\mathcal{K}$-shortest paths, the request is blocked. For a possible RWA solution, the $\mathcal{Q}$ factor is estimated at destination. If it is satisfying with respect to the threshold, the connection is established. Otherwise, the lightpath is regenerated on every regeneration site over the assigned path. The quality of each transparent segment on the path is also estimated; if at least one segment cannot provide a good $\mathcal{Q}$ factor, the connection is blocked.

As we can see, systematically regenerating weak requests in terms of $\mathcal{Q}$ factor, adds more regenerators than necessary ones. Besides, if the chosen translucent nodes are excessive, even more regenerators are activated in the network.

In this thesis, we propose an enhancement of the regenerator allocation strategy and compare it to our own approach under static traffic assumption and the same QoT estimation environment. More details about the proposed enhancement are provided in Section 5.5.4.2.

### 4.2.7 Study of Manousakis *et al.*

In [64], the authors consider ASE, CD, PMD, Xtalk, SPM and XPM in the estimation of the $\mathcal{Q}$ factor at the destination of a lightpath. They propose to divide the IA-RWA and RP problem into three consecutive steps:

- The first step aims to find the lightpath requests that cannot be established in a transparent way, on any of their $\mathcal{K}$-shortest paths. Five approaches (an exact approach via an Integer Linear Programming (ILP) formulation and four heuristic algorithms) are considered to decide on the way to decompose the problematic lightpath into subsequent successive lightpaths in order to place regenerators at their separating nodes. At the end of this step, a new (transformed) traffic matrix is obtained from the transparent lightpaths.

- In the second step, an ILP formulation is run over the transformed traffic matrix performing IA-RWA. The connections that are not established at this phase are left

to the third step.

- The third step tries the different re-routing possibilities in order to establish rejected lightpath requests at the previous step, using the remaining resources in the network.

### 4.2.8 Study of Pan *et al.*

The authors in [45] address the translucent network design considering linear physical impairments first, then linear and non-linear physical impairments. For the linear IA-RWA and RP, an ILP formulation is proposed, with the objective of minimizing the number of regenerators as well as the blocking ratio of traffic requests, with more stress over the second objective. A heuristic-based algorithm is also proposed, made of three steps.

- The first step finds a route for every request regardless of the effective WA or the QoT. This step aims at minimizing the number of blocked requests as well as minimizing the average hop number traversed by the successful lightpaths.

- In the second step, lightpaths resulting from the previous step are processed sequentially. WA is carried out according to the FF[2] strategy. Under the wavelength continuity constraint, some lightpath may present the need for wavelength conversion. The priority is given to the wavelengths that allow the establishment of the lightpath using the least umber of regenerators. In this step too, the QoT is neglected.

- In the third and last step, the QoT at destination of the lightpaths resulting from the previous step is estimated. When a lightpath presents unacceptable QoT, it is decomposed into the minimum number of subsequent lightpaths providing admissible end-to-end QoT.

One drawback of this algorithm is that rejected lightpaths at the first step due to wavelength contention, are not addressed after the third step in order to benefit from possible flexibility driven by the wavelength conversion operations happening in step 2.

As for the non-linear IA-RWA and RP, a QoT tool called Q-NL takes into account linear and non-linear physical impairments (ASE, Xtalk, XPM, SPM, FWM, and PMD, considering that the CD has been completely compensated). An iterative RP heuristic is proposed, copying steps 1 and 2 of the previous heuristic algorithm. The third step does not take in consideration the WA resulting from step 2, only WC locations are retained. An ILP formulation is considered to assign wavelengths to the transparent lightpaths minimizing the noise variance caused by non-linear impairments. Then the QoT is checked at the end of each lightpath and more regenerators are inserted if the connection necessitates regeneration.

[2]In the FF wavelength assignment strategy, wavelengths are indexed in their order of presence in the considered spectrum. The assignment seeks the first free wavelength in the increasing order of indices.

### 4.2.9 Study of Doumith *et al.*

In [13, 34] the authors propose an exact approach for translucent WDM network design under scheduled traffic consideration (SLDs[3]). The main objective is to maximize the number of satisfied requests and to minimize the number of required regenerators. This approach is divided in two steps. In the first step routing and regenerator placement are formulated by an ILP aiming at minimizing, at the same time: (*i*) the number of regenerators, (*ii*) the number of regeneration sites, and (*iii*) the number of rejected SLDs. The QoT considered for the regeneration decision is that of the central wavelength (1550 nm).

In the second step, WA and additional RP (WARP) are performed. Rejected SLDs from the previous step are not considered. The input SLDs fed to the WARP ILP are the all-optical segments resulting from the regeneration at the first step. The objective of this second ILP is the minimization of the number of regenerators and the number of regeneration sites, simultaneously.

Results show that regenerators are reused at different time periods by different SLDs which is important in today's networks seeking to alleviate both the number of deployed equipment and the inherent operational costs. Besides, it is worth noting that the second step adds at most 2 regenerators to those deployed in the first step, which means that even though the approach was developed in two steps for the sake of scalability, the optimality of the global solution is barely altered.

Due to the dependency of the results on the traffic sets, the authors extend their study in [44] to consider different traffic patterns (PLDs and SLDs) simultaneously in order to guarantee traffic establishment under traffic uncertainty. results show that a network cost reduction of up to 42 % can be achieved in comparison to a classic translucent WDM network design where traffic forecasts are considered separately.

## 4.3 Conclusion

In this chapter we surveyed research works from the literature tackling the problem of translucent network design under sparse regeneration. To the best of our knowledge, even though some research addressed cost minimization of networks, it has not been considered as the goal of the design solution. It has rather been discussed as a consequence among others. In this thesis, not only do we consider the CapEx costs of regeneration, but also the inherent OpEx costs. In the next chapter, we present the cost function translating our view for overall regeneration cost in the network and discuss our approach for IA-RWA within the design solution.

[3]Scheduled lightpath demands, requiring a full-channel capacity each.

# Chapter 5

# COR2P: an innovative tool for translucent network design

## 5.1 Introduction

In this chapter, we introduce a translucent network design solution that also solves the IA-RWA problem. The explicit objective of this tool is to minimize both the requests' rejection ratio, and the network cost related to the activation of regenerator pools in the nodes. The consequences of this approach are not only the minimization of the total number of regenerators in the network, but also the reduction of the number of regeneration sites.

This chapter is organized as follows. We first introduce the sparse regeneration principle and then explain into detail our cost model inherent to regeneration deployment at the nodes. A cost function is then provided to represent the cost of RWA and regeneration relative to a lightpath establishment. Indeed, a lightpath is established through a wise choice of a physical route, optical channels and adequate regeneration placement, in order to provide an admissible QoT at the destination node.

Our tool, called COR2P for Cross Optimization for RWA and Regenerator Placement, incorporates this cost function when dealing with impaired signals. COR2P is based on three main steps and utilizes BER-Predictor in order to estimate the QoT at the destination of such lightpaths.

## 5.2 Translucent Network Design

As aforementioned in Chapter 2, sparse regeneration in translucent network design performs 3R regeneration in sparsely placed nodes of the network. These nodes are translucent nodes since a transit lightpath can bypass the electrical layer of the node, or be switched to the 3R regenerator bank in order to recover from degradations due to accumulated impairments. The other nodes of the network are transparent, the only electrical operations being related to signal insertion (*resp.*, extraction) into (*resp.*, from) the optical layer (Add/Drop). Translucent network design, in the sparse regeneration context, considers a

transparent network topology and adds 3R regeneration banks to sparsely chosen nodes from the network.

### 5.2.1 Problem Statement

Designing a translucent network consists in judiciously choosing which network nodes are to present 3R regeneration facility. In this respect, the design issue is closely related to the traffic load to be established in the network. The higher the traffic load, the more numerous the required optical channels. This has two major impacts:

- Wavelength contention: with high traffic loads, more optical channels are allocated. Without WC, wavelength assignment is subject to the wavelength continuity constraint. Therefore, some lightpaths may be unable to find an end-to-end free wavelength over all of their paths' links. In this case, WC is needed at an intermediate node. As we already mentioned in Chapter 2, 3R regenerators also provide WC facility.

- QoT deterioration: regardless of the traffic load, paths present physical impairments that accumulate with each traversed network element. With more traffic on the links, interactions between the signals and the optical medium become severer and non-linear effects are accentuated. With the knowledge of the network's usage, QoT can be monitored at any point of the network, and 3R regeneration is deployed when needed.

This design problem requires a good knowledge of the network's topology and capacity, as well as of the operator's expectations and quality requirements.

Besides, when a node is chosen to become a regeneration site (translucent node), additional network costs are to be considered. Indeed, a 3R regeneration bank will add extra fees (Capital and Operational expenditures) to the network, including:

- Deployment fees: related to the intrinsic price of the equipment and to their installation (3R regenerator pool, additional racks, installation staff fees).

- Operation fees: related to the costs inherent to the usage of the equipment (extra power-feeding and air-conditioning, supervision and maintenance) assuming that floor rental is still the same.

In this thesis, for the sake of simplicity, we consider a dedicated personal staff for the supervision of 3R regenerators, in order to represent not only the additional human intervention accounted for OpEx, but also fixed operational expenses as power and cooling. Therefore, a 3R regenerator pool requires a dedicated staff responsible for the good operation of the pool.

We can describe the translucent network design problem as follows.

***Given***

*Network specifications*:

- A physical network topology wherein all nodes are *a-priori* transparent;
- A set of wavelengths, available per fiber-link;

*Traffic load*:

- A set of Permanent Lightpath Demands (PLDs), where each connection demand requires a full channel bandwidth[1];

***Objective***

The aim of translucent network design is to guarantee the QoS that the network operator offers to its clients, while also minimizing the network's expenses. We can enumerate the network's expectations as follows:

- Respect a maximum rejection ratio, *i.e.*, establish the maximum possible number of PLDs, by guaranteeing (*i*) enough resources to carry the connection demands, and (*ii*) a good QoT at destination. This issue is an objective and a constraint at the same time.
- Minimize additional costs inherent to the deployment of 3R regenerators, (*i*) by minimizing the number of regeneration sites in order to reduce CapEx cost inherent to site deployment and OpEx cost inherent to site operation, and (*ii*) by minimizing the number of regenerators in each regeneration site, in order to reduce CapEx cost represented by the prices of a single regenerator and additional racks.

***Subject to***

*Quality of transmission requirements:*

An admissible QoT threshold is fixed by the network operator. It is represented by the BER ($\text{BER}_{th}$) threshold or the $\mathcal{Q}$ factor threshold[2] ($\mathcal{Q}_{th}$). In order to be established successfully, a lightpath should present an acceptable BER at its destination node, *i.e.*, not exceeding $\text{BER}_{th}$.

*Wavelength continuity constraint:*

In the absence of any wavelength conversion, a lightpath should be routed using the same wavelength along its route. Introducing regenerators relaxes this constraint.

*Regeneration capacity per site:*

The number of regenerators that can be deployed in a regeneration site is upper-bounded due to power supply or footprint constraints.

[1]This assumption has been explained in Chapter 2

[2]In the following, notions of BER and $\mathcal{Q}$ factor are equivalent and mentioning one implies the other.

### 5.2.2 Cost Model

In this thesis, we propose a solution to the translucent network design problem, and address two main corporate objectives: QoS and minimal network cost. This solution resolves the IA-RWA and regenerator placement problems. Indeed, two kinds of network resources are addressed: optical resources, and electrical resources. On one hand, optical resources can be expressed in terms of wavelengths, since a lightpath requires a wavelength per link along its route. Optical resources, in this respect, are limited by network's capacity, or, more simply, by the number of wavelengths deployed per link. On the other hand, electrical resources are related to the client cards and 3R regenerators deployed to establish a lightpath. As we have already elaborated, we do not take into consideration client cards (transceivers or Add/Drop transponders) in this part, since they constitute the fixed variable needed for transmission/reception of established lightpaths. Therefore, electrical resources are represented by the regenerators needed to maintain the QoT of lightpaths, and relax the WC constraint.

Following the previous reasoning, the cost of establishing a connection request can be presented as a weighting between optical and electrical resources costs:

$$Cost_{(connection)} = \alpha \times Cost_{(optical\ resources)} + (1 - \alpha) \times Cost_{(electrical\ resources)} \quad (5.2.1)$$

Optical resources are related to the assigned channels on the links traversed by the lightpath. It is important to note that the number of optical channels, regardless of their wavelength, solely impacts the optical resources cost. As a result, the number of hops spanned by the lightpath from source to destination can represent this cost.

The electrical resources cost depends on the regeneration site configuration along the considered route. Since our objective is to design a translucent network, the electrical resources cost can be expressed by the CapEx/OpEx costs in which the operator needs to invest:

$$Cost_{(electrical\ resources)} = Cost_{(regeneration)} = Cost_{CapEx} + Cost_{OpEx} \quad (5.2.2)$$

Each regeneration scenario has its specific cost calculation according to the characteristics of the network node where the regeneration has to take place. These *scenarii* can be summarized by the following cases:

- If a node is transparent, the investment in order to make it translucent has to be accounted. The lightpath will need one 3R regenerator from its bank. We represent the cost corresponding to such a case by the CapEx cost of environment equipment (rack, power supply, cooling device, and 3R regeneration pool). Since a first regenerator has to be activated, an OpEx cost is considered, in order to monitor its performance.

- If a node is already considered as a regeneration site, the activation of an additional regenerator is the only operation to perform. This adds an additional OpEx cost for monitoring.

- If the node is translucent, but its regenerator pool is fully used, there are two possible options: (*i*) invest in a new pool deployment that increases the CapEx cost, or (*ii*) make it impossible to deploy the current node as a regeneration site for the considered lightpath.

  In our vision, the regeneration pool size is upper-bounded with a high value in order to have a clear methodology. We do not allow adding more regeneration pools if the deployed pool is fully-used.

#### 5.2.2.1 OpEx cost of a regenerator

When a first regenerator is activated at a network node, an operator staff is needed to operate it, monitor its performance and intervene in case of component failure. As we mentioned earlier in Section 5.2, we consider a dedicated personal for the monitoring of the regeneration pool.

When a second regenerator needs to be activated, the same staff is in charge of its monitoring, but monitoring two regenerators is not the same as monitoring one regenerator. The same as monitoring '$x$' regenerators is not the same as monitoring a single regenerator. But OpEx cost, unlike CapEx cost, cannot be deduced by simple proportional relationship with the number of deployed equipment, especially OpEx cost corresponding to human intervention. This is why we consider the OpEx cost to be a decreasing function of the number of regenerators held in the site.

Figure 5.1 illustrates our approach for additional OpEx cost per activated regenerator, with respect to its order of activation in the pool.

#### 5.2.2.2 CapEx and OpEx costs of a translucent node

Given the aforementioned CapEx and OpEx cost considerations, the cost of deploying a regeneration site at a given network node is made of the fixed CapEx cost, and of the variable OpEx cost. The total OpEx cost in a translucent node is given by the cumulative cost of all deployed regenerators. Therefore, it is an increasing concave function of the number of regenerators (since the individual OpEx cost per regenerator is adecreasing convex function). Figure 5.2 illustrates the total cost of a translucent node.

#### 5.2.2.3 Total cost of a lightpath

The total regeneration cost of a lightpath depends not only on how many times a lightpath is regenerated over the route it follows, but also on the intrinsic regeneration capacity of

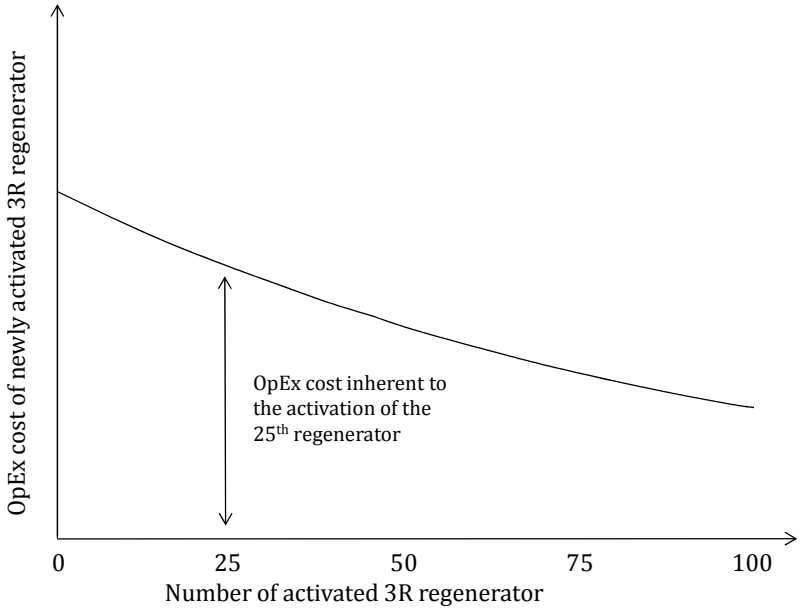


Figure 5.1: OpEx cost of additional regenerators, according to their order of activation.

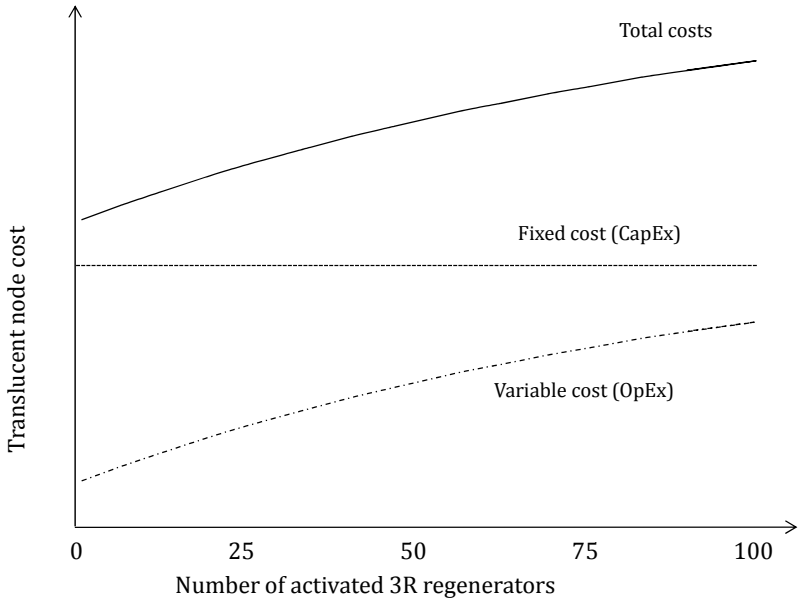


Figure 5.2: Total cost of a translucent network node.

the sites where it should undergo regeneration. In this respect, the regeneration cost of a lightpath can be expressed by Equation 5.2.3:

$$Cost_{regeneration} = \sum_{i=1}^{\mathcal{H}-1} \mathcal{C}_{\mathcal{R}}(v_i) \tag{5.2.3}$$

wherein "$\mathcal{H}-1$" is the number of intermediate nodes ($v_i$) between the source and destination of the given route ($\mathcal{H}$ being the number of hops it spans).

$\mathcal{C}_{\mathcal{R}}(v_i)$ is the regeneration cost at node $v_i$. It can be detailed, according to Section 5.2.2 as follows:

$$\mathcal{C}_{\mathcal{R}}(v_i) = \begin{cases} 0 & \text{if } v_i \text{ is not a regeneration site for the considered lightpath,} \\ \mathcal{C}_C + \mathcal{C}_O \cdot e^{-\frac{1}{\mathcal{X}}} & \text{if } v_i \text{ is considered a regeneration site for the first time,} \\ \mathcal{C}_O \cdot e^{-\frac{x_0+1}{\mathcal{X}}} & \text{if } v_i \text{ already has } x_0 (< \mathcal{X}) \text{ active regenerators,} \\ \infty & \text{if } x_0 = \mathcal{X} \textit{ i.e.}, \text{ the regenerator pool at } v_i \text{ is fully used and the} \\ & \text{considered lightpath attempts to be regenerated at } v_i. \end{cases} \tag{5.2.4}$$

In the latter equation, $\mathcal{C}_C$ and $\mathcal{C}_O$ are weighting factors that depend on the vendor prices and the operator's deployment strategy (cooling, staff handling). $\mathcal{X}$ is the regenerator pool size. We considered this form of exponential function, in order to obtain a convex function of the OpEx cost related to activating an additional regenerator in a regenerator site. Other functions could also be considered, with more knowledge of the operator's investment.

According to these assumptions, the total cost of a connection can be expressed in the following equation:

$$Cost_{(connection)} = \alpha \times \frac{\mathcal{H}}{\overline{\mathcal{H}}} + (1-\alpha) \times \sum_{i=1}^{\mathcal{H}-1} \mathcal{C}_{\mathcal{R}}(v_i) \tag{5.2.5}$$

In this equation, $\mathcal{H}$ and $\overline{\mathcal{H}}$ are respectively, the hop number along the route, and the average hop number over all possible routes between the source and destination nodes (*e.g.*, over the $\mathcal{K}$-shortest paths). The variable $\overline{\mathcal{H}}$ is needed in order to impose comparable orders of magnitudes between the two weighted parts of Equation 5.2.2.3.

## 5.3 COR2P

In this Section, we describe COR2P, an original solution for translucent network design. It consists of a heuristic-based algorithm dealing with the IA-RWA problem as well as the regenerator placement problem. COR2P stands for "***Cross-Optimization for RWA and Regenerator Placement***". We explain in detail each of its three steps, and

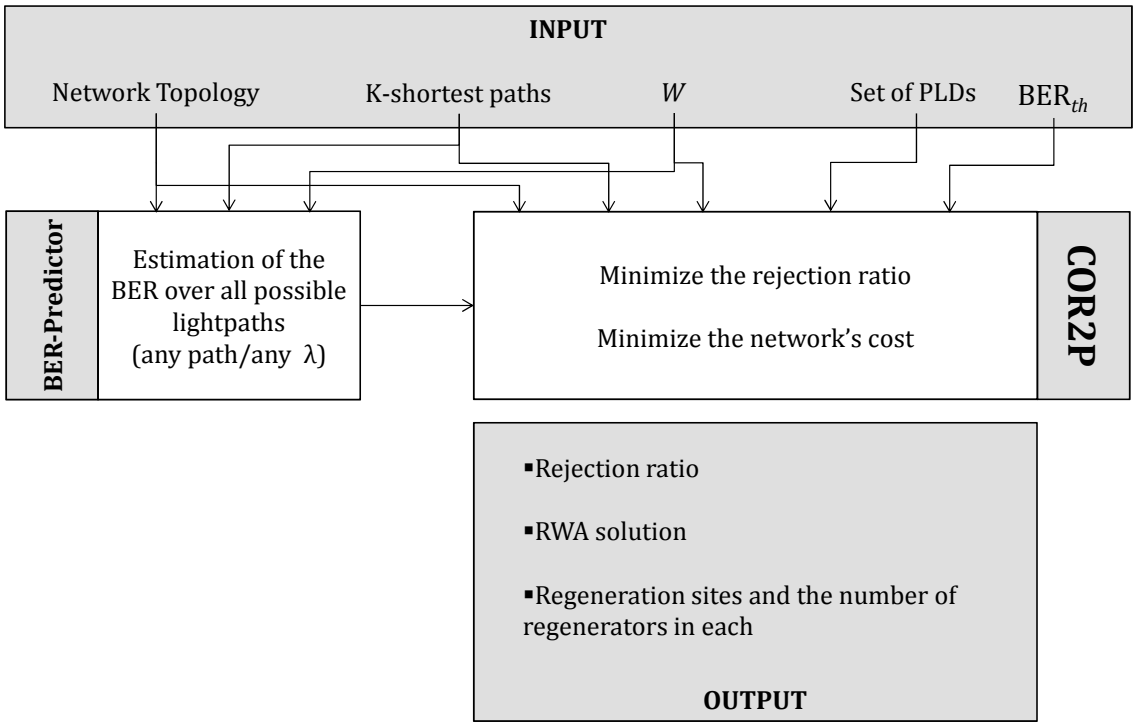


Figure 5.3: Overview of the input and output of COR2P, and its main objectives.

investigate different parameters that impact regenerator concentration in some sites among the set of nodes of the network. The originality of COR2P lies within its CapEx/OpEx cost function, and its influence on regenerator concentration in a few nodes.

COR2P, seen as a black box, can be summarized in Figure 5.3. Indeed, COR2P utilizes data from the BER-Predictor (Cf. Chapter 3). in order to make decisions on lightpath establishment and regeneration or blocking. The network topology and the BER-Predictor tool enable to evaluate the QoT at destination for all the $\mathcal{K}$-shortest paths between two network nodes. The network topology includes, not only the connectivity graph between the nodes, but also all the localizations of the transmission equipment used along each hop. The $\mathcal{K}$-shortest paths of all source/destination couples are computed beforehand in km. $W$ is the number of available channels per fiber-link. In the following, we explain the notations used for the description of COR2P, then include a discussion of its different steps.

### 5.3.1 Notations

In this chapter, we use the following notations and typographical conventions.

- $\mathcal{G} = (\mathcal{V}, \mathcal{E}, \xi)$ is a directed graph representing the network topology. $\mathcal{V}$ represents the set of nodes and $\mathcal{E}$ represents the set of links. $\xi$ is a cost function $\xi : \mathcal{E} \rightarrow \mathbb{R}^+$ mapping the physical length of the links. Links in $\mathcal{E}$ are unidirectional, but if $\xi$

includes a link from node $v_a$ to node $v_b$, it is mandatory to also include a link from node $v_b$ to node $v_a$. This assumption corresponds to the real situation in carriers' networks.

- $N = |\mathcal{V}|$ denotes the number of the network nodes.
- $W$ denotes the number of wavelengths per fiber-link.
- $\mathcal{D}$ is the set of PLDs to be set up in the network.
- A PLD, denoted $d_i (1 \leq i \leq |\mathcal{D}|)$, is a connection demand between two nodes $S_i$ and $D_i$ in $\mathcal{V}$.
- $\mathcal{P}_i$ is the set of available paths connecting $S_i$ and $D_i$. These paths (the $\mathcal{K}$-shortest paths, if they exist) are computed beforehand according to Eppstein's algorithm [32]. computed between all PLDs to be set up.
- $p_{ik}$ denotes the $k^{th}, 1 \leq k \leq \mathcal{K}$ shortest path in $\mathcal{P}_i$ between $S_i$ and $D_i$.
- $\mathcal{H}_{ik}$ denotes the number of hops of the path $p_{ik}$.
- $\mathcal{R}$ is the initial number of regeneration sites in the network while $\mathcal{R}^*$ is the number of effectively used regeneration sites[3] at the end of the execution of the COR2P algorithm.
- $\mathcal{X}$ is the maximum number of regenerators per regeneration site, *i.e.*, the regenerator pool size.

### 5.3.2 Synopsis of COR2P

COR2P is a heuristic-based algorithm that aims to find an RWA solution to a set of PLDs and places regenerators in appropriate nodes in order to satisfy the quality of transmission. Its originality lies not only in minimizing the number of required regenerators in the network but also in minimizing the number of regeneration sites. COR2P can be divided into three consecutive steps as follows.

#### 5.3.2.1 Step 1 - Preliminary Routing

In this step, COR2P proceeds to a preliminary routing in a transparent network environment. The wavelength continuity constraint and the finite number of optical channels per fiber are the main constraints considered in this step.

We first compute an estimate ($BER_{ik}$) of the BER over all the $\mathcal{K}$-shortest paths ($p_{ik}$) of PLDs $d_i$, using BER-Predictor. For this estimation, we consider flat spectral response of the network elements (flat systems), *i.e.*, all the wavelengths present the same BER at

[3]This notion will be explained in Section 5.3.2.3.

the destination. Typically, this BER corresponds to the central wavelength of the given spectrum (the C-band). We recall that the "best" path is not necessarily the shortest path since the BER estimation depends on the transmission elements along the routes. On one hand, the higher the hop number of a path, the higher the non-linear impairments added by nodes connections, regardless of the distance in km of the path. Indeed, the passage through more switching fabrics, potentially induces more crosstalk and non-linear effects. On the other hand, the shorter a path (in km), the lower linear effects. Therefore, the QoT of a lightpath over a given route, depends on the interaction between linear and non-linear impairments, and is not trivial to predict. PLDs are then sorted in the decreasing order of their best BER ($BER_i^*$ over their candidate routes. This how, the first PLD presents, at its destination, the worst QoT of all PLDs, while the last one presents the best QoT.

Second, the PLDs are processed one by one in the previously defined order as follows. Respecting the flat-systems environment, we search for an end-to-end lightpath (path & wavelength) for the given PLD, over one of its $\mathcal{K}$-shortest paths, respecting the wavelength continuity constraint. If no solution is available, due to lack of resources over some of the hops, the processing of the PLD is postponed to Step 3. Such PLDs may then be established thanks to the relaxation of the wavelength continuity constraint provided by regeneration in Step 3.

#### 5.3.2.2 Step 2 - Potential Regenerator Placement

At this step, COR2P determines the nodes that are most likely to become regeneration sites. In this respect, each node "$v_i$" is assigned a counter "$c_i$", that reflects the amount of needed regeneration at its level.

Established[4] lightpaths in Step 1 are considered. For each of these lightpaths, a QoT follow-up is performed over the intermediate nodes until the destination. Whenever the observed QoT drops beneath the admissible threshold fixed by the operator, the counter of the preceding node is incremented. Recursively, the quality test is performed until the destination, assuming each time, that the node wherein the counter is incremented, is the source node of the remaining route followed by the lightpath.

Once all the lightpaths are processed, the network nodes are sorted in decreasing order of their counters. As mentioned in Section 5.3.1, we introduce $\mathcal{R}$ as the initial number of regeneration sites in the network. It can be considered as an additional input to COR2P. Accordingly, the first $\mathcal{R}$ nodes from the sorted list are those where regeneration is most likely needed. The number of regeneration sites at the end of COR2P is not restricted to $\mathcal{R}$ as we explain in the following paragraph. The number of regeneration sites to be effectively deployed in the network can be reduced.

[4]Lightpaths in Step 1 are not exactly "established", since their QoT has only been checked at the central wavelength of the operational transmission band. Step 1 mainly guarantees for some of the PLDs to have stepped over the resources contention constraint.

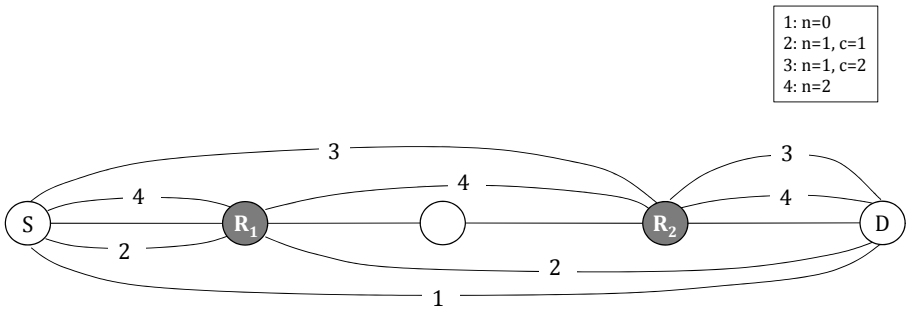


Figure 5.4: Regeneration possibilities.

#### 5.3.2.3 Step 3 - Effective RWA and Regenerator Placement

In this step, real transmission systems are taken into account. In such environment, the signal quality depends on the given wavelength (non-flat system), effective wavelength assignment being applied in this step.

First, we consider the PLDs that have been provided a lightpath in Step 1. The Best-BER-Fit (BBF) strategy is adopted for the wavelength assignment procedure. Given a path and a set of wavelengths, BBF consists in choosing the first available wavelength that guarantees the quality of transmission requirements[5] [79]. Subsequently, BBF saves the best suited wavelengths in terms of BER for weaker lightpaths. If no available wavelength can satisfy the quality of transmission requirements, the lightpath requires one or more signal regenerations. In addition, PLDs which processing has been postponed until this step, can benefit from the relaxation of the wavelength continuity constraint, thanks to the possibility to use regenerators at the deployed sites.

Second, PLDs that remain with no RWA solution, are processed as follows. For each PLD, COR2P first verifies if it can be routed without the need for any regeneration. If not, COR2P tries all possible combinations of regeneration over the K-shortest paths, provided that available wavelengths can assure its routing over the subpaths delimited by regeneration sites. If multiple possible solutions exist, COR2P chooses the one providing the lowest cost, according to the cost function represented by Equation 5.2.2.3. This function aims not only to optimize the number of deployed regenerators but also to concentrate them in a few nodes in order to reduce the network management cost.

Under high traffic loads, wavelength contention is most likely to occur, and some PLDs might be faced by the impossibility to benefit from the existing regeneration sites in order to be established. In this case, COR2P allows for one regeneration site to be added, but only over the shortest path. Step 3 synopsis is given in Pseudo-Code 1. Function GET_COST(*path*) detailed in Pseudo-Code 2, tries different placements for the regeneration along the *path* and computes the cost related to each combination. It then chooses the *solution* that gives the lowest total cost.

It is important to note that the number of regeneration sites at the end of COR2P

[5]The free wavelength providing the closest QoT to the acceptable threshold.

**Pseudo-Code 1** Synopsis of COR2P-Step 3

Let $\Theta$ be the set of demands to be regenerated.
Let $\Delta$ be the set of demands rejected in Step 1.
**Initialization**
$\Theta = \Delta$
$\mathcal{R}$ nodes are considered regeneration sites
**Processing**
**for all** $d_i \in \mathcal{D} \backslash \Delta$ **do**
  $\lambda^*$=Get_BBF[1]($p_{ik^*}$) {$p_{ik^*}$ *is the path assigned to* $d_i$ *in Step 1*}
  **if** ($\lambda^* \neq -1$) **then**
    Assign $\lambda^*$ to $d_i$
    Update network resources
  **else**
    $\Theta = \Theta \cup \{d_i\}$
  **end if**
**end for**
**for all** ($d_i \in \Theta$) **do**
  $cost_i = \infty$
  **for** ($k = 1$ to $k = \mathcal{K}$) **do**
    $cost_{ik} = Get\_Cost^2(p_{ik})$
    $cost_i = min(cost_i, cost_{ik})$
  **end for**
  **if** ($cost_i = \infty$) **then**
    **if** ($p_{i1}$ supports no regeneration site) **then**
      **if** (one or more links on $p_{i1}$ present full spectrum usage) **then**
        $d_i$ is blocked
      **else**
        $h = 2$
        **while** ($h \neq \mathcal{H}_{i1}$) **do**
          Estimate $BER_1$ and $BER_2$, BERs relative to the BBF wavelengths at the end of subpaths ($v_1 - ... - v_{h^*}$) and ($v_{h^*} - ... - v_{(\mathcal{H}_{i1}+1)}$)
          **if** (($BER_1 \geq BER_{th}$) & ($BER_2 \geq BER_{th}$)) **then**
            $d_i$ is blocked
          **else**
            **if** (($BER_1 \geq BER_{th}$) || ($BER_2 \geq BER_{th}$)) **then**
              $h^{*}++$
            **else**
              $v_h$ is considered a regeneration site
              A regenerator is deployed in $v_h$
              $d_i$ is established
              $h = \mathcal{H}_{i1}$
            **end if**
          **end if**
        **end while**
      **end if**
    **else**
      $d_i$ is blocked
    **end if**
  **else**
    Solution of the Get_Cost($p_{i1}$) function provides places to add regenerators along with an RWA solution
  **end if**
**end for**

[1] Get_BBF(*path*) is a function that returns the Best-BER-Fit wavelength, available over the parameter *path*. Get_BBF(*path*) returns $-1$ if no available wavelength guarantees the quality of transmission requirements.
[2] Pseudo-code of the Get_Cost(*path*) function is provided in Pseudo-code 2.

(*i.e.*, the effectively used sites $\mathcal{R}^*$) is not necessarily equal to $\mathcal{R}$. As we have discussed, the insertion of a new regeneration site in the network is possible. It is also possible to use some of the $\mathcal{R}$ fixed regeneration sites.

Figure 5.5 depicts the flowchart according to which the PLDs that remain unrouted are processed in Step 3. We assume $N_r^{ik}$ regeneration sites over the path $p_{ik}$ ($1 \leq k \leq \mathcal{K}$), thus $C_{N_r^{ik}}^{n}$ combinations of $n$ regeneration sites ($0 \leq n \leq N_r^{ik}$). Figure 5.4 presents an assimilation of the different regeneration possibilities over the $k^{th}$ path of a PLD $d_i$ from $S$ to $D$. At most, two regenerators at nodes $R_1$ and $R_2$, can be used to regenerate a lightpath along the illustrated path. Four possibilities for request establishment can then be exploited:

- No regeneration is considered: in this case, the signal is routed all-optically from node $S$ to node $D$.
- A single regeneration along the path is considered: in this case, two possibilities are present:
  - A regeneration is considered at regeneration site $R_1$, resulting in two all-optical lightpaths: from $S$ to $R_1$, and from $R_1$ to $D$.
  - A regeneration is considered at regeneration site $R_2$, resulting in two all-optical lightpaths: from $S$ to $R_2$, and from $R_2$ to $D$.
- Two regenerations are considered at $R_1$ and $R_2$, resulting in three lightpaths: ($i$) from $S$ to $R_1$, ($ii$) from $R_1$ to $R_2$, and ($ii$) from $R_2$ to $D$.

Figure 5.4 also illustrates the subpaths corresponding to each regeneration possibility.

**Pseudo-Code 2** Synopsis of Get_Cost (*path*)

**Initialization**
Let $\mathcal{H}$ be the number of hops of "*path*"
Let $s$ and $d$ be the source and destination of "*path*"
Let $\mathcal{N}_R$ be the number of regeneration sites over "*path*"
$minCost = \infty$
**for** ($n = 1$ to $n = \mathcal{N}_R$) **do**
  Consider the $n$-combinations from the set of $\mathcal{N}_R$ sites
  **for** ($c = 1$ to $c = C(n, \mathcal{N}_R)$ **do**
    $v_1, v_2, \ldots v_n$ are used as regeneration sites over "*path*", according to combination '$c$'
    Find a set of BBF free wavelengths $\{\lambda_p : p = 1...n+1\}$ over the subpaths of "*path*" delimited by $v_i$, $1 \leq i \leq n$. These wavelengths should provide good QoT.
    **if** (Such set exists) **then**
      Compute the cost $Cost_c$ relative to the use of "*path*" with the combination '$c$' of regeneration sites, using the *Cost Function* { *Equation* (5.2.3) }
    **end if**
    **if** ($Cost_c < minCost$) **then**
      $minCost = Cost_c$
      Store this "*solution*"("*path*", '$c$', $\{\lambda_p : p = 1...n+1\}$)
    **end if**
  **end for**
**end for**
Return "*solution*"

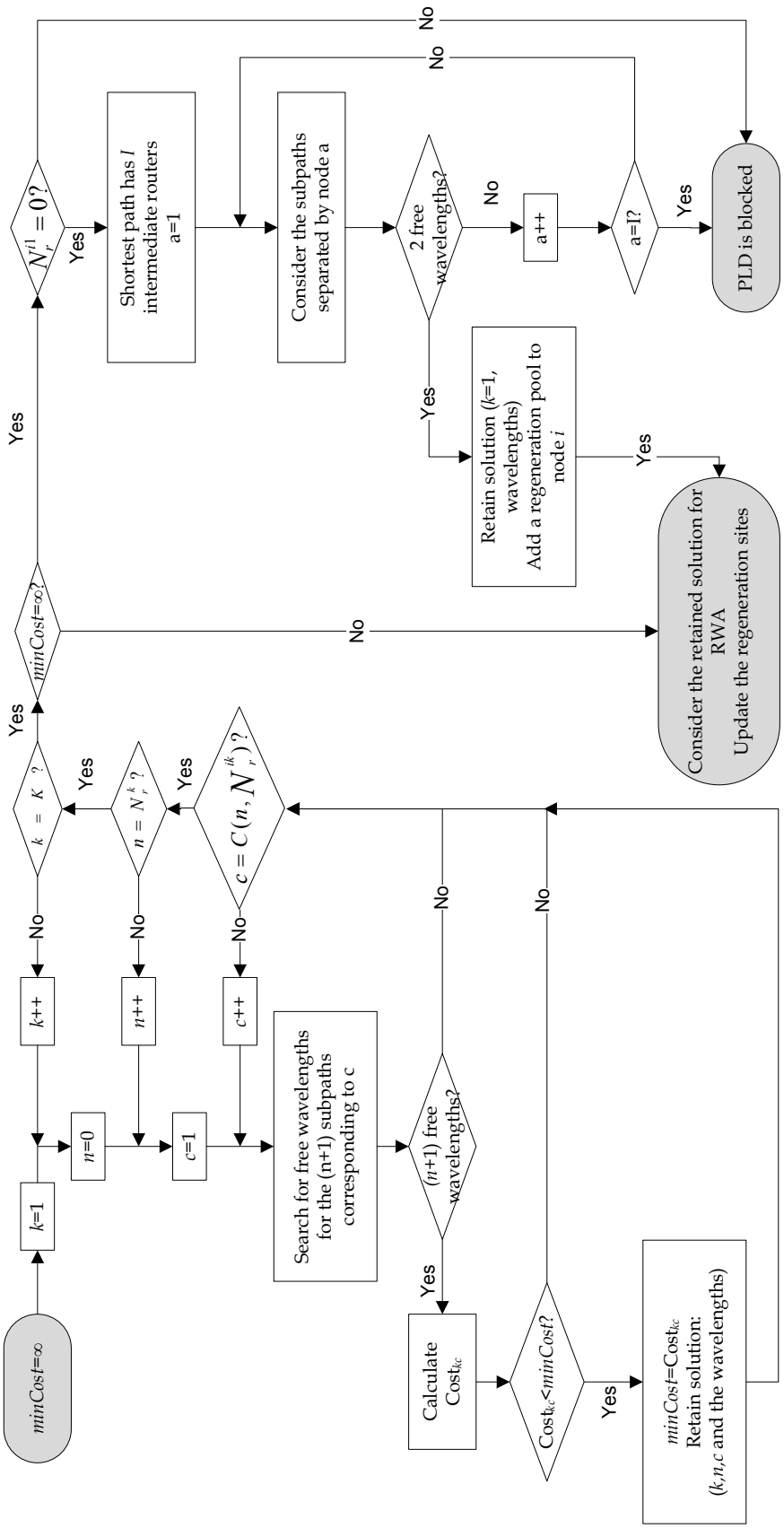


Figure 5.5: PLD processing in Step 3.

## 5.4 Illustrative case study

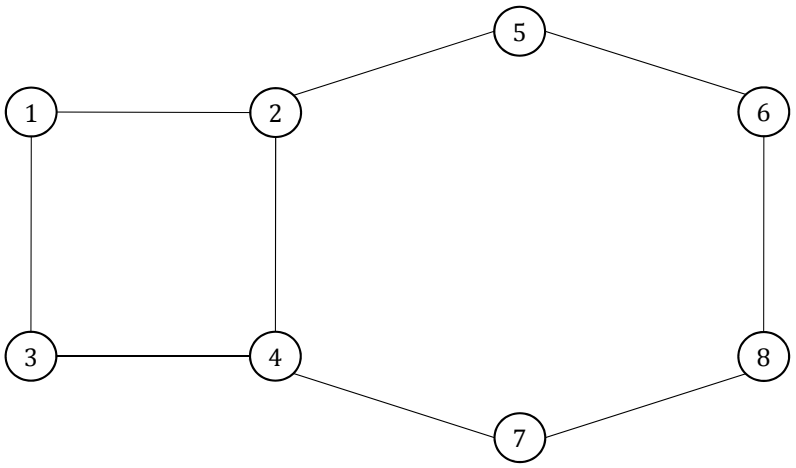


Figure 5.6: Considered network in the case study.

In this section, we provide an illustrative example of COR2P. The considered network is shown in Figure 5.6, it is made of 8 nodes and 18 fiber-links. We consider 2 wavelengths ($\lambda_1$, $\lambda_2$) deployed at each fiber ($W = 2$), and 2 shortest paths for each source/destination couple ($\mathcal{K} = 2$). The QoT for this network is estimated in relation to the hop-number spanned by the lightpaths. We represent by $Q_i$ the QoT provided at the destination of a path made of $i$ hops, under flat-systems consideration. For example, $Q_3$ represents the QoT at three-hop-long path, under flat-systems. In such an environment, we make the following assumption: $Q_1 > Q_2 \geq \mathcal{Q}_{th} > Q_3 > \cdots$. Under non-flat-systems, we consider $Q_{th}$ as follows:

- $Q_{\lambda_1} \geq Q_{th}$ when spanning only **3** hops while $Q_{\lambda_1} < Q_{th}$ at the fourth hop.
- $Q_{\lambda_2} \geq Q_{th}$ when spanning only **2** hops while $Q_{\lambda_2} < Q_{th}$ at the third hop.

The set of PLDs to be established in the network is represented in Table 5.1. Their shortest paths and their QoT under flat systems are also shown in this table.

Finally, the number of potential regeneration sites is considered to be equal to 2 ($\mathcal{R} = 2$).

| PLD | S | D | first path | second path |
|---|---|---|---|---|
| $d_1$ | 2 | 7 | 2-4-7 ($Q_2$) | 2-5-6-8-7 ($Q_4$) |
| $d_2$ | 2 | 8 | 2-4-7-8 ($Q_3$) | 2-5-6-8 ($Q_3$) |
| $d_3$ | 2 | 5 | 3-1-2-5 ($Q_3$) | 3-4-2-5 ($Q_3$)) |
| $d_4$ | 6 | 4 | 6-5-2-4 ($Q_3$) | 6-8-7-4 ($Q_3$)) |
| $d_5$ | 7 | 1 | 7-4-2-1 ($Q_3$) | 7-4-3-1 ($Q_3$)) |
| $d_6$ | 8 | 3 | 8-7-4-3 ($Q_3$) | 8-7-4-2-1-3 ($Q_3$)) |

Table 5.1: PLDs to be established in the network.

COR2P resolves the IA-RWA in three steps:

- Step 1:

  First, PLDs are sorted in the decreasing order of their best performance over their $\mathcal{K}$-shortest paths. The resulting order is the following: $d_2 \rightarrow d_3 \rightarrow d_4 \rightarrow d_5 \rightarrow d_6 \rightarrow d_1$

  Second, PLDs are assigned wavelengths respecting the wavelength continuity constraints. The assignment goes as follows:

  - $d_2$ is routed on its first path, and assigned $\lambda_1$: 2-4-7-8 ($\lambda_1$).

  - $d_3$ is routed on its first path, and assigned $\lambda_1$: 3-1-2-5 ($\lambda_1$).

  - $d_4$ is routed on its first path, and assigned $\lambda_2$, because $\lambda_1$ is occupied by $d_2$ on link 2-4: 6-5-2-4 ($\lambda_2$).

  - $d_5$ is routed on its first path, and assigned $\lambda_1$: 7-4-2-1 ($\lambda_1$).

  - $d_6$ is routed on its first path, and assigned $\lambda_2$, since $\lambda_1$ is occupied by $d_5$ on link 7-4: 8-7-4-3 ($\lambda_2$).

  - As for $d_1$, on its first path 2-4-7, both $\lambda_1$ and $\lambda_2$ are occupied over link 2-4. Due to wavelength contention, the second path is also checked: 2-5-6-8-7. $\lambda_1$ is not free over link 2-5, being occupied by $d_3$. $\lambda_2$ is also not free over link 8-7, being occupied by $d_6$. Consequently, $d_1$ cannot be routed without wavelength conversion, and its processing is postponed to Step 3.

  In this step, wavelengths are treated as a "dummy" variable, without more influence than that of the wavelength continuity constraint. The aim of this step is to provide a preliminary routing, the wavelength assignment, however, takes place in Step 3.

- Step 2:

  In this step, node counters are calculated according to the QoT assumption under flat-systems consideration, *i.e.*, QoT becomes unacceptable within the third hop of the path. Whenever QoT drops, a regeneration is needed at the preceding node, *i.e.*, the counter of the third node on the path is incremented in our case.

  Nodes are then sorted in the decreasing order of their counters: $2 \rightarrow 4 \rightarrow 7$. The first $\mathcal{R}$ nodes are considered potential regeneration sites ($\mathcal{R} = 2$). Therefore, nodes 2 and 4 are considered installed regeneration sites in Step 3. This favors the use of these two sites for regeneration in the next step, but does not limit the regeneration in the network at each of them; as aforementioned, other regeneration sites can also be deployed.

- Step 3:

  First, let us consider $\Theta = \{d_1\}$, where the processing of $d_1$ was postponed until this step.

  Routed demands in Step 1 are considered one by one. For each, COR2P fetches for its BBF wavelength on its dedicated path, providing an acceptable QoT, assuming non-flat systems. $d_2$, $d_3$, and $d_5$ are assigned $\lambda_1$ on their paths, while $d_4$ and $d_6$ could

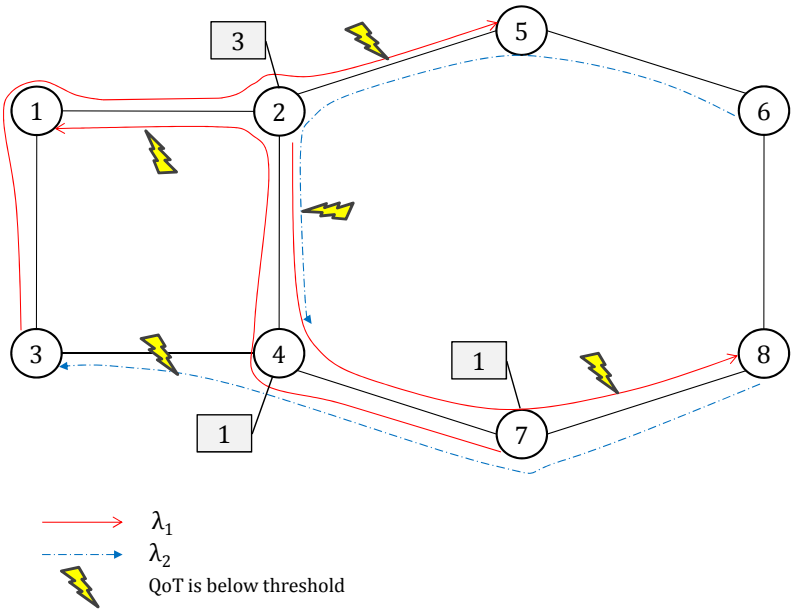


Figure 5.7: Illustration of Step 2 and node counter computation.

not be assigned $\lambda_2$ because it provides unacceptable QoT at destination. The set $\Theta$ is then updated: $\Theta = \{d_1, d_4, d_6\}$.

*Processing of PLDs in* $\Theta$*:*

- Processing of $d_1$: on its first path 2-4-7, $\lambda_2$ is the BBF wavelength for this path. It also provides an acceptable QoT at destination. Thus $d_1$ can be established without the need for regeneration.

- Processing of $d_4$: on its first path 6-5-2-4, there is no more free wavelength on link 2-4. On its second path 6-8-7-4, only $\lambda_2$ can be used, but it provides a bad QoT at node 4. And since there are no regeneration sites over this path, and because COR2P does not allow for adding a new regeneration site except on the first path, $d_4$ is rejected.

- Processing of $d_6$: on its first path 8-7-4-3, the BBF wavelength is $\lambda_2$, but provides a bad QoT at node 3. Since this path comprises a regeneration site at node 4, benefiting from a regeneration at this site provides a good QoT at destination, and $d_6$ can then be successfully established.

In the end, one PLD has been blocked, and one effective regeneration site (at node 4) has been deployed, neglecting node 2, although considered as a potential regeneration site in Step 2.

## 5.5 Results and discussion

### 5.5.1 Simulation environment

In this part of the thesis, we consider the 18-node American National Science Foundation backbone network (NSFNet-18), wherein the optical switching fabrics are assumed to be MEMS-based. Losses and impairments intrinsic to this type of fabric are given in Table 3.3. Figure 5.8 illustrates the NSFNet-18. SMFs are deployed at the fiber-links covering the C-band (around 1550 nm) with a 100 GHz channel spacing, providing $\mathcal{W} = 40$ wavelengths on each fiber. The nominal capacity per wavelength is assumed to be of 10 Gbps. Double-stage EDFA amplifiers are deployed at each fiber-span (80 km) in order to recover from fiber losses. In order to cope with dispersion at the spans, DCF fibers are deployed at the central stage of the in-line amplifiers. Their provided dispersion slope is equal to -100 ps/nm per span. Pre-compensation is also deployed at the nodes, with a dispersion slope of -800 ps/nm. Gain equalizers are deployed every 400 km (5 spans). More details concerning the characteristics of the transmission system can be found in [88].

In the current study, the considered threshold of the $\mathcal{Q}$-factor ($\mathcal{Q}_{th}$) is 12.6 dB. This value corresponds to a BER of $10^{-5}$ assuming forward error correction (FEC) at the destination. We also consider an acceptable blocking ratio of 1% for the QoS criterion.

Without any loss of generality, and since the OpEx cost cannot be evaluated explicitly according to the statement of different operators, we consider the ratio $\mathcal{C}_C/\mathcal{C}_O$ equal to 1 (Cf. Equation (5.2.4)). We consider 5 shortest paths between each source/destination node pair ($\mathcal{K} = 5$). The regenerator pool size $\mathcal{X}$ is set to 100 according to the assumption made in Section 5.2.2, unless otherwise is stated.

Simulations cover five traffic loads ranging from 100 to 500 connection requests. For each traffic load, 10 static traffic matrices are generated randomly according to a uniform distribution. Therefore, all the presented results are mean values of 10 simulations.

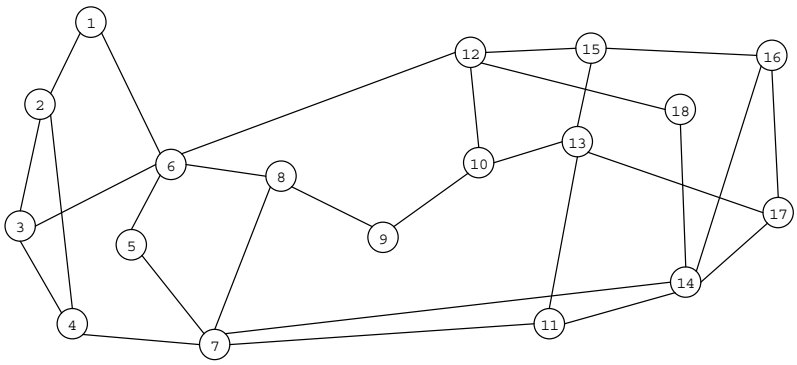


Figure 5.8: The American 18-nodes NSF backbone network topology (NSFNet-18).

### 5.5.2 Regeneration Concentration

COR2P performs a cross-optimization between two main objectives: minimization of the rejection ratio, and minimization of the network cost. We recall that the connection cost considered in COR2P can be represented as a weighting between the optical resources cost and the electrical resources cost. For practical referencing, we recall Equation (5.2.2.3) from Chapter 5:

$$Cost_{(connection)} = \alpha \times \frac{\mathcal{H}}{\overline{\overline{\mathcal{H}}}} + (1-\alpha) \times \sum_{i=1}^{\mathcal{H}-1} \mathcal{C}_{\mathcal{R}}(v_i) \tag{5.5.1}$$

This equation is used whenever an impaired lightpath needs an RWA and regeneration solution in order to be established. When the focus needs to be made over the regeneration cost (electrical resources), the parameter $\alpha$ in Equation 5.5.1 should be set to a small value. In this way, the regeneration cost becomes more eminent than the optical resources cost and COR2P should seek activating regenerators from the most used sites, as long as doing so serves the establishment of the lightpaths. Indeed, at the processing of a severely impaired lightpath, the use of already deployed regeneration sites will only take into consideration the OpEx cost relative to activating a regenerator. In addition, the higher the number of activated regenerators in a node, the lower the OpEx cost corresponding to the activation of an additional one. This drives lightpaths to undergo regeneration in the most used sites, resulting in regeneration concentration in some of the network nodes. This concentration of lightpath regeneration in the sites is possible on condition that enough optical resources exist on the ingress and egress links of the regeneration sites.

When existing regeneration sites cannot provide a solution for the establishment of a lightpath, a regeneration site can be added over the shortest path of the lightpath, in order to release the wavelength continuity constraint and drive in a regeneration solution. In this case, the CapEx cost of the site installation is considered. By inserting new regeneration sites in the network, COR2P allows some flexibility in network design while concentrating the regenerators in the most used sites.

In Step 2, COR2P chooses a given number $\mathcal{R}$ of nodes to become regeneration sites, and deploys a regenerator pool at each. In this respect, when a first regenerator is to be activated within such nodes, the CapEx cost of pool installation is not taken into account, considering that it has already been considered. Only CapEx related to additional regeneration site installation is accounted, so that regeneration stays concentrated in the first chosen sites. According to the choice of $\mathcal{R}$, we define our flexibility towards the concentration of regenerators. But it is worth noting that even with $\mathcal{R} = \mathcal{N}$ ($\mathcal{N}$ being the number of nodes of the network) COR2P does not use all of them, since it always tries to activate regenerators in the most previously used sites. In this respect, we define $\mathcal{R}^*$ as the number of effective regeneration sites provided at the end of COR2P. These regeneration sites are those having activated regenerators ($\mathcal{R}^* \gtreqless \mathcal{R}$).

Let us consider $\rho = \frac{\mathcal{R}}{N}$ representing the ratio of regeneration sites among the network nodes. In [101] we discussed the regenerator concentration according to the value of $\rho$.

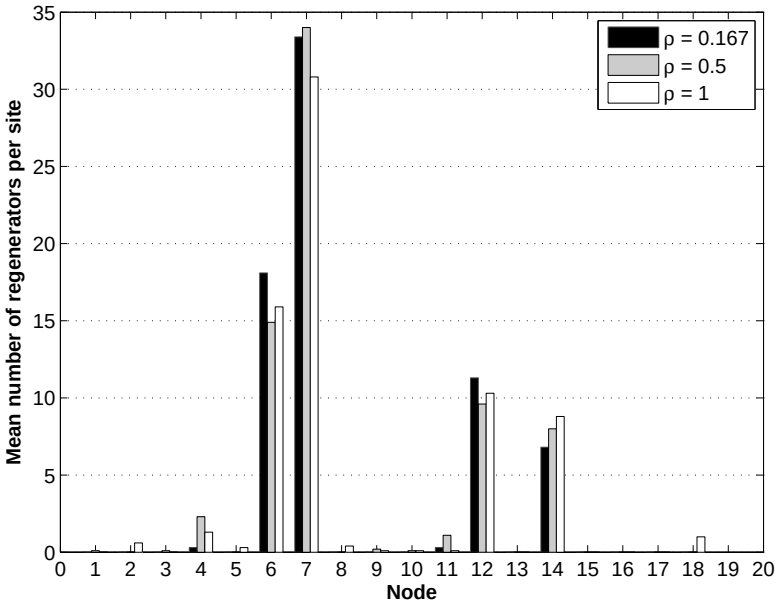


Figure 5.9: Regenerator distribution for a traffic load of 400 PLDs.

In order to favor regeneration concentration, we set the value of $\alpha$ to 0.1. We consider three values of $\rho$: 0.167, 0.5 and 1, corresponding to $\mathcal{R} = 3, 9$, and 18, respectively. It is worth reminding that selected '$\mathcal{R}$' nodes are translucent nodes, which means that even with $\rho = 1$, the network is not considered an opaque network, since optical signals are not systematically regenerated at each node.

Figure 5.9 illustrates the distribution of regenerators over the sites for a traffic load of 400 PLDs and for the considered values of $\rho$. From these results we can drive out the following conclusions:

- The higher the ratio $\rho$, the higher the number of effective regeneration sites $\mathcal{R}^*$. Indeed, when allowing a higher number of regeneration sites than the exact need of the network, some sites are used for a very small number of regenerators (see small bars on the figure). This is costly for the operator where not only should a regenerator pool be installed at the node, but also, a monitoring team should operate the pool even though only few regenerators are activated within. The Return On Investment (ROI) in such regeneration sites is far too small in comparison to sites that can be considered as hotspots for regeneration.

- The predominantly used regeneration sites (nodes 6, 7, 12, and 14) have the highest nodal degrees and longest average distances with their first neighbors (Cf. Figure 5.8).

Figure 5.10 depicts the number of effectively used regeneration sites with regard to the traffic load and $\rho$. We first point out that for for $\rho = 1$, and for the highest considered

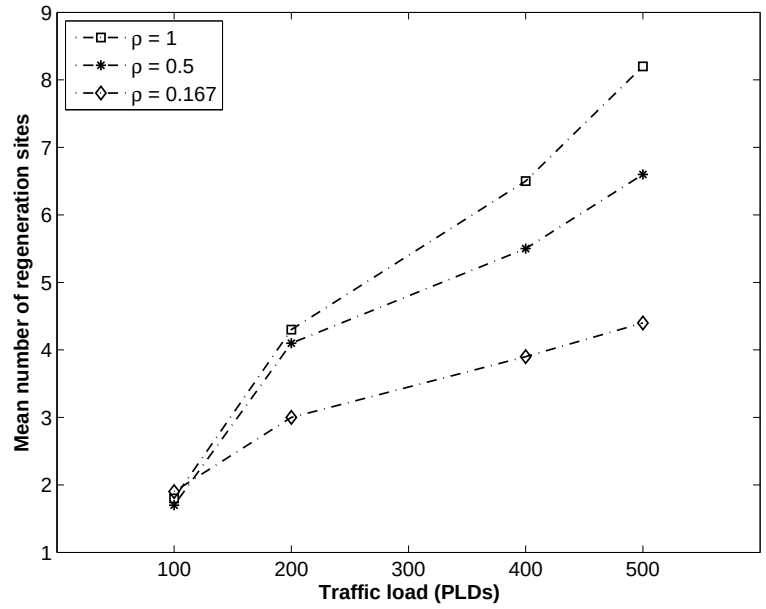


Figure 5.10: Effective number of regeneration sites w.r.t. $\rho$.

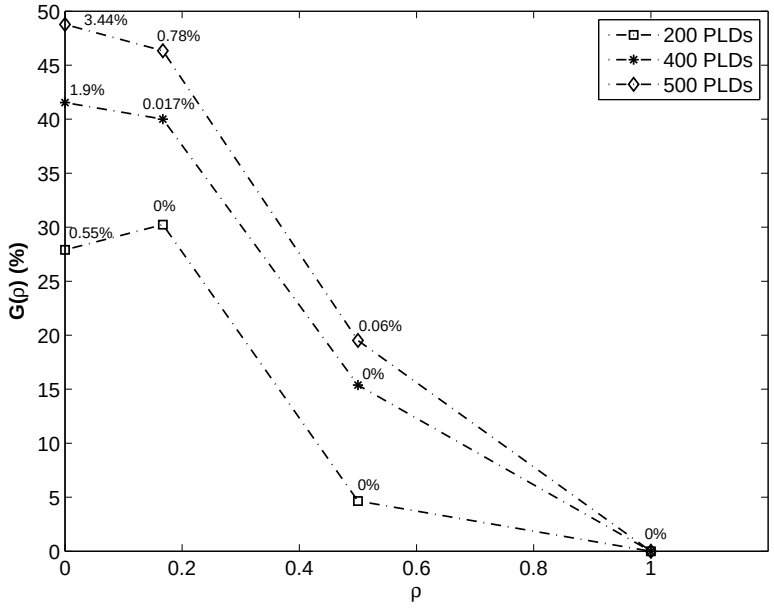


Figure 5.11: Effective number of regeneration sites w.r.t. $\rho$.

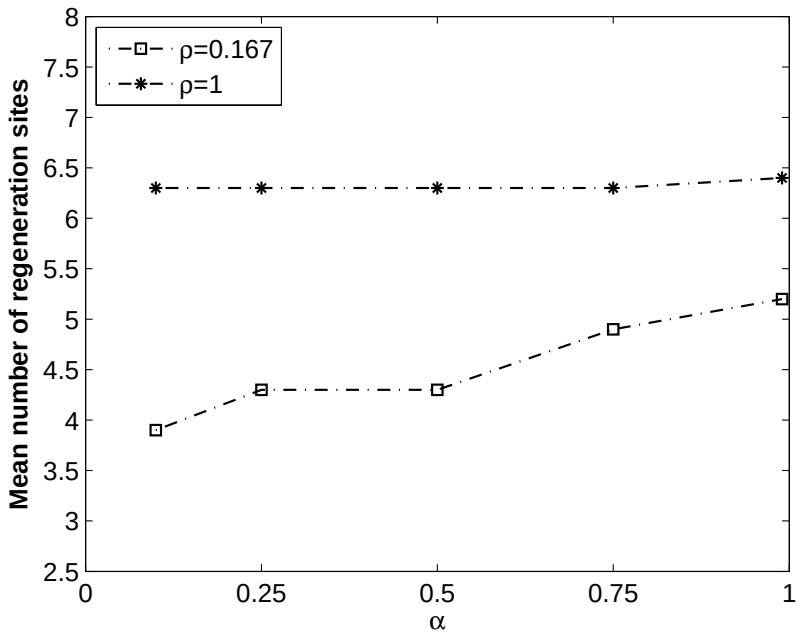


Figure 5.12: Effective number of regeneration sites w.r.t. $\alpha$.

traffic load (500 demands) an average of only 8.2 sites is effectively used. This means that, even though COR2P allows the use of all of the network nodes for regeneration, less than half of the network nodes are effectively used. This strongly highlights the concentration of the regenerators urged by the cost function implemented within COR2P.

Collaterally, for $\rho = 0.167$ and for a traffic load of 500 demands, an average of 4.4 ($> 3$) regeneration sites is effectively used. This means that COR2P allowed the installation of pools of regenerators in other sites than those considered at the end of Step 2, in order to successfully establish the lightpaths.

Let us consider the case $\rho = 1$ as a reference case. In Equation (5.5.2), we introduce $G(\rho)$ as the gain in the number of effective regeneration sites with respect to our reference case. This gain is illustrated in Figure 5.11.

$$G(\rho) = \frac{\mathcal{R}^*_{(\rho=1)} - \mathcal{R}^*_{\rho}}{\mathcal{R}^*_{(\rho=1)}} \tag{5.5.2}$$

Our concern is to find the best value of $\rho$ that leads to the optimum number of regeneration sites with regard to the acceptable blocking ratio ($< 1\%$). In the figure, we have coupled to each value of $G(\rho)$ the corresponding blocking ratio. For traffic loads of 400 and 500 PLDs, the optimum value of $\rho$ is 0.167 corresponding to $\mathcal{R} = 3$ whilst lower numbers of effective regeneration sites can be achieved with $\rho = 0$ at the price of unacceptable blocking ratios. Under 200 PLDs, $\rho = 0.167$ enables the highest gain with null blocking ratio [101].

Figure 5.12 depicts the impact of $\alpha$ over the effective number of regeneration sites for a

traffic load of 400 demands. We considered $\rho = 0.167$ and $\rho = 1$ (the optimum and worst *scenarii* in terms of the number of effective regeneration sites w.r.t. an acceptable blocking ratio). For $\rho = 1$, all network nodes are regenerating, thus the CapEx cost related to the installation of a pool of regenerators does not exist, which explains how $\alpha$ barely impacts the number of regeneration sites. While for $\rho = 0.167$, the concentration due to the value of $\alpha$ is eminent ($\alpha = 0.1$). Small values of $\alpha$ concentrate the regenerators in fewer sites because the CapEx cost of installing new regeneration pools weighs more than when $\alpha$ takes higher values.

In the end, the values of $\alpha$ and $\rho$ jointly affect the concentration of regenerators in a limited number of regeneration sites.

### 5.5.3 Regenerator pool sizing

In the previous section, we showed that whatever the value of $\rho$, COR2P concentrates regenerators in less than half the network nodes. In addition, we have pointed out the two values: $\rho = 1$ and $\rho = 0.167$, as those leading to the highest and lowest mean numbers of effective regeneration sites $\mathcal{R}^*$, respectively, while still providing an acceptable QoS. In this section, we investigate the optimum size of the regenerator pool to be deployed in the translucent nodes.

We recall that $\mathcal{R}^*$ represents the number of effectively used regeneration sites and represent by $\mathcal{X}_i^*$ the number of regenerators activated in regeneration site $v_i$. We also introduce $\mathcal{X}^* = \max_i \mathcal{X}_i^*$.

In the following, we consider two traffic loads made of 400 and 500 PLDs, respectively. Figure 5.5.3 plots $\mathcal{X}^*$ and $\mathcal{R}^*$ under the considered traffic loads for $\rho = 0.167$ and $\rho = 1$.

For $\rho = 1$, regeneration is potentially possible in all the network nodes. Hence, PLDs have further regeneration possibilities than the case of $\rho = 0.167$ where regeneration is more concentrated. In this respect, the number of required regenerators per site should be less for $\rho = 1$ in comparison to the other case. Therefore, we consider different values of initial pool size $\mathcal{X}$, in order to finally choose the effectively needed pool size $\mathcal{X}^*$.

- For $\rho = 1$, and under 400 PlDs, 7 regeneration sites holding 25 regenerators each are sufficient to guarantee a good QoS, whereas, 8 regeneration sites holding 26 regenerators each are required under 500 PLDs.

- For $\rho = 0.167$, 5 regeneration sites holding 30 regenerators within, are necessary to guarantee a good QoS under 400 demands, and 6 regeneration sites having 44 regenerators are needed under 500 demands.

Choosing a lower number of istes holding a larger number of regenerators, or, inversely, a higher number of sites holding fewer regeneratros depends on the carrier's strategy.

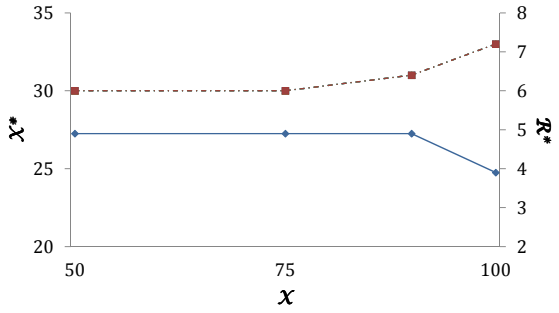


(a) 400 PLDs, $\rho = 0.167$

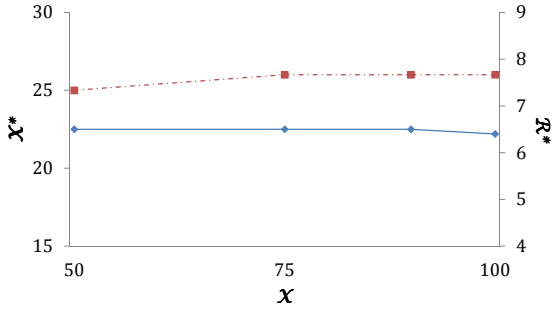


(b) 400 PLDs, $\rho = 1$

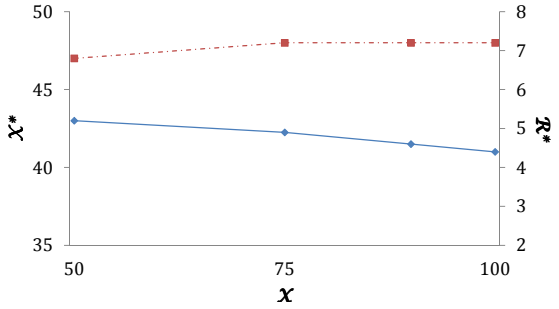


(c) 500 PLDs, $\rho = 0.167$

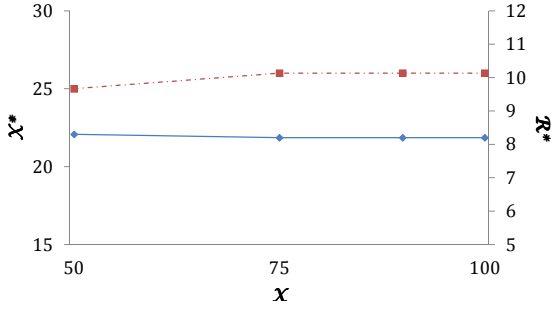


(d) 500 PLDs, $\rho = 1$

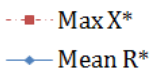


Figure 5.13: Mean $\mathcal{R}^*$ and maximum $\mathcal{X}^*$ values w.r.t. $\mathcal{X}$ for: (a) 400 PLDs and $\rho = 0.167$, (a) 400 PLDs and $\rho = 1$, (a) 500 PLDs and $\rho = 0.167$, and (a) 500 PLDs and $\rho = 1$.

### 5.5.4 Comparison with other RP approaches

In the previous section we have focused on an important feature of COR2P: the concentration of regenerators in some of the network nodes. In this scope, we highlighted (*i*) the cost function within COR2P and (*ii*) the choice of certain regeneration sites before the effective RWA and regeneration phase.

In this section, we provide a performance analysis of COR2P by means of comparison with two regenerator placement algorithms from literature, namely RP-CBR+ and LERP. We call RP-CBR+ an amelioration we made to the approach proposed by Pachnicke et *al.*, in [85, 86] in [102, 103]. In this respect, we shortly recall the important steps of the two algorithms and provide in Section 5.5.4.3 a comparative summary of the essential characteristics of COR2P RP-CBR+, and LERP, before proceeding to numerical results in Section 7.4.

#### 5.5.4.1 LERP

In [63], authors introduce a heuristic-based algorithm called LERP for *Lightpath Establishment and Regenerator Placement*. LERP aims at minimizing the number of required regenerators in the network while optimizing the resource utilization w.r.t. QoT requirements. In a first step, LERP uses a Random-Search-based (RS-based) scheme to find an RWA solution for a given set of PLDs. Rejected requests due to lack of network resources are stored for processing in a third step. In a second step, LERP runs a QoT-Test over the lightpaths given out in the previous step respecting the order provided by the mentioned RS scheme. Each lightpath is tested hop-by-hop and when a regeneration is required, the lightpath is dispatched into two lightpaths: an established lightpath, prior to regeneration and a residual lightpath. The residual lightpath is added to a new traffic matrix made of only residual lightpaths. After all lightpaths provided by the first step are tested, the residual lightpath matrix constitutes an input for another RS-based RWA module. This operation is repeated each time for the new RWA solution respecting the updated set of available resources until no more residual lightpaths exist. In the third and last step of LERP, the rejected demands at the first step are reconsidered in a third RS-based RWA module that takes into account the residual network resources. The same iterative operation including the QoT-Test and the residual lightpath matrix as in the second is applied, only this time some residual parts of requests may be actually rejected by lack of resources.

#### 5.5.4.2 RP-CBR+

In [85], [86], Pachnike et *al.*, propose a regenerator placement (RP) and a Constraint-Based Routing (CBR) strategies. In [102], we proposed an improved version of Pachnicke's algorithm, called RP-CBR+.

In its first phase, Pachnicke's algorithm relies on a heuristic proposed in [81] to determine regeneration sites. Connection requests between all node pairs are considered

assuming unlimited network capacity under flat systems. In other terms, each of these traffic requests is routed over its shortest path. At this step, the algorithm computes for each node the number of non-QoT-admissible connections that could be established if the considered node was equipped with an infinite-size regeneration pool. Let $\phi_{n_i}$ be the set of such connections for node $n_i$. Once all the nodes have been investigated, the node $n_1$ with the highest $|\phi_{n_1}|$ is considered as an effective regeneration site. The operation of computing $\phi_n$ for all nodes then choosing an effective regeneration site is repeated each time for the set of demands that remain non-QoT-admissible until all the demands become admissible, *i.e.*, $\phi_n = \emptyset, \forall n$.

In its second phase, Pachnicke's approach treats the traffic requests of a given traffic matrix in an arbitrary order. Effective regenerator placement occurs along with RWA under limited network capacity. We have improved Pachnicke's original algorithm in order to minimize the number of regenerators. The $\mathcal{K}$-shortest paths are computed for each demand and starting from the first path, different regenerator placement combinations are investigated. The first QoT-admissible combination providing the least number of regenerators is considered as the retained solution. For each combination, the algorithm tries to find free wavelengths over the resulting transparent sections of the path, the First-Fit (FF) strategy being adopted under non-flat systems. We recall that under the FF WA strategy, wavelengths are indexed in their order of presence in the spectrum, and the first free wavelength is assigned to the considered lightpath. The $\mathcal{Q}$-factor is evaluated at the end of each section. In case of non-admissible QoT for all the combinations inherent to the $k^{th}$ shortest path, the $(k+1)^{th}$ shortest path is considered. RP-CBR+ aims to reduce the number of required regenerators in comparison with the original version of Pachnike's algorithm.

| Criterion | RP-CBR+ | COR2P | LERP |
|---|---|---|---|
| **Dedicated phase for choosing regeneration sites?** | Yes | Yes/No (adaptive: $\rho = 1$ or $\rho \leq 1$) | No |
| **Number of regeneration sites** | Fixed (restricted to the first phase's result) | Adaptive<br>With pertinent values of $\rho$ and $\alpha$, regeneration concentration in some sites is manageable.<br>-choosing $\rho < 1$ and $\alpha$ near 0 urges COR2P to stay as much as possible within the first $\mathcal{R}$ sites.<br>-choosing $\rho = 1$ and $\alpha$ near 1 gives COR2P more freedom in terms of regenerator placement in all the network nodes, but still won't eliminate concentration. | All nodes are potential regeneration sites |
| **Processing order of demands** | Arbitrary | -QoT-dependent order for demands successfully routed in Step 1<br>-Arbitrary order for demands rejected in Step 1 due to capacity limitations. | a Random Search chooses the best sequence of demands providing the lowest rejection ratio |
| **Wavelength assignment strategy** | FF | BBF | BBF |

Table 5.2: Comparative summary of RP-CBR+ , COR2P and LERP.

#### 5.5.4.3 Comparative summary

Table 5.2 summarizes the essential differences between COR2P, RP-CBR+ and LERP. It is important to note how RP-CBR+ restricts the regenerator placement to the sites that it determines in its first phase, while LERP allows inserting regenerators in any site of the network. COR2P, in comparison, can be adapted to each of the two scenarios. On one hand, choosing $\alpha$ near 0 urges COR2P to respect as much as possible the regeneration sites ($\mathcal{R}$) considered at the third step of COR2P. On the other hand, choosing $\alpha$ near 1 allows more freedom for regenerator placement even in new sites if needed, as explained in Section 5.5.2. In the following we will precise the different values of COR2P's parameters in order to compare it to the two algorithms.

#### 5.5.4.4 Comparison results

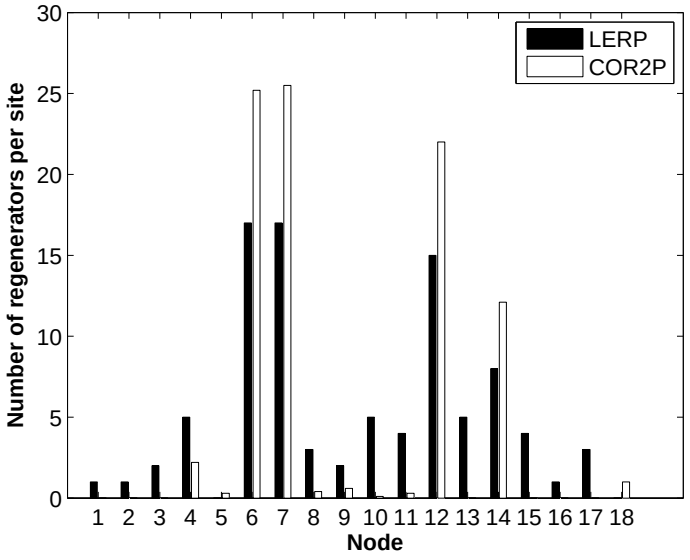


Figure 5.14: LERP vs. COR2P: Regenerators distribution under 400 demands

**5.5.4.4.1 Comparison with LERP** In order to compare COR2P to LERP, COR2P's parameters should meet LERP's environment. Thus, since LERP does not consider a limited regeneration capacity per site, we choose to set $\mathcal{X}$ to 100 in COR2P: a ceiling that is not reached for the traffic matrices considered in our simulations. Moreover, since LERP does not concentrate the regenerators, we consider $\alpha = 0.99$[6]. $\rho$ is also set to 1.

Figure 5.14 shows the distributions of the regenerators over the network nodes under COR2P and LERP. The considered traffic load is made of 400 PLDs. We notice that LERP places 16 regenerating nodes while the mean number of effective sites in COR2P over the 10 matrices is 6.4, *i.e.*, COR2P provides a difference of 60% of regeneration sites

[6]We do not choose $\alpha = 1$ in order to save the comparison between the alternative $\mathcal{K}$-shortest paths.

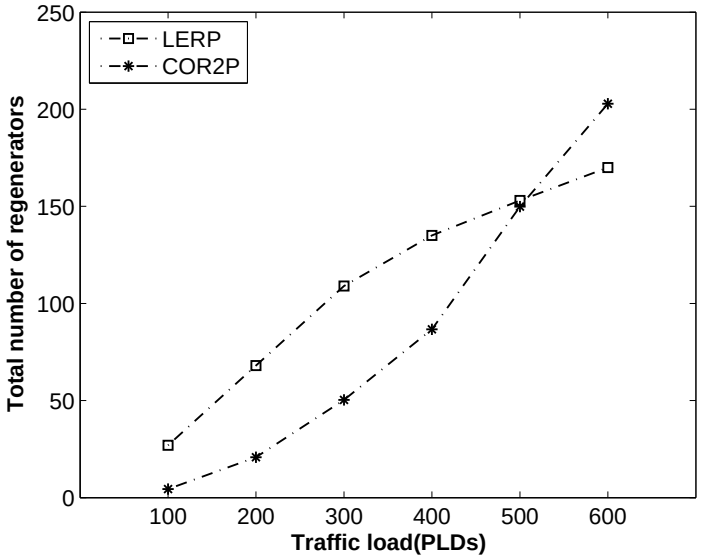


Figure 5.15: LERP vs. COR2P: Total number of regenerators w.r.t. traffic load.

in comparison to LERP. The total number of regenerators under COR2P is equal to 89.7 regenerators whereas it is equal to 135 under LERP.

Figure 5.15 shows the evolution of the mean number of required regenerators with respect to traffic load. This figure shows the limits of impact of the QoT-dependent order according to which the traffic requests are considered for RWA in COR2P. For low and moderate traffic loads (*i.e.*, less than 500 demands), sorting the demands in the aforementioned order allows better use of network resources than LERP. As a result, COR2P presents advantageous number of required regenerators in comparison to LERP. As for high traffic loads, this QoT-dependent order is not very effective since the network is overloaded and faces blocking due to lack of resources. In this case, LERP outperforms COR2P for the reason that it uses the best combination for the RWA solution in order to minimize the number of regenerators, while COR2P processes the demands needing regeneration sequentially in its third step. As a conclusion for identical scenarios, and for low or moderate traffic loads, COR2P reduces both the total number of regenerators and the number of sites compared to LERP. As for higher traffic loads, COR2P's feature of ordering demands in a QoT-dependant order has negligible effect, and demands needing regeneration should consider a non-sequential order in the last step.

**5.5.4.4.2 Comparison with RP-CBR+** Simulation run over the NSFNet-18 under RP-CBR+ defines six *a priori* regeneration sites: $4, 6, 7, 12, 14, 17$. For $\rho = 0.33$ ($\mathcal{R} = 6$), the first phase of COR2P provides the same set of sites. Moreover, RP-CBR+ assumes unlimited-size regeneration pools, thus, for comparable *scenarii*, we have chosen "$\mathcal{X} = 100$" and set '$\alpha$' to 0.1 under COR2P.

Figure 5.16 illustrates the blocking ratio versus the traffic load for both algorithms.

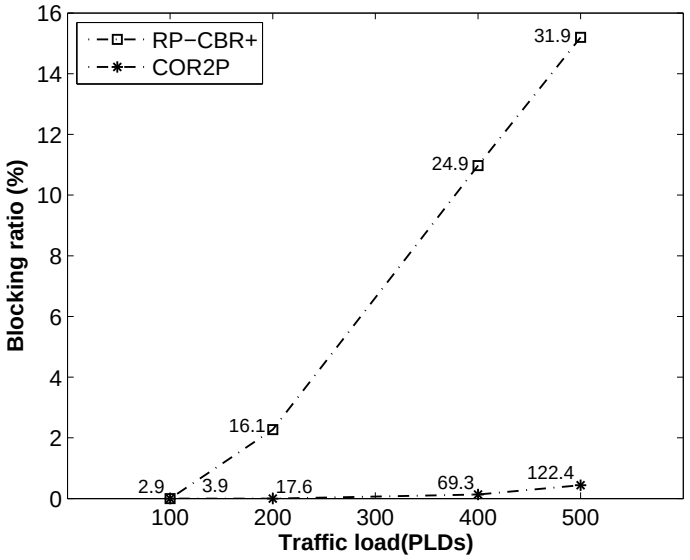


Figure 5.16: COR2P vs. RP-CBR+: Blocking ratios w.r.t. traffic load.

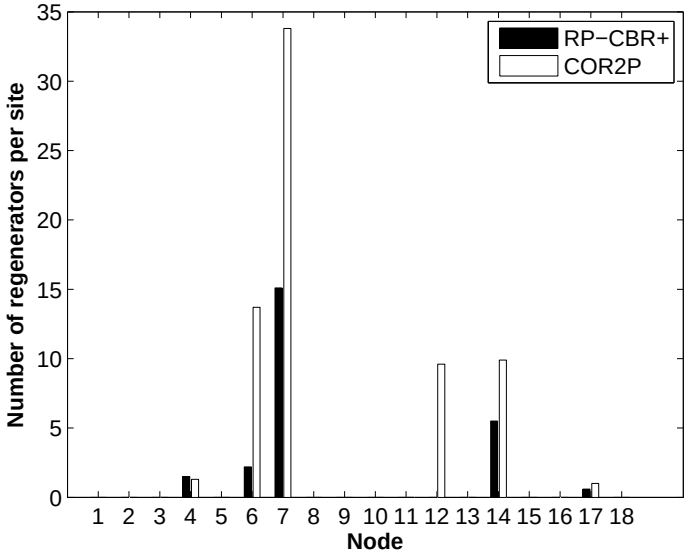


Figure 5.17: COR2P vs. RP-CBR+: Regenerators distribution under 400 PLDs.

The values attached to the plotted curves in the figure represent the average numbers of regenerators. Figure 5.17 depicts the regenerator distribution over the network nodes under 400 traffic requests. load. Figure 5.16 also compares the two algorithms in terms of blocking ratio. We notice a big difference between COR2P and RP-CBR+ in terms of blocking ratios. On one hand, for a traffic load of 200 PLDs, COR2P accepts all traffic demands whereas RP-CBR+ presents a blocking ratio of 2.5%, although having the same number of regenerators. On the other hand, under higher traffic loads, COR2P keeps reasonable blocking ratios while they reach 11% and 15% for 400 and 500 PLDs, respectively. This gap of blocking ratios between the two algorithms is compensated by regenerators in the network; COR2P inserts a lot more regenerators than RP-CBR+ . It is worth noting that for 400 PLDs, COR2P does not add regeneration sites to the first fixed six (see Figure 5.17).

We justify the flexibility in terms of successfully established lightpaths presented by COR2P by two important criteria:

- First, the order by which COR2P processes PLDs: in decreasing order of QoT over the best path (Cf. Step 1 in Section 5.3.2.1 of Chapter 5).
- Second, the wavelength assignment strategy adopted by COR2P: BBF, is more adapted to the impairement constraints than the FF strategy adopted in Pachnicke's approach [79].

At last, for traffic loads higher than 500 PLDs, COR2P adds isolated regenerators in new nodes (*e.g.*, for 500 PLDs, nodes 8 and 10 hold a regenerator each), which also helps establishing lightpaths. lightpaths.

As a conclusion, COR2P presents a blocking ratio 100 times lower than RP-CBR+ under high traffic loads, a benefit obtained at the price of a greater number of regenerators.

## 5.6 Conclusion

In this chapter, we have introduced a new tool for translucent network design adopting the sparse regeneration approach. This tool, called COR2P, reduces the rejection ratio as well as the regeneration cost of the lightpaths that are most impaired in the network.

We have explained in details our approach for the cost evaluation of lightpath establishment. For that purpose, we have provided a cost function that enables regeneration concentration in some of the network nodes.

In addition, we have discussed simulation results that show the different features of COR2P. In order to highlight the benefits of COR2P, we have compared it to two heuristic-based algorithms from the literature. We have shown that allowing flexible regeneration in the network nodes helps minimize the regeneration ratio of traffic requests. We have also provided a regenerator pool sizing strategy that depends on the operator's criteria. Finally,

we focused on the influence of impairment-aware request processing and WA strategies on the total number of regenerators and the rejection ratio.

# Part II

# Energy-Aware WDM Network Design

# Chapter 6

# Green Networking in core networks

## 6.1 Introduction

The telecommunication industry has become prone to offer high capacity services to their clients, as major advances are undergoing in silicon industry, routing/switching control and fiber transport. The power consumption of networks, in this regard, has driven a lot of concern lately, with the increasing green consciousness. In this chapter, we highlight the motivations behind power-aware networking, and identify the candidate components for power consumption minimization at the WDM layer, given a practical network architecture. We also provide a review of related work in order to further highlight our contribution in this field.

## 6.2 Power-awareness in networks: drivers

In order to cope with data volume growth and new broadband services requirements, network operators are increasingly deploying high performance equipment, from access to core. Consequently, the evolution of inherent energy consumption in the Information and Communications Technology (ICT) sector has become of major concern. *Green networking* has become an important field of discussion for two reasons. At one hand, climate change due to Greenhouse Gas (GHG) emission has become a world-wide interest. In this respect, reducing high energy consumption induces lower CO2 emission intensity. At the other hand, environmental consciousness has driven governments to rise energy price in order to penalize non-eco-friendly industries and encourage energy awareness. As a consequence, operational costs induced by electrical power needs grow opposite to the operators' expectations.

Statistics of network energy consumption show tremendous increases in overall energy consumption. For instance, in 2007, almost 10 % of the UK's power consumption was due to operating ICT equipment. In 2006, power consumption of Telecom Italia increased by

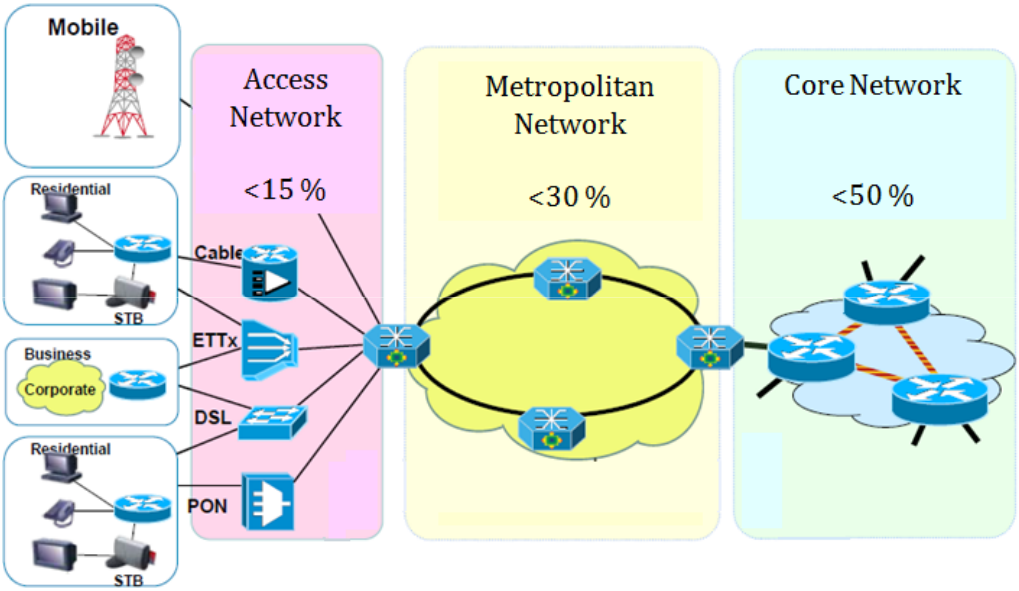


Figure 6.1: Effective device utilization in internet networks.

7.95 % with respect to the year 2005. Operating network infrastructures and data centers accounted for 90 % of this power consumption. Deutsche Telekom reported in 2007, that 20 % of energy waste was inherent to cooling systems [21].

It is now almost confirmed that future internet capacity will not be limited by the networking equipment capacity, but by energy constraints. Besides, it is worth noting that power throughput in networks is less than 50 % [55]. This is illustrated in Figure 6.1.

Figure 6.2 depicts operational estimations in a typical operator network deployed nowadays. Although only 6 % of network devices are deployed at the metro and core networks, inherent energy needs constitute 30 % of overall network consumption. In fact, operational power requirements of networking equipment depends on the capacity they handle. The more towards the core network, the more power-greedy the equipment.

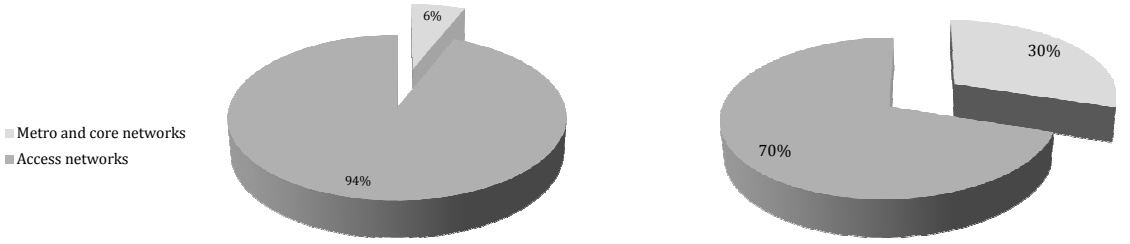


(a) Percentage in number of devices per network level.

(b) Energy requirements per network level.

Figure 6.2: Energy requirements in typical carrier networks.

The data plane has been identified as the most power-consuming throughout the network levels. This is justified by the complex functionalities it tackles at very high speeds

(packet processing and forwarding, buffering, etc...). Considering the sole example of a core IP-router, estimations of power consumption show that data-plane, control plane and heat management account for 54 %, 11 %, and 35 %, respectively [93]. This explains, in part, the gap between network devices number and energy requirements between the access level on one hand, and the transport and core levels on the other hand. Indeed, transport and core networks present more sophisticated data plane than the access networks.

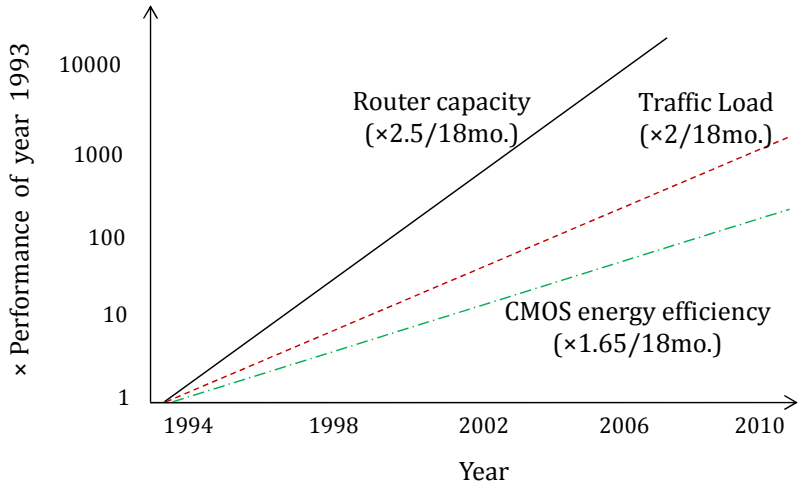


Figure 6.3: Evolution of router capacity, traffic load and CMOS energy efficiency.

While traffic evolution follows Moore's law by doubling every 18 months, routers capacity increases 2.5 times in the same time period. Silicon-based technologies, present lower level power increase (at a factor of 1.65), allowing lower power consumption augmentation of designed routers [21, 50]. However, generalizing throughout the network, introducing new low consumption networking technologies (all-optical equipment, silicon-based technologies...) is not sufficient to meet total energy cost. New network architectures -including equipment architectures-, energy-aware protocols and equipment usage management help achieve better eco-sustainability. In addition, it is stated that 2 W of electricity for cooling systems are required for every consumed watt at the central offices [50]. Therefore, power consumption corresponding to heat dissipation, as well as inherent operational costs can be alleviated thanks to power-aware networking solutions.

In the short-term, solutions targeting the existing infrastructures must be provided until the emergence of green-networking technologies and equipment.

## 6.3 Power-awareness at the WDM core

Our study considers energy-awareness in core WDM networks. Two main approaches are generally adopted to improve energy efficiency in such context:

- *Design of power-aware devices*: introducing new architectures relying on energy-efficient technologies aim at indulging more energy-efficiency in network devices. Some researches address future highly-integrated all-optical processing components like optical buffers, wavelength converters and switching fabrics [56, 39]. These equipment should also be able to offer adaptability with different technologies from previous generations and different vendors. This field of investigation is vast and faced with too much challenges including standardization constraints. In [23] energy conservation is tackled through *best-of-breed* technology aiming at removing all unnecessary computation for packet processing. The research covers Central Power Unit (CPU), memory and chipset design for network equipment. In [22] authors propose an optical core architecture where an intermediate OXC is inserted between the router and transponders to achieve power efficient behavior in comparison to currently deployed core architecture. At the access level, devices allowing data rate adaptation to the effective traffic are highly promising, following the launch of the Energy Efficient Ethernet (EEE) IEEE 802.3az task force [2, 48, 49, 47]. *Elastic* Optical Line Terminals (OLT) which accommodation ability depends on the required rate of each service both in upstream and downstream communications are discussed in [53].

- *Power-efficient control plane*: control plane can manage the optimization of device utilization according to the traffic needs. Protocols and routines can be defined in order to modulate dynamic adaptation of network usage to traffic evolution in time. As an example of such control plane solutions, power-aware cooperation between Content Providers (CP) and Internet Service Providers (ISP) is proposed in [26]. This cooperation differs from classic cooperation in considering power consumption as an objective to minimize. Preliminary results show important power savings. Some devices including links, whole nodes and network cards can be switched off at off-peak periods while residual traffic is established using the remaining subset of devices [61, 29, 28, 52]. Sleep cycle protocols under Quality of Service (QoS) constraints are also proposed [16]. Power-aware traffic engineering solutions (routing and grooming) [36, 62, 57, 98, 10], based on power calculations and statistics at different network levels seem to be an open field of discussion since they can offer effective solutions for short term realization in actual networks.

In general, power savings -whether achieved through operational or design solutions- can pay off for capital and operational costs. As previously mentioned, power and cost increase slowly in a network's lifetime in comparison to requested capacity as new optical networking technologies are emerging.

In the context of WDM core networks, the introduction of more optics allows not only a huge transmission capacity, but also the reduction of energy-greedy optical-to-electrical-to-optical (OEO) conversions, not to mention cost reduction. Nevertheless, as mentioned in Chapter 2, due to current limitation in optics technology, OEO devices are still deployed

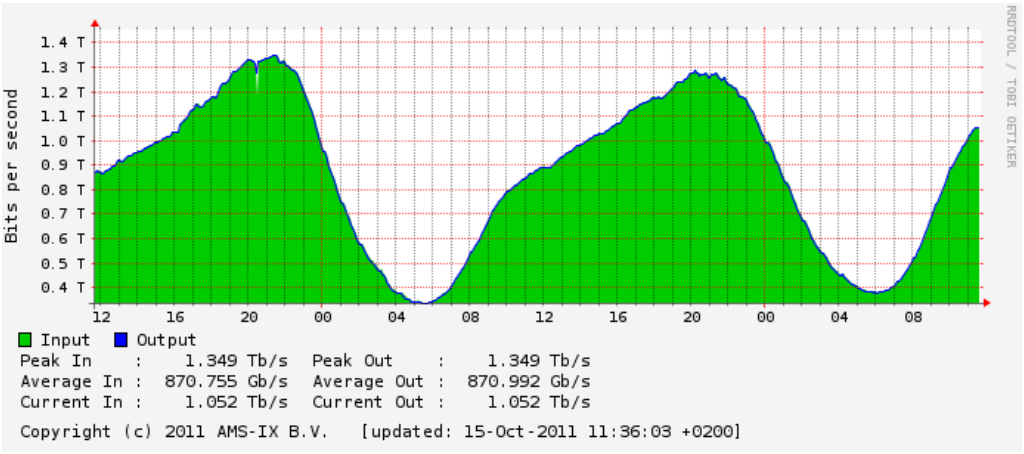


Figure 6.4: Daily graph of traffic load.

for Add/Drop functionality between the optical switching core and the core router, as well as for regeneration functionality [20]. As elaborated previously, in this part of the thesis, we address power consumption at the WDM network considering only transceivers. We do not take in consideration QoT, since doing so adds too much complexity to our problem. Our work can be considered as a step towards considering QoT and power-aware networking, jointly.

## 6.4 Toward dynamic networks

In a typical optical network, once optical channels are provisioned, no channel reconfiguration occurs until end-of-life [92]. Currently, new broadband services and applications are emerging. Nevertheless, such services can have random duration and set-up dates as well as variable capacity needs. Indeed, traffic load is not constant throughout a given observation period (*e.g.*, a day, a week...), it is determined by the human behavior. Figure 6.4 depicts the profile of traffic load in the Netherlands over 48 hours. These data re provided by the Amsterdam Internet Exchange (AMS-IX) service provider [6]. We notice that high traffic loads happen during the daytime and especially in the evening. Low traffic loads can be witnessed during late night and early morning hours.

Traditional networks are designed in such a way to support peak-hour traffic. Routers and client cards are always switched on, ready to be used for transmission at any time, even at off-peak hours. This is a considerable cause of useless power consumption in the network. Idle and sleep modes are suggested to be implemented in the equipment of the future in order to cope with such energy waste [29, 28, 52]. Some research also propose to completely turn-off whole links and nodes [31, 27]. Since these last solutions provoke constraints at the control level, solutions optimizing existing infrastructure utilization are more advantageous for the meanwhile.

In general, a dynamic network should be able to offer the needed capacity bandwidth to its clients with a minimal response time, and minimal bandwidth waste. So far, transmission on fiber uses fixed SONET/SDH data rates (2.5, 10, 40 Gbps). If the channel capacity is less than the requested service capacity, multiple optical channels might be required. Otherwise, a single channel is sufficient, but remaining capacity on the channel might not be used. In both cases, there is a gap between the needed and the offered capacities, and the operator should optimize the utilization of its resources in order to achieve maximum return on investment (ROI). Channel reconfiguration is a key element in this matter. Until now, capacity reconfiguration of a channel is not possible. New research in the field of flexible data rate transceivers is emerging [89, 51]. Such transceivers should be able to switch from a data rate to another, on demand. In addition, such technology allows the network to adapt its transmission to proper data rates depending on performance characteristics over transmission paths[1] [75]. However, channel reconfiguration in terms of carried data is already in service. A channel serves different requests in its lifetime, and sometimes, multiple requests at the same time by means of traffic grooming.

Reconfigurability in order to converge to a dynamic network is an active subject for research. With the invents in mid-link spectral-inverter-based systems, transmission has become transparent to data rates and modulation formats that transit at the same time. These systems are DCF-free[2]. Unlikely, classic DCF-based systems require different dispersion maps for different data rates and formats [83]. In this context, a single spectral inverter supporting multiple WDM channels has been proved to be able of restoring signals with different data rates and modulation formats, transmitted simultaneously.

In addition, significant research has been carried out in the field of multiple data-rate transmission, in order to exploit already deployed networking systems. Currently installed systems are able to transport channels at 40 Gbps and perhaps the next generation 100 Gbps channels. Indeed, 40 Gbps components are marketed since the early 2000's. A key feature of these components is their ability to transport 40 Gbps channels simultaneously with the operated WDM channels at lower data rates. Modulation formats such as the Differential Phase-Shift-Keying (DPSK), the Phase-Shape Binary Transmission (PSBT), and the Polarization Division Multiplexing Quadrature PSK (PDM-QPSK) allow the co-propagation of 40 Gbps channels along with 10 Gbps. DPSK presents high performance transmission allowing twice the optical reach provided by PSBT. The main drawback of this modulation format is its need for complicated filtering at the receiver in order to apply to transmission with 50 GHz spacing between channels. Otherwise, it is a perfect candidate for 100 GHz spacing systems [104]. PDM-QPSK is more appropriate for 100 Gbps transmission because of its efficiency and robustness against linear impairments

[1]The monitoring system of networks supervises channels' performance from end-to-end. If, under high traffic loads, the QoT of some channels drops below the acceptable threshold, the control plane can switch the transmission over such channels to lower data rates. Lower data rates have better performance than higher ones over long distances.

[2]Only tunable post-compensation is used at the end of the transmission line in order to cope with residual dispersion accumulated over the signal.

that become crucial at this data-rate [70, 59, 74, 25].

Deploying multiple data rate transceivers at the network nodes helps achieve a better network capacity usage. With knowledge of traffic profile, operators can dimension their network in such a way to obtain the minimum needed resources. Traffic engineering also plays a key role in determining network equipment to deploy. This dimensioning plan does not require new technology equipment, nor sophisticated control plane functionalities like controlling sleep/active modes of proposed equipment with such possibility.

With traffic varying in time, operators can implement traffic establishment algorithms (RWA) considering the space-time correlation between underlying lightpaths at the optical layer. Grooming traffic can be of great benefit in order to optimize the throughput of transceivers. Optical bypass provided by transparent switching cores also plays an important role minimizing the number of used transceivers. Although being opposite in principle, grooming and optical bypass, together, can provide optimum network design (exact need in equipment) as well as optimum network usage (best traffic routing solution to maximize network equipment efficiency).

## 6.5 Considered node architecture: practical constraints

As aforementioned, we do not take in consideration the quality of transmission of lightpaths in this part of the thesis. Therefore, 3R regenerator banks can be neglected from the node architecture depicted in Figure 2.7 of Chapter 2. In this part of the thesis, WSS-based OXCs are considered. In comparison to MEMS-based OXCs, WSS-based OXCs are made of directionally independent modules, incorporating Mux and Demux functionalities. MEMS-based OXCs are especially inconvenient because the switching fabric acts as a single point of failure. Any failure at any point of the fabric will affect multiple directions whereas a failure at the level of a WSS will only affect the associated direction [41].

In WSS-based OXCs, local add and drop can be considered as a node degree. Figure 6.5 illustrates the architecture of a network node with a connectivity degree equal to 3. The shown ADM is made of a single $(1 \times N)$ WSS and a splitter. The WSS receives signals from the transmitters, multiplexes them into a composite signal, while the splitter does fairly the reverse operation sending single channel signals to the receivers. The input and output of WSS and splitters at the different degrees (including the Add/Drop side) of the OXC are composite signals. The disposition of the ADM in this architecture adds a constraint to the transmission/reception: a given wavelength can only be added (*resp.*, dropped) once. In this respect, the wavelength assignment operation should take in consideration this constraint so that all signals that need to be added at (*resp.*, Dropped) a given node have different wavelengths. In order to alleviate this constraint, another local add and drop degree (and ADM) should be deployed as illustrated in Figure 6.6 where two incoming signals at the same wavelength (designated by the blue lines) need to be dropped at the node.

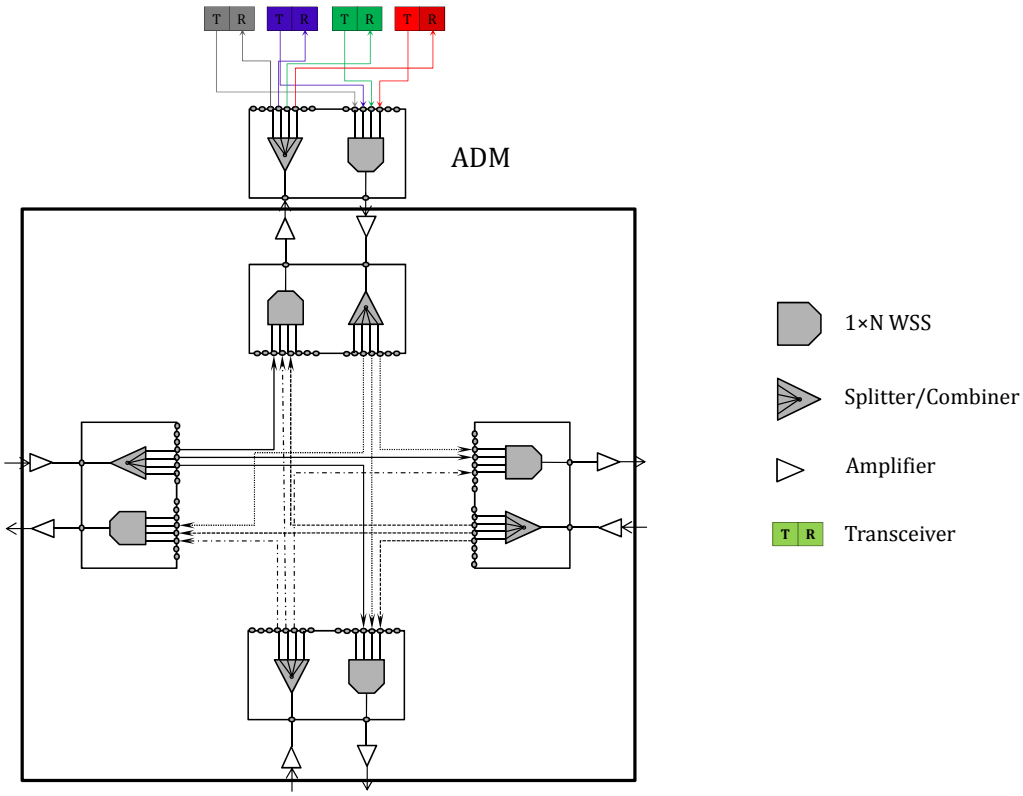


Figure 6.5: Bloc diagram of a 3-degree network node.

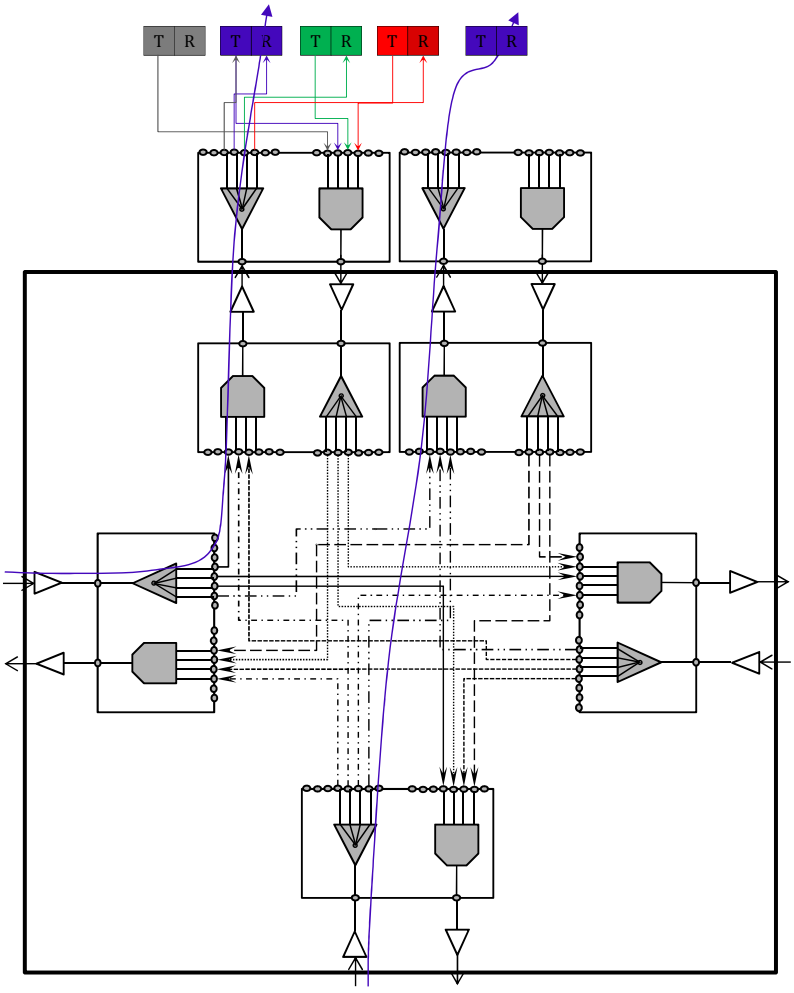


Figure 6.6: WSS-based OXC: dropping signals with the same wavelength.

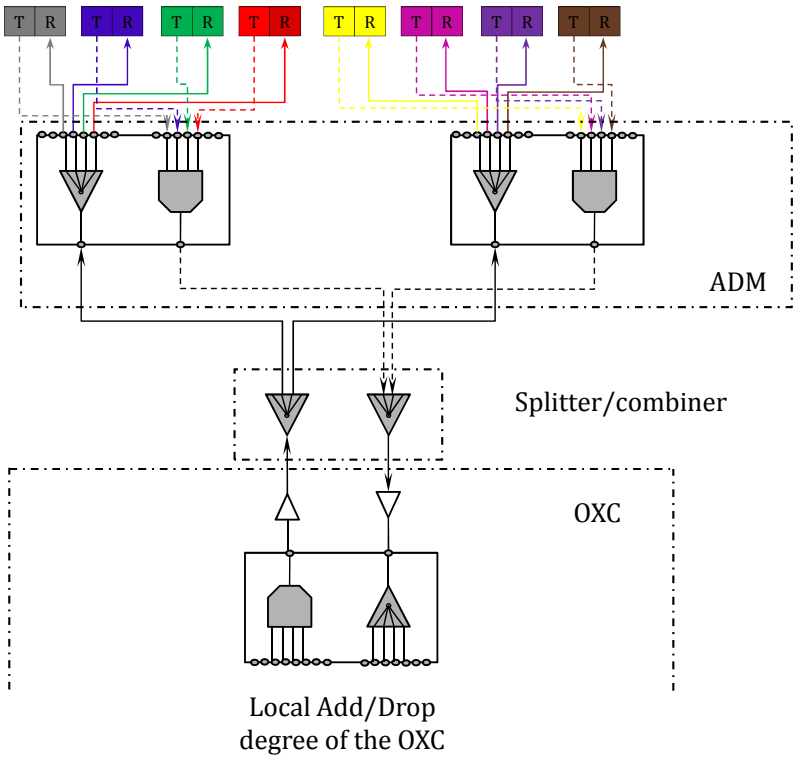


Figure 6.7: WSS-based OXC: adding more wavelengths.

Another issue to consider, is the number of wavelengths dropped or added simultaneously. As depicted in Figure 6.5, $(1 \times N)$ WSS are used at the ADM, which means that only $N$ wavelengths can be used. Inserting a splitter/combiner of size $(1 \times N)$ after the local add/drop degree allows connecting $N$ ADMs and hence, $N^2$ distinct wavelengths can be served. In Figure 6.7 inserted splitters between the local add/drop and the ADM allowed the activation of 4 more transceivers having different wavelengths (at a given time). Another solution is to use WSSs with higher port count ($(1 \times N')$ WSS where $(N' > N)$).

Transceivers, on their turn, have their constraints and specifications. The transmitter and receiver of the equipment, have been historically used in pairs (dual-channel transceivers), and remain so. Single-channel transceivers (transmitter *or* receiver) are commercialized, but still less deployed than dual-channel transceivers. Besides, even though wavelength reconfigurability is provided in today's transceivers, the transmitter and receiver are still deployed at the same wavelength at a given time. Reconfigurability in terms of data rate is not yet a mature technology, and therefore, deployed transceivers nowadays are characterized by their fixed data rate.

In this work, we consider WSS-based OXCs at the nodes with constraints of single-wavelength add/drop with no limitation on the WSS size. The transceivers are dual-channel and have a fixed data rate. In this respect, another constraint is present. In fact, since a transceiver is dual-channel, and the OXC does not allow for two signals tuned to the same wavelength $\lambda$ to be added (*resp.* dropped) except once at a given time, it is

certain that an added signal and a dropped signal, having the same carrier $\lambda$ are related to the same transceiver. Consequently, at a given time, two signals tuned to $\lambda$ where the first one is added and the second one is dropped, need to have the same data rate.

## 6.6 Related work

As elaborated, our study is concerned with the optimization of electrical transceivers at the WDM layer. In this context, some research has been carried out under different assumptions, resorting to grooming and optical bypass approaches.

### 6.6.1 Study of G. Shen *et al.*

In [42], G. Shen et *al.*, propose a design solution for IP-over-WDM networks aiming to establish a set of static traffic requests while minimizing the consumed power. They propose a power consumption model that considers electrical ports, optical switching and optical amplifiers at the fiber-links. It is worth noting that the proposed approach allows to turn-off nodes and links that are not traversed by traffic, which has no practical purpose in operational networks. The authors also take into account the deployment of parallel fibers on the same link neglecting the end equipment allowing the connection with the OXCs.

The proposed approach is translated into three solutions: an exact solution based on an ILP model, and two heuristic-based algorithms. Results show that RWA solutions under grooming possibility can reduce the power consumption of the network by 25 % to 45 % according to network size, with respect to direct-bypass RWA solutions.

### 6.6.2 Study of Xia *et al.*

In [62], Xia et *al.*, propose a traffic engineering approach based on traffic grooming and optical bypass under power constraints. The objective of this approach is to minimize the total power consumption of connections' provisioning. The transmission in the IP and WDM layers is emulated and power consumption of transmission equipment is expressed per 10 Gbps channel. The proposed algorithm chooses a routing and grooming solution for every connection request according to power consumption estimations on the shortest paths. Compared to a classic traffic-grooming approach, the authors show that green traffic routing and grooming provide less power, which proves that minimizing the number of network interfaces without considering their intrinsic utilization is not enough to guarantee an optimal power consumption reduction. The study considered fixed data rate interfaces at 10 Gbps and static traffic. No wavelength assignment was taken into account in the routing process. Regardless of the fact that the operation is sequential and the connection requests order has not been justified, one drawback of this approach is the per-channel power consumption considered especially at the in-line optical amplifiers and at the OXC.

Indeed, these components are fully switched-on permanently, their power consumption is independent of the actual throughput they hold.

### 6.6.3 Study of Idzikowski *et al.*

In [52], Idzikowski et *al.*, propose three approaches that aim to switch network interfaces on when needed, and off when unused following a scheduled traffic pattern. These approaches rely on rerouting the traffic at both the IP and WDM layers. The traffic they consider is sampled and routed at each sample period. Thus some traffic ranging over more than one period might be disrupted and re-routed on another path/lightpath. Which may lead to a great amount of calculations at the control plane, which might not be practical in an actual network even if the considered traffic and its variation are known in advance. The resources used by a demand should serve it until its tear-down time in order to reduce the number of operations that the routers will have to endure. Wavelength assignment is also left for a final phase after each routing period, which also adds more processing to handle.

### 6.6.4 Study of Yetginer *et al.*

In [36], Yetginer et *al.*, formulate the power consumption of electrical operations used for the establishment of a lightpath as the sum of a fixed term and a linear function of the traffic. This formulation is based on the statements in [24, 100] considering on one hand, a non-negligible power consumed in equipment even when no traffic is routed, and on the second hand, a linear dependence on traffic at the switching components. The considered components are the input and output ports of the EXC, as well as the Add/Drop transponders. The total power consumption of the network is then expressed in terms of the number of established lightpaths and the total amount of traffic switched at the electrical layer. The authors address the grooming problem through an exact approach. Three objective functions are considered for the proposed ILP formulation:

- The first objective function is to minimize the number of active electrical ports. This is inherent to the classical grooming operation commonly tackled in the literature. Minimizing the number of active ports means minimizing the number of lightpaths used to establish the traffic load. The authors call the ILP under this objective function: minL.

- The second objective function is to minimize the number of electronically switched traffic. The concerned traffic includes lightpaths that are sent back to the electrical layer at intermediate nodes in order to be groomed with other requests. The ILP is called minT under this objective function.

- The third objective function is to minimize the total power consumption of the network. This corresponds to ILP: minP.

As can be expected, minT achieves very low switching levels at the cost of a high number of lightpaths, avoiding intermediate grooming. minL requires higher amounts of traffic grooming. minP, at its turn results in a moderate amount of traffic grooming at intermediate nodes, proving that minimizing the number of lightpaths or the amount of groomed traffic is not sufficient to minimize the overall power consumption of the network.

### 6.6.5 Study of W. Shen *et al.*

The authors in [95] include in their RWA and grooming strategy the possibility for multiple data rate routing over the links, introducing a more close perspective to the granularity of traffic requests. The approach considers static traffic only. The objective function of the proposed exact approach is based on the approach described in the previous section. Compared to cost-efficient design, power-efficient design yields less overall consumption, which emphasize the fact that minimizing the cost (number or price) of network equipment is not sufficient to drive power consumption minimization.

## 6.7 Conclusion

In this chapter, we overviewed the main drivers for power-awareness at the networks, and more specifically at the core networks. We also discussed the increasing need for a dynamic network and the possible architectures that can be deployed in the near future in order to drive more flexibility at the core. In a dedicated section, we discussed important physical constraints that are necessary to consider under a WSS-based OXC infrastructure. Finally, we surveyed studies from the literature that target the WDM network design under power constraints.

Our research extends the aspects discussed by the above work and includes more constraints to the design and RWA phase in order to fit real-world networks. Indeed, none of the above research considered intrinsic constraints at the nodes, especially that related to the Add/Drop module and transceivers. In addition, we offer in our study the possibility to handle not only static traffic patterns, but also scheduled traffic patterns. The next chapter will describe in detail our approach for power-efficient WDM network design under multiple data rate transmission environment.

# Chapter 7

# Power-Aware Multi-Rate WDM Network Design

## 7.1 Introduction

In this chapter, we explain in detail our approach toward network's transceivers dimensioning. We first show the benefits, as well as the complexity, of traffic grooming and transceiver reutilization. Our approach considers the possibility for splitting the scheduled traffic requests into small fractions. These fractions are routed independently through the network, with respect to the network constraints. Their establishment includes their routing and wavelength assignment, as well as defining their grooming with other requests, and the grooming locations at the nodes. An exact approach, as well as a meta-heuristic algorithm are formulated and explained in the following sections.

## 7.2 Network resources optimization

Currently deployed networking equipment do not have the option of a low power consumption mode. They are always powered-on even during inactivity periods. Our study focuses on the transceivers at the core network. Dimensioning a dynamic network under current on-the-shelf technologies rely strongly on the traffic management at the control plane. Indeed, minimizing the number of transceivers at the nodes alone is not sufficient to minimize the inherent power consumption. It is of equal importance to optimize their usage (*i.e.*, their throughput), in order to provide the closest capacity to the traffic load.

The traffic we consider is represented by a set of scheduled (pre-planned) traffic requests (scheduled demands (SDs)) which arrival dates and activation periods are known in advance. Considering their time-correlation, the control plane can choose among their different possible routing solutions in order to also introduce a space-correlation notion.

Time-space-correlation adds a huge flexibility to optimize the resource dimensioning problem. In fact, time-space-correlation has an important impact on the routing, grooming and wavelength assignment (RGWA) procedure of the traffic requests. The transceivers that need to be deployed in the network will be used in two fashions, under the concept of resource sharing:

- *Resource sharing at the same time*: a transceiver can be used by different time-correlated traffic requests by means of grooming. Table 7.1 provides the characteristics of 2 SDs. The tuple $(S_i, D_i, \alpha_i, \beta_i, \gamma_i)$ represents an SD to be established from node $S_i$ to node $D_i$. Its set-up and tear-down dates are $\alpha_i$ and $\beta_i$, respectively. The requested capacity is $\gamma_i$. In this example, the SDs need to be routed in the 6-node network provided in Figures 7.1 and 7.2. One data rate $C$ is considered in the example. $SD_1$ and $SD_2$ are active at the same time between 16:00 and 18:00. Two routing solutions are illustrated. The first solution, depicted in Figure 7.1 adopts the first path in the routing table of the SDs. Four transceivers are needed in this case. In Figure 7.2, alternative paths are chosen (1-2-3-6 and 2-3-6). Therefore, $SD_1$ is first routed from node 1 to node 2, then from node 2 to node 6. In the time period [16:00-18:00] where the two SDs are active simultaneously, the control plane grooms them at the EXC of node 2, to be routed over the same lightpath. This solution needs only three transceivers, and thus, is more economically and power-wise advantageous than the previous one. This *grooming* operation is only possible because the sum of requested capacity is less than a channel capacity.

Table 7.1: Sample SDs for grooming example.

| $i$ | $S_i$ | $D_i$ | $\alpha_i$ | $\beta_i$ | $\gamma_i$ |
|---|---|---|---|---|---|
| 1 | 1 | 6 | 14:00 | 18:00 | 0.25 $\times C$ |
| 2 | 2 | 6 | 16:00 | 17:00 | 0.5$\times C$ |

- *Resource sharing at different times*: a transceiver can be used by different sets of traffic requests at different time periods. These sets of SDs are disjoint in time. Consider the SDs of Table 7.2. $SD_3$ has a zero time-correlation with the other two SDs. Therefore, a transceiver at node 1 can first serve $SD_3$, then $SD_1$, instead of dedicating a transceiver for each (Cf. Figure 7.3). This resource sharing is quite important in networks where a good knowledge of the traffic's space-time-correlation can avoid deploying unnecessary equipment.

Table 7.2: Sample SDs for resource sharing example.

| $i$ | $S_i$ | $D_i$ | $\alpha_i$ | $\beta_i$ | $\gamma_i$ |
|---|---|---|---|---|---|
| 1 | 1 | 6 | 14:00 | 18:00 | 0.25 $\times C$ |
| 2 | 2 | 6 | 16:00 | 17:00 | 0.5$\times C$ |
| 3 | 1 | 5 | 11:00 | 12:00 | 1$\times C$ |

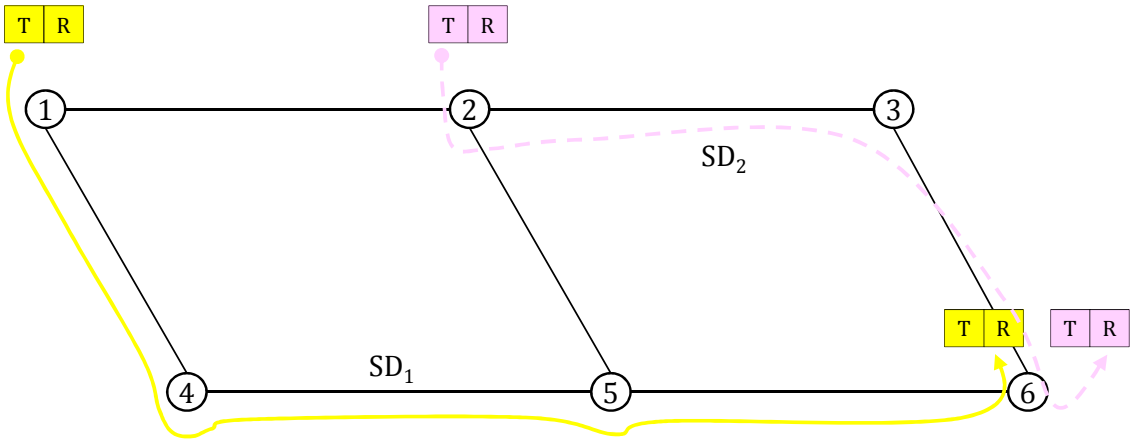


Figure 7.1: Routing over the first path.

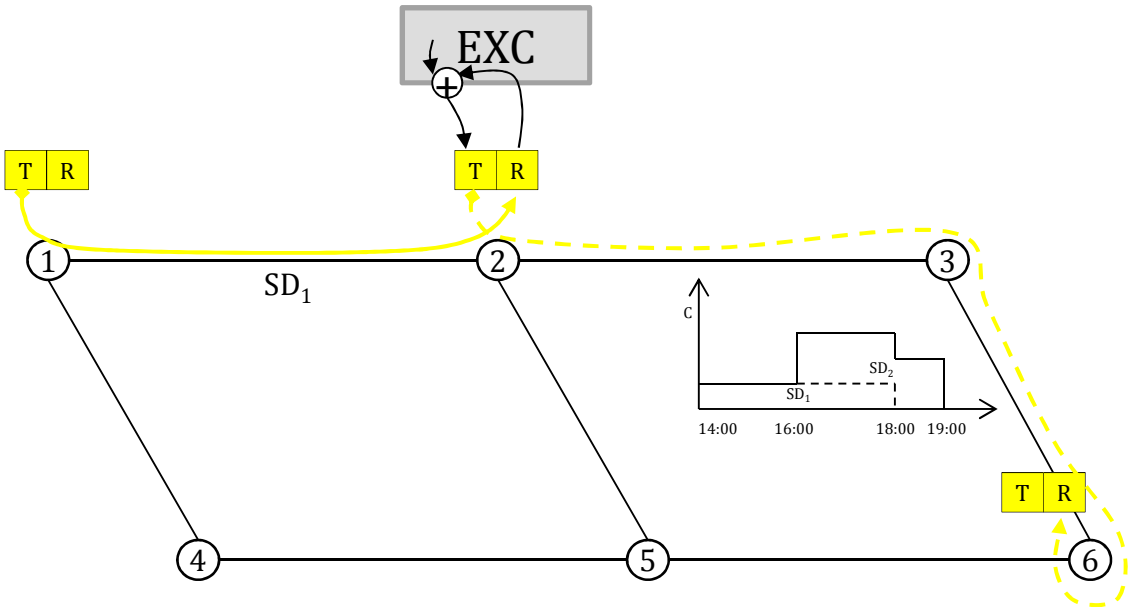


Figure 7.2: Routing solution allowing grooming at an intermediate node.

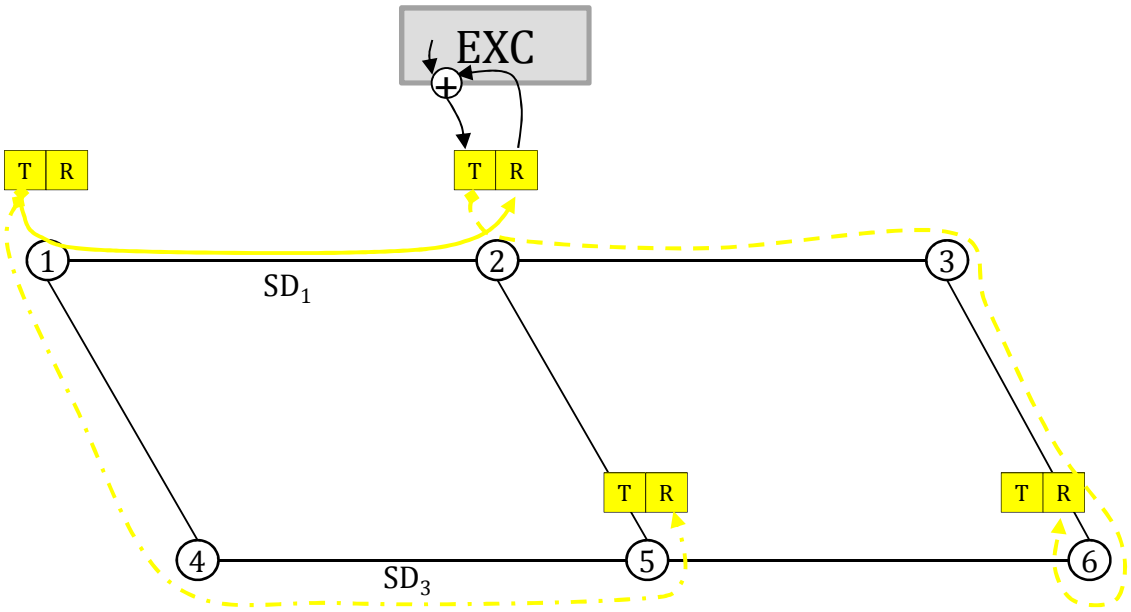


Figure 7.3: Transceiver reutilization.

Traffic grooming and resource sharing have been widely discussed in optical networks under the "Grooming" label. Classic grooming solutions aim to minimize the network cost and maximize the network's throughput [20]. In our context, the objective is to dimension the transceiver map (number and types at each node) providing the least power consumption under a given traffic set. In general, the grooming problem is solved by first adopting a virtual topology in parallel to the physical topology. The virtual topology is made of virtual links between the network nodes. These links can span one or more physical links. Figure 7.4 illustrates an example of a virtual topology constructed over a 10-node physical network. The virtual lightpaths are represented by grey curves. We can notice that some of the network nodes have been *bypassed* in this virtual topology (nodes 2, 3, 8, and 10). The curves follow the physical links spanned by each lightpath. After the virtual topology is constructed, traffic requests are assigned a succession of lightpaths from their source to their destination. Afterwards, the evolution of cumulative capacity over each lightpath is inspected to finally obtain the number of resources that can meet the required capacity. The wavelength assignment procedure is usually the last subproblem to be investigated.

Classic traffic grooming solutions consider a single data rate over the channels. Considering multiple data rate transmission adds a new degree of complexity to traffic RGWA.

We can describe the power-aware network dimensioning as follows.

***Given***

*Network specifications*:

- a physical network topology wherein all OXCs are WSS-based;

- a set of wavelengths, available per fiber-link;
- a set of transceiver types, characterized by their data rates and power consumptions;

*Traffic load*:

- a set of traffic requests. We essentially target the case of SDs, but since permanent requests (Permanent Demands (PDs)) can be considered as a particular case of SDs, activated over the whole observation period, our approach also applies for PDs.

***Objective***

The aim of the power-aware network dimensioning is to establish a set of traffic requests at the minimum rejection ratio and power consumption.

***Subject to***

*Constraints related to the OXC and transceiver architecture:*

- a wavelength '$\lambda$' can be dropped only once at a given time;
- '$\lambda$' can be added only once at a given time;
- if '$\lambda$' is added and dropped at the same time, the 2 corresponding channels should have the same data rate;

*Wavelength continuity constraint:*

Lightpaths routed on the virtual topology bypass intermediate nodes in the physical topology. In this respect, it is assigned the same wavelength over all the underlying links at the physical topology. A traffic request that spans more than one lightpath on the virtual topology, can eventually be assigned different wavelengths over these lightpaths.

In current networks, optical network design is mainly based on the concept of PDs even if in reality, the connections at the electrical layer are not permanently active. In order to evaluate the impact of electrical connections' burstiness at the session level, we compare, in the following, the global power consumption for a given set of SDs with the global power consumption required by the same traffic requests assuming permanent activity period.

## 7.3 Power consumption optimization in WDM mixed data rates transmission

In our approach, we consider the possibility to split the data volume of an SD into different flows, having *any* granularity. This fluid approximation at the electrical layer results in multiple *partial* SDs (p-SD), belonging to the same original SD. p-SDs are processed separately, as if they were independent. They can be assigned different routes on the physical

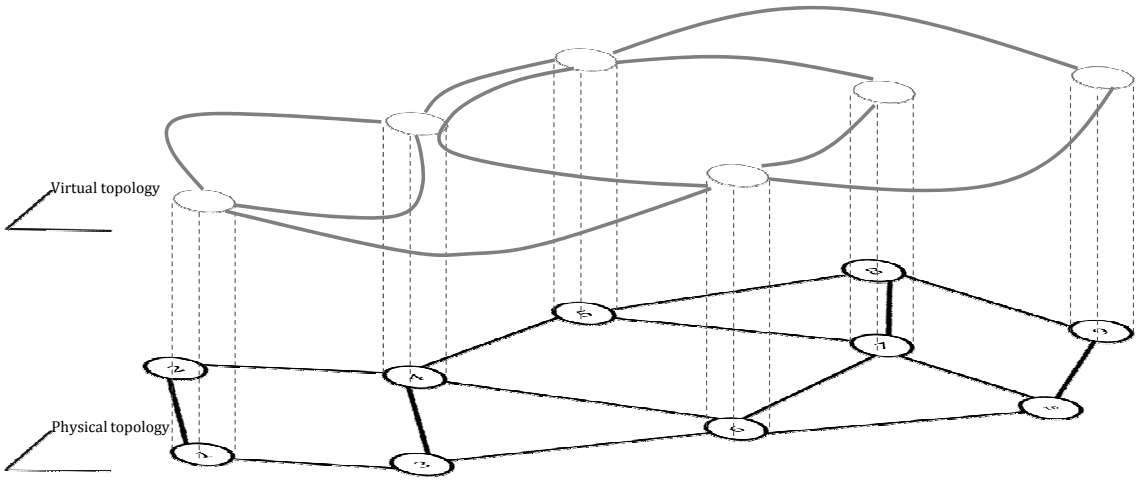


Figure 7.4: A virtual topology example.

topology (bifurcated routing). As for their virtual routes, they also are assigned a succession of one or more lightpaths, and a wavelength over each lightpath. In Figure 7.5, we illustrate an example of an SD decomposition into 3 p-SDs. We assume a connection request $SD_i$ from node 1 to node 7, having a requested capacity of $\gamma_i$. The SD is decomposed into three p-SDs: p-$SD_{i1}$ (dots), p-$SD_{i2}$ (dashes and dots), and p-$SD_{i3}$ (dashes), where $(\sum_{k=1}^{k=3} \gamma_{ik} = \gamma_i)$. In the figure, we show the different virtual paths followed by each p-SD, and the assigned wavelengths over each lightpath. We notice that p-$SD_1$ and p-$SD_2$ follow the same path after the passage by node 4. On the lightpath between nodes 4 and 5, they are assigned different wavelengths ($\lambda_1$, $\lambda_2$), and hence different transceivers at the nodes. On the lightpath between nodes 5 and destination node 7, they are assigned the same wavelength $\lambda_1$. This means that they are routed on the same channel, using the same transceivers. In this respect, $(\gamma_{i1} + \gamma_{i2})$ should not exceed the data rate of the considered transceiver.

The set of all lightpaths in the network defines a virtual topology which is mapped/routed over the physical topology. Under these assumptions, the overall problem can be divided into four inter-dependent sub-problems as follows:

- *SD routing over a virtual topology*: As aforementioned, SDs are split into p-SDs, each routed in the virtual topology over one or more consecutive lightpaths from its source to its destination.

- *Lightpath routing on the physical topology*: This consists in assigning each lightpath a continuous route from its source node to its destination node, while intermediate nodes (if any) are transparently bypassed.

- *Transceiver assignment to lightpaths*: A lightpath is served with a pair of transceivers at its ends. The lightpath uses only the transmitter of one transceiver at its source node and the receiver of one transceiver at its destination node. Both transceivers

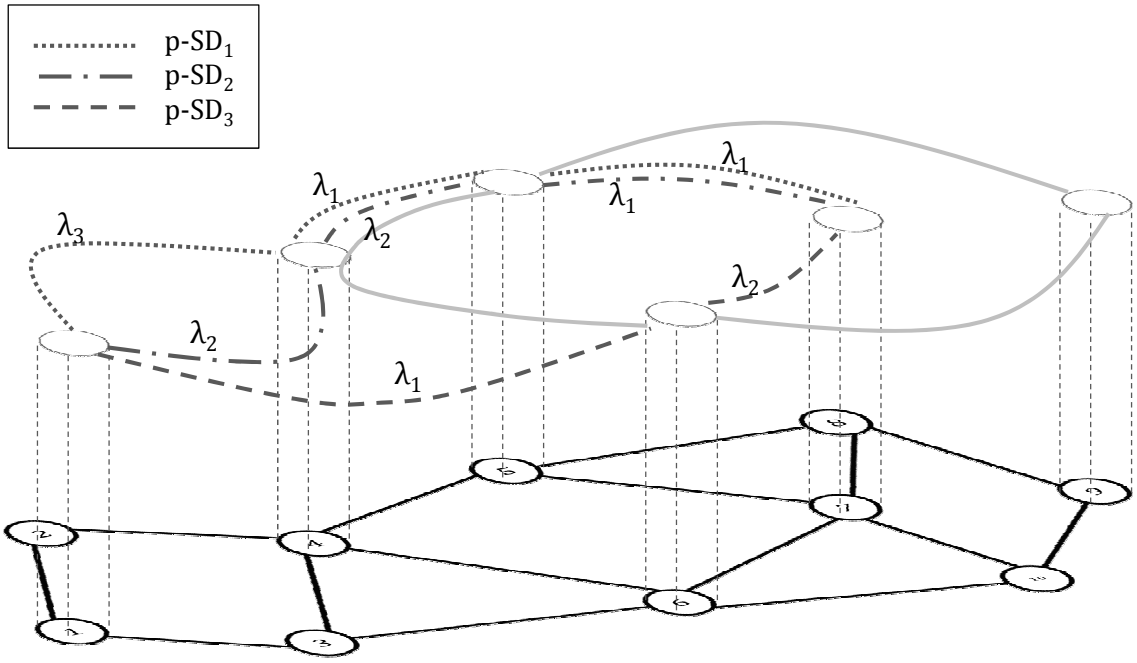


Figure 7.5: Example of p-SD establishment under bifurcated routing assumption.

are tuned to the same wavelength and should have the same data rate.

- *Wavelength assignment to lightpaths*: A lightpath is assigned a single wavelength along all the links of its path during its active period, respecting the constraints cited above.

### 7.3.1 Exact approach via linear programming

In this section, we solve the global power consumption optimization problem in the context of mixed data rate transmission by means of an ILP formulation.

#### 7.3.1.1 Parameters

- $\mathcal{N} = \{n_i\}_{i=1}^{\mathbb{N}}$: set of network nodes.
- $\mathcal{E} = \{l_v\}_{v=1}^{\mathbb{E}}$: set of unidirectional links in the network. A link can be expressed as an oriented vector $l_v = \overrightarrow{n_a n_b}$ where $a, b \in \{1...\mathbb{N}\}$ and $a \neq b$.
- $\mathcal{D} = \{\delta_d\}_{d=1}^{\mathbb{D}}$: set of SDs to be established in the network. $\delta_d = (S_d, D_d, \alpha_d, \beta_d, \gamma_d)$ is an SD having $S_d$ as source node and $D_d$ as destination node. Its set-up and tear-down times are $\alpha_d$ and $\beta_d$, respectively. $\gamma_d$ is its requested data rate.
- $\mathbb{W}$ : number of available wavelengths over each link.
- $\mathbb{C}$ : number of types of transceiver cards that can be deployed at the nodes. A transceiver card of type $c$ has a data rate $\Gamma_c$ and a power consumption $P_c$.

- $\mathcal{T}$ : set of sorted set-up and tear-down dates:

$$\mathcal{T} = \bigcup_{d=1}^{\mathbb{D}} \{\alpha_d, \beta_d\} = \{\epsilon_1, \epsilon_2, ...\epsilon_{\mathbb{T}}\} \text{ such that } \epsilon_1 < \epsilon_2 < ... < \epsilon_{\mathbb{T}}$$

#### 7.3.1.2 Variables

- $\zeta_i^c$ : number of cards of type $c$ at node $n_i$.

  $\lambda_{ij}^{c\omega t}$ : binary variable specifying whether an established lightpath from node $n_i$ to node $n_j$ is using wavelength $\omega$ at data rate $\Gamma_c$, at time $\epsilon_t$.

- $\upsilon_{dij}^{c\omega}$ : data volume of one p-SD of $\delta_d$ sent over a lightpath established from node $n_i$ to node $n_j$ using wavelength $\omega$ at data rate $\Gamma_c$, ($\upsilon_{dij}^{c\omega} \geq 0$).

- $\Delta_{dij}$ : Cumulated data volume of all p-SDs inherent to $\delta_d$ routed over a set of lightpaths established from node $n_i$ to node $n_j$, ($\Delta_{dij} \geq 0$).

- $\varsigma_i^{c\omega t}$ : binary variable denoting whether a card of type $c$ at node $v_i$ is tuned to wavelength $\omega$ or not, at time $\epsilon_t$. This variable is due to the fact that the same card is tunable to different wavelengths at different times.

- $\xi_{ijab}^{\omega t}$ : binary variable specifying whether an established lightpath from node $n_i$ to node $n_j$ is using wavelength $\omega$ over physical link $\overrightarrow{n_a n_b}$, at time $\epsilon_t$.

- $A_d$: binary variable denoting whether a demand $\delta_d$ is accepted or not.

#### 7.3.1.3 Constraints

In the following Integer Linear Programming (ILP) equations, $i$, $j$, $a$, and $b$ are nodes' indices in the set of network nodes $\mathcal{N}$, $i, j, a, b \in \{1...\mathbb{N}\}$. $d$, $\omega$, $t$, and $c$ represent the indices of an SD, a wavelength, a time instant, and a card type, respectively: $d \in \{1...\mathbb{D}\}$, $\omega \in \{1...\mathbb{W}\}$, $t \in \mathcal{T}$, and $c \in \{1...\mathbb{C}\}$.

**Traffic routing over the virtual topology** The following equations account for the multi-commodity flow equations for bifurcated traffic routing in the virtual network. Equation (7.3.1a) ensures that the traffic flow relative to an SD $\delta_d$ entering a node $n_i$ is equal to the traffic flow of the same SD $\delta_d$ leaving the same node. This is applicable to all nodes except the source and destination nodes of the SD. At the source node, the traffic flow of the request -if accepted- is only leaving the node. This is ensured by Equations (7.3.1b) and (7.3.1d). Similarly, at the destination node, the traffic flow of the request -if accepted- is only entering the node. This is ensured by Equations (7.3.1c) and (7.3.1e).

$$\sum_{k=1}^{\mathbb{N}} \Delta_{dak} = \sum_{k=1}^{\mathbb{N}} \Delta_{dka} \ , \forall d, a : n_a \neq S_d, n_a \neq D_d \tag{7.3.1a}$$

$$\sum_{k=1}^{\mathbb{N}} \Delta_{dka} = 0 \ , \forall d, a : n_a = S_d \tag{7.3.1b}$$

$$\sum_{k=1}^{\mathbb{N}} \Delta_{dak} = 0 \ , \forall d, a : n_a = D_d \tag{7.3.1c}$$

$$\sum_{k=1}^{\mathbb{N}} \Delta_{dak} = A_d \times \gamma_d \ , \forall d, a : n_a = S_d \tag{7.3.1d}$$

$$\sum_{k=1}^{\mathbb{N}} \Delta_{dka} = A_d \times \gamma_d \ , \forall d, a : n_a = D_d \tag{7.3.1e}$$

**p-SD traffic grooming** Equation (7.3.2) ensures that the cumulated data volume of all p-SDs inherent to $\delta_d$ routed between $n_i$ and $n_j$ is properly split into lightpaths delimited by appropriate transceivers tuned to suitable wavelengths. Moreover, Equation (7.3.3) ensures that whatever the p-SDs served by a lightpath between nodes $n_i$ and $n_j$ using a transceiver pair of type '$c$', the data rate $\Gamma_c$ is never exceeded.

$$\sum_{\omega=1}^{\mathbb{W}} \sum_{c=1}^{\mathbb{C}} \upsilon_{dij}^{c\omega} = \Delta_{dij} \ , \forall i, j, d \tag{7.3.2}$$

$$\sum_{d:\alpha_d \leq t < \beta_d} \upsilon_{dij}^{c\omega} \leq \lambda_{ij}^{c\omega t} \times \Gamma_c \ , \forall i, j, c, \omega, t \tag{7.3.3}$$

It is worth noting that the variables $\upsilon_{dij}^{c\omega}$ are time-independent. Thus, each lightpath has a unique tuple (transceiver type, wavelength, physical route) during its active period. Consequently, a p-SD maintains a fixed RGWA solution from its set-up time until its tear-down time.

**RWA**

$$\sum_{a:\overrightarrow{n_a n_b} \in \mathcal{E}} \xi_{ijab}^{\omega t} = \sum_{a:\overrightarrow{n_b n_a} \in \mathcal{E}} \xi_{ijba}^{\omega t} \ , \forall i, j, \omega, t, b : b \neq i, b \neq j \tag{7.3.4a}$$

$$\sum_{a:\overrightarrow{n_a n_i} \in \mathcal{E}} \xi_{ijai}^{\omega t} = 0 \ , \forall i, j, \omega, t \tag{7.3.4b}$$

$$\sum_{a:\overrightarrow{n_j n_a} \in \mathcal{E}} \xi_{ijja}^{\omega t} = 0 \ , \forall i, j, \omega, t \tag{7.3.4c}$$

$$\sum_{a:\overrightarrow{n_i n_a} \in \mathcal{E}} \xi_{ijia}^{\omega t} = \sum_{c=1}^{\mathbb{C}} \lambda_{ij}^{c\omega t} \ , \forall i, j, \omega, t \tag{7.3.4d}$$

$$\sum_{a:\overrightarrow{n_a n_j} \in \mathcal{E}} \xi_{ijaj}^{\omega t} = \sum_{c=1}^{\mathbb{C}} \lambda_{ij}^{c\omega t} \ , \forall i, j, \omega, t \tag{7.3.4e}$$

A lightpath is assigned a route along with a wavelength. This assignment is subject to the wavelength continuity constraint insured by Equation (7.3.4a). In this respect, if a lightpath enters node $n_k$ using a certain wavelength $\omega$, it should leave $n_k$ using the same wavelength. The remaining equations (7.3.4b), (7.3.4c), (7.3.4d), and (7.3.4e) ensure that a lightpath is only entering (*resp.* leaving) its destination node (*resp.* source node).

$$\xi_{ijab}^{\omega t} - \xi_{ijab}^{\omega t^+} \leq 2 - \sum_{c=1}^{\mathbb{C}} \lambda_{ij}^{c\omega t} - \sum_{c=1}^{\mathbb{C}} \lambda_{ij}^{c\omega t^+} \ , \forall i,j,\omega,t,a,b : \overrightarrow{n_a n_b} \in \mathcal{E} \tag{7.3.5a}$$

$$\xi_{ijab}^{\omega t^+} - \xi_{ijab}^{\omega t} \leq 2 - \sum_{c=1}^{\mathbb{C}} \lambda_{ij}^{c\omega t} - \sum_{c=1}^{\mathbb{C}} \lambda_{ij}^{c\omega t^+} \forall i,j,\omega,t,a,b : \overrightarrow{n_a n_b} \in \mathcal{E} \tag{7.3.5b}$$

Equations (7.3.5a) and (7.3.5b) ensure that if a lightpath is active at consecutive times $t$ and $t^+$, it should maintain its physical route and wavelength.

Equation (7.3.6) ensures that a wavelength is used at most once over a physical link at any time.

$$\sum_{i=1}^{\mathbb{N}} \sum_{j=1}^{\mathbb{N}} \xi_{ijab}^{\omega t} \leq 1 \ , \forall \omega,t,a,b : \overrightarrow{n_a n_b} \in \mathcal{E} \tag{7.3.6}$$

**Transceiver-related constraints** Equations (7.3.7a) and (7.3.7b) ensure that a transceiver card contains a transmitter and a receiver operating at the same wavelength and data rate.

$$\varsigma_i^{c\omega t} \geq \sum_{j=1}^{\mathbb{N}} \lambda_{ij}^{c\omega t} \ , \forall i,c,\omega,t \tag{7.3.7a}$$

$$\varsigma_i^{c\omega t} \geq \sum_{j=1}^{\mathbb{N}} \lambda_{ji}^{c\omega t} \ , \forall i,c,\omega,t \tag{7.3.7b}$$

Equation (7.3.8) ensures that a wavelength can be added/dropped at most once at any time.

$$\sum_{c=1}^{\mathbb{C}} \varsigma_i^{c\omega t} \leq 1 \ , \forall i,\omega,t \tag{7.3.8}$$

$$\zeta_i^c \geq \sum_{\omega=1}^{\mathbb{W}} \varsigma_i^{c\omega t} \ , \forall i,c,t \tag{7.3.9}$$

$\zeta_i^c$ in Equation (7.3.9) represents the number of transceivers of type $c$ deployed at node $n_i$.

#### 7.3.1.4 Objective

$$\min \ \left( \phi \cdot \sum_{i=1}^{\mathbb{N}} \sum_{c=1}^{\mathbb{C}} \zeta_i^c \times P_c - \psi \cdot \sum_{d=1}^{\mathbb{D}} A_d \right) \tag{7.3.10}$$

This objective function is two-folds. It seeks to minimize the overall power consumption of the network while satisfying the maximum number of requests. $\phi$ and $\psi$ are weighting factors used to stress one fold or the other.

### 7.3.2 ILP complexity

The time performance of linear programs depends on their proper number of variables and constraints. We are interested with how our ILP scales with the input network and traffic matrix. Table 7.3 recalls our ILP's parameter settings. We can thus determine the computational complexity inherent to the variable and constraint calculations as follows:

| Number of ... | Symbol |
|---|---|
| Network nodes | $\mathbb{N}$ |
| Network links | $\mathbb{L}$ |
| Card types | $\mathbb{C}$ |
| Wavelengths | $\mathbb{W}$ |
| Traffic requests | $\mathbb{D}$ |
| Time periods | $\mathbb{T}$ |

Table 7.3: Reminder of parameters' dimensions.

Let $T_v(\mathbb{N})$ and $T_c(\mathbb{N})$ be the complexities inherent to the variables computation and the constraints computation, respectively, driven by the number of nodes $\mathbb{N}$.

$$\begin{aligned} T_v(\mathbb{N}) &= \mathbb{N} \cdot \mathbb{C} \\ &\quad + \mathbb{N} \cdot \mathbb{N} \cdot \mathbb{C} \cdot \mathbb{W} \cdot \mathbb{T} \\ &\quad + \mathbb{N} \cdot \mathbb{N} \cdot \mathbb{C} \cdot \mathbb{W} \cdot \mathbb{C} \\ &\quad + \mathbb{N} \cdot \mathbb{D} \cdot \mathbb{W} \\ &\quad + \mathbb{N} \cdot \mathbb{W} \cdot \mathbb{C} \cdot \mathbb{T} \\ &\quad + \mathbb{N} \cdot \mathbb{N} \cdot \mathbb{L} \cdot \mathbb{W} \cdot \mathbb{T} \\ &\quad + \mathbb{D} \\ &\quad = O(\mathbb{N}^2) \end{aligned} \tag{7.3.11}$$

$$\begin{aligned} T_c(\mathbb{N}) &= \mathbb{D} \cdot (\mathbb{N} - 2) + \mathbb{D} + \mathbb{D} + \mathbb{D} + \mathbb{D} \\ &\quad + \mathbb{D} \cdot \mathbb{N} \cdot \mathbb{N} + \mathbb{N} \cdot \mathbb{N} \cdot \mathbb{C} \cdot \mathbb{W} \cdot \mathbb{T} \\ &\quad + \mathbb{N} \cdot \mathbb{N} \cdot (\mathbb{N} - 2) \cdot \mathbb{W} \cdot \mathbb{T} + \mathbb{N} \cdot \mathbb{N} \cdot \mathbb{W} \cdot \mathbb{T} \\ &\quad + \mathbb{N} \cdot \mathbb{N} \cdot \mathbb{W} \cdot \mathbb{T} + \mathbb{N} \cdot \mathbb{N} \cdot \mathbb{W} \cdot \mathbb{T} + \mathbb{N} \cdot \mathbb{N} \cdot \mathbb{W} \cdot \mathbb{T} \\ &\quad + \mathbb{N} \cdot \mathbb{N} \cdot \mathbb{W} \cdot \mathbb{T} \cdot \mathbb{E} + \mathbb{N} \cdot \mathbb{N} \cdot \mathbb{W} \cdot \mathbb{T} \cdot \mathbb{E} \\ &\quad + \mathbb{W} \cdot \mathbb{T} \cdot \mathbb{E} \\ &\quad + \mathbb{N} \cdot \mathbb{C} \cdot \mathbb{W} \cdot \mathbb{T} + \mathbb{N} \cdot \mathbb{C} \cdot \mathbb{W} \cdot \mathbb{T} \\ &\quad + \mathbb{N} \cdot \mathbb{W} \cdot \mathbb{T} + \mathbb{N} \cdot \mathbb{W} \cdot \mathbb{T} \\ &\quad = O(\mathbb{N}^3) \end{aligned} \tag{7.3.12}$$

Using the *big O notation*, the total computational complexity can be expressed as: $T_{ILP}(\mathbb{N}) = \mathcal{F}(T_v(\mathbb{N}), T_c(\mathbb{N})) = O(\mathbb{N}^2, \mathbb{N}^3)$. Consequently, the computational time of the proposed ILP scales cubically with the number of nodes in the network.

Similarly, we can find that the computational time scales linearly with the number of traffic requests.

### 7.3.3 Heuristic approach

It is well known that the RWA problem is NP-complete [19]. RGWA, on its turn, is more complex than the classic RWA where requests have full wavelength capacity and an infinite duration (permanent lightpath demand, PLD). Indeed, time-space correlation of the SDs, and their different capacity values add more complexity to the RWA problem. The ILP equations can be solved with means of commercial software over a small network, and/or for limited traffic loads. This is due to the fact that the complexity of the ILP, expressed in terms of the number of variables and equations, increases with the network size and the given traffic load. Heuristic algorithms can help extend the research over larger networks, and for heavier traffic loads. In our proposed heuristic approach, we adopt the genetic algorithm (GA) optimization method. GAs have been found to provide good solutions for complex optimization problems, avoiding local minima. They are a branch of evolutionary algorithms (EA) that mimic natural evolution in societies and species. Particularly, GAs use aspects of species reproduction like *inheritance*, *mutation*, *selection*, and *crossover*.

In a genetic algorithm, a population of *chromosomes* encodes candidate solutions (individuals). The chromosomes' encoding depends on the given optimization problem. In general, binary encoding is the most used in GAs. The first population is generated randomly. Each individual is evaluated by a fitness procedure (normally, a single function) in order to provide an image of its survivability among the population. Some GAs keep the best individuals and pass their genotypes to the next generation (population), this mimics "*natural selection*". Selection is also used to stochastically choose parents, in order to reproduce the rest of the new population individuals. This selection can also rely on the individuals' fitness. The reproduction operation happens through "*crossover*" and "*mutation*". Crossover is the operation of choosing the genotypes to inherit to children chromosomes. It can take place at several points in the parent chromosomes. Mutation, in its turn, applies random variation in the genotype, in order to maintain a genetic diversity from one generation to another. The evolution is only stopped when (*i*) either a maximum number of generations, or (*ii*) a satisfactory level, has been reached. In the first case, there is a chance that a satisfactory solution has not been produced.

In the following we present our GA approach for solving the problem of power consumption optimization in mixed data rates networks. We illustrate the chromosome encoding, and provide a summary of the calculation of individuals' fitness, and a general skeleton of the adopted GA.

#### 7.3.3.1 Mathematical formulation

We use the following mathematical formulation to describe our GA approach:

- $\mathcal{N} = \{n_i\}_{i=1}^{\mathbb{N}}$ is the set of network nodes.
- $\mathcal{E} = \{l_v\}_{v=1}^{\mathbb{E}}$ is the set of unidirectional links in the network.
- $\mathcal{D} = \{\delta_d\}_{d=1}^{\mathbb{D}}$: set of SDs to be established in the network. ($\delta_d = (S_d, D_d, \alpha_d, \beta_d, \gamma_d)$)
- $\omega = 1...\mathbb{W}$ : available wavelengths over each link.
- $c = 1...\mathbb{C}$: available card types. A card of type '$c$' accounts for a data rate of $\Gamma_c$ and a power consumption of $P_c$.
- $\mathbb{P}_d = \{p_{d,k}\}_{k=1}^{\mathcal{K}}$ is the set of shortest paths between nodes $S_d$ and $D_d$ of SD $\delta_d$. In order to simplify our mathematical representation, we consider that all source/destination pair have $\mathcal{K}$ shortest paths even if, in reality, some node pairs may have less than $\mathcal{K}$ paths. The considered shortest paths are calculated in hop number, according to Eppstein's shortest path calculation [32].

  A path $p_{d,k}$ is made of $h_{d,k}$ hops. A *layout* $L_{d,k}^{l}$ is a set of transparent subpaths, or lightpaths, that cover the links of $p_{d,k}$ from source to destination. At most, $p_{d,k}$ can have $2^{h_{d,k}-1}$ layouts. For instance, the path $n_1 - n_2 - n_3 - n_4$ can have $2^{3-1} = 4$ different layouts as follows:

  1. $L^1 = \{[n_1{-}n_2{-}n_3{-}n_4]\}$ spanning only one subpath (no intermediate grooming point).
  2. $L^2 = \{[n_1{-}n_2][n_2{-}n_3{-}n_4]\}$ spanning two subpaths (one intermediate grooming point at node $n_2$).
  3. $L^3 = \{[n_1{-}n_2{-}n_3][n_3{-}n_4]\}$ spanning two subpaths (one intermediate grooming point at node $n_3$).
  4. $L^4 = \{[n_1 - n_2][n_2 - n_3][n_3 - n_4]\}$ spanning three subpaths (two intermediate grooming points at nodes $n_2$ and $n_3$).

- $\mathcal{L}_{d,k} = \{L_{d,k}^{l}\}_{l=1}^{2^{h_{d,k}-1}}$ represents the set of layouts relative to path $p_{d,k}$.
- $\Lambda_d = \bigcup_{k=1}^{\mathcal{K}} \mathcal{L}_{d,k} = \{\mathbb{L}_{d,\theta}\}_{\theta=1}^{\Theta_d}$ represents all possible layouts on the $\mathcal{K}$-shortest paths between $S_d$ and $D_d$. $\Theta_d = \sum_{k=1}^{\mathcal{K}} 2^{h_{d,k}-1}$. It is an ordered set, first, in terms of $k$, second, in terms of $l$. $\mathbb{L}_{d,\theta}$ is made of $\tau_{d,\theta}$ subpaths.
- $\Pi = \{SP_\pi\}_{\pi=1}^{N_{sp}}$ represents all possible subpaths in the network. $SP_\pi$ can be expressed by the tuple: $(S_\pi, D_\pi, \mathcal{E}_\pi)$ where $S_\pi$ and $D_\pi$ are its source and destination nodes, and $\mathcal{E}_\pi = \{l_{\pi,e}\}_{e=1}^{NL_\pi}$ is the set of links spanned by the subpath. There are $NL_\pi$ links bypassed by $SP_\pi$.

- $\mathcal{T}$ : set of sorted set-up and tear-down dates:

$$\mathcal{T} = \bigcup_{d=1}^{\mathbb{D}} \{\alpha_d, \beta_d\} = \{\varepsilon_1, \varepsilon_2, ...\varepsilon_{\mathbb{T}}\} \text{ such that } \varepsilon_1 < \varepsilon_2 < ... < \varepsilon_{\mathbb{T}}$$

Since we adopt the bifurcated routing under fluid approximation assumption, we split our SDs into several partial SDs (p-SDs). Each p-SD has a requested capacity equal to the finest granularity that we allow. Let '$\varrho$' be this finest granularity. In this respect, each SD $\delta_d$ can be split into $\rho_d = \frac{\gamma_d}{\varrho}$ p-SDs. In this respect, a new traffic set $\mathcal{D}'$ needs to be established in the network:

$$\mathcal{D}' = \{\delta'_{d,\epsilon}\}_{d=1,\epsilon=1}^{d=\mathbb{D},\epsilon=\rho_d}$$

where p-SD $\delta'_{d,\epsilon}$ can be represented by the tuple $(S_d, D_d, \alpha_d, \beta_d, \varrho)$.

The solution to our optimization problem can be represented by a routing solution for each p-SD (route+layout), and a set of (wavelength/transceiver type) couple over each subpath of the layout. Appropriate grooming at the nodes and over the lightpaths is necessary in order to validate the solution with respect to the different constraints mentioned above. The solution providing the least power consumption is to be adopted for the network and the given traffic load. Let $\Sigma$ be the solution to our optimization problem:

$$\mathcal{D}' = \{\delta'_{d,\epsilon}\}_{d=1,\epsilon=1}^{d=\mathbb{D},\epsilon=\rho_d} \longmapsto \Sigma = \{\mathbb{S}_{d,\epsilon}\}_{d=1,\epsilon=1}^{d=\mathbb{D},\epsilon=\rho_d}$$

where $\mathbb{S}_{d,\epsilon}$ refers to the RWA solution of p-SD $\delta'_{d,\epsilon}$:

$$\mathbb{S}_{d,\epsilon} = (\mathbb{L}_{d,\theta}, \Omega_{d,\epsilon})$$

$$\Omega_{d,\epsilon} = \{(c, \omega)\}_{l=1}^{l=\tau_{d,\theta}})$$

where $\theta \in 1..\Theta_d$ , $c \in \{1..\mathbb{C}\}$ , and $\omega \in \{1..\mathbb{W}\}$.

Having fixed the number '$\mathcal{K}$' of possible paths between the nodes, and the finest granularity '$\varrho$', the solution will not be the optimum (sub-optimal solution).

#### 7.3.3.2 Chromosome encoding

In order to unify the RWA solution of the p-SDs, we consider the layout having the highest number of subpaths in the network. It corresponds to the longest path among all shortest paths between the nodes, with passage to the electrical layer at every intermediate routing. Let us consider $\mathbb{H} = \max_{d,k}\{h_{d,k}\}$. In this order, we can encode the RWA solution of a p-SDs as depicted in Figure 7.6 over $(\mathbb{H}+1)$ integer fields. The first field is that of the layout to be assigned to the p-SD $\delta_{d,\epsilon}$. The next '$\mathbb{H}$' fields encode the card type and the wavelength given to $\delta_{d,\epsilon}$ over the corresponding subpaths. Not all of the fields are useful, since '$\mathbb{H}$' is the highest number of lightpaths over the layouts. In this order, only the first $\tau_{d,\theta}$ fields are significant, and the rest are padding fields. For the individuals of the first population, the value of the first field is chosen randomly among the possible '$\Theta_d$' layout

solutions (p-SD $\delta'_{d,\epsilon}$), while the rest of the fields are random numbers from 1 to $\mathbb{C} \times \mathbb{W}$. For instance, if a field's value is $x \in \{1..\mathbb{C} \times \mathbb{W}\}$, '$c$' and '$\omega$' can be calculated as follows:

$$c = (x-1)\text{div}(\mathbb{W}) + 1 \text{ and: } \omega = (x-1)\text{mod}(\mathbb{W}) + 1$$

where "*div*" and "*mod*" are integer division and modulo operations, respectively.

The whole chromosome is a concatenation of all p-SDs' solutions. A chromosome is depicted in Figure 7.7. It is made of $(\sum_{d=1}^{\mathbb{D}} \rho_d)$ RWA solutions related to all p-SDs in $\mathcal{D}'$.

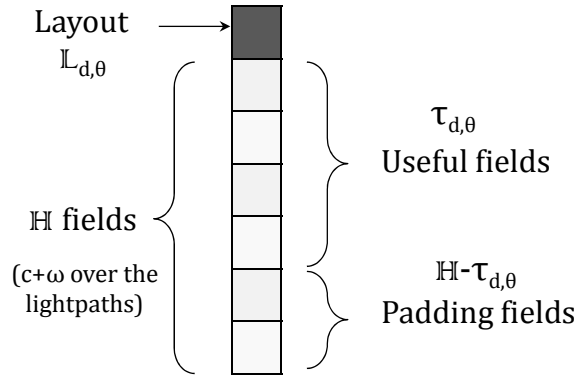


Figure 7.6: Routing solution encoding for p-SD $\delta'_{d,\epsilon}$.

#### 7.3.3.3 Fitness calculation

Due to the different constraints of this problem, some chromosomes might not present a valid RGWA solution. For instance, if a link happens to carry the same wavelength twice (or more), using different data rates, the solution cannot be considered valid. In this case, we cannot calculate the power consumption of the network. Only valid solutions can be used for power consumption calculation. In this respect, our fitness criterium is the power consumption, set to the exact value inherent to valid solutions, and to *infinity* in the case of invalid solutions.

Pseudo-code 3 resumes the validation process of a chromosome. The most-fitted individual of a population is the one having the least power consumption.

#### 7.3.3.4 Crossover and mutation

Crossover and mutation are two basic operators that affect the performance of GAs. They depend on the encoding of the chromosomes as well as the considered optimization problem. Crossover between two *parent* chromosomes produces two *children* chromosomes by rearranging solutions inside the same individual. Figure 7.8 illustrates a crossover operation happening at two locations in the chromosomes. A single, or multiple crossover points can be considered according to the genetic algorithm modeling.

As for mutation, it occurs at stochastically chosen fields in the chromosome. In binary encoding, mutation only inverts the chosen bits. In our encoding, mutation happens at

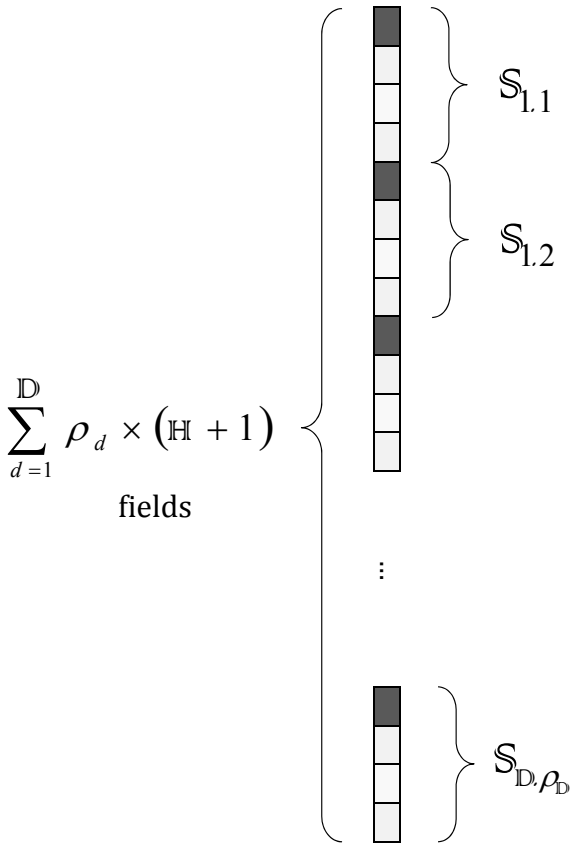


Figure 7.7: Chromosome encoding.

**Pseudo-Code 3** Synopsis of the chromosome validation.

**Input: Chromosome** $\Sigma$
**for all** $\pi \in \{1...N_{sp}\}$ **do**
  **for all** $\omega \in \{1...\mathbb{W}\}$ **do**
    **for all** $t \in \{1...\mathbb{T}\}$ **do**
      Load $C^t_{c,\omega} = \{c : \exists(d,\epsilon) : (SP_\pi \in \mathbb{L}_{d,\epsilon})\&((c,\omega) \in \Omega d,\epsilon \text{ over } SP_\pi)\&(\alpha_d < \varepsilon_t < \beta_d)\}$
      Calculate $Nb^{\pi,\omega}_{p-SD} = card(\{\delta'_{d,\epsilon} : (SP_\pi \in \mathbb{L}_{d,\epsilon})\&(\exists c : (c,\omega) \in \Omega d,\epsilon \text{ over } SP_\pi)\})$
      **if** $card(C^t_{c,\omega} > 1)$ (Multiple lightpaths use wavelength $\omega$ over $SP_\pi$, at the same time using more than one card types.) **then**
        **if** $(\varrho \times Nb^{\pi,\omega}_{p-SD}) > \Gamma_{\mathbb{C}}$ **then**
          Return[1] $\infty$
        **else**
          Replace '$c$' by the appropriate card type[2] in the chromosome itself.
        **end if**
      **end if**
    **end for**
  **end for**
**end for**
**for all** $v \in \{1...\mathbb{E}\}$ **do**
  **for all** $\omega \in \{1...\mathbb{W}\}$ **do**
    **for all** $t \in \{1...\mathbb{T}\}$ **do**
      Load $\mathcal{SP}^t_{\pi,\omega} = \{\pi : (l_v \in \mathcal{E}_\pi)\&(\exists c,d,\epsilon : (c,\omega) \in \Omega_{d,\epsilon})\&(\alpha_d < \varepsilon_t < \beta_d)\}$
      **if** $card(\mathcal{SP}^t_{\pi,\omega}) > 1$ (wavelength conflict over link $l_v$.) **then**
        Return $\infty$
      **end if**
    **end for**
  **end for**
**end for**
**for all** $i \in \{1...\mathbb{N}\}$ **do**
  **for all** $t \in \{1...\mathbb{T}\}$ **do**
    **for all** $\omega \in \{1...\mathbb{W}\}$ **do**
      **if** $\omega$ is used for transmission at node $n_v$ more than once at time $T_t$ **then**
        Return $\infty$
      **else**
        **if** $\omega$ is used for reception at node $n_v$ more than once at time $T_t$ **then**
          Return $\infty$
        **end if**
      **end if**
    **end for**
  **end for**
**end for**
**for all** $i \in \{1...\mathbb{N}\}$ **do**
  **for all** $c \in \{1...\mathbb{C}\}$ **do**
    Calculate $N_{v,c}$[3]
  **end for**
**end for**
Return $Power = \sum_{v=1}^{\mathbb{N}} \sum_{c=1}^{\mathbb{C}} N_{v,c} \times P_c$

[1] The *Return* command stops the execution of the routine and exists the whole instance.
[2] The appropriate card type has enough data rate to carry the needed cumulated capacity, while other card type having lower data rates cannot be used.
[3] $N_{v,c}$ is the number of cards of type $c$ used at node $N_v$.

a small probability $\mathcal{P}_m$. The field to be mutated undergoes a special mutation according to its type. On the one hand, if the field corresponds to a layout decision for $\delta'_{d,\epsilon}$, the mutation chooses randomly another layout from the $\Theta_d$ layouts. On the other hand, if the field was

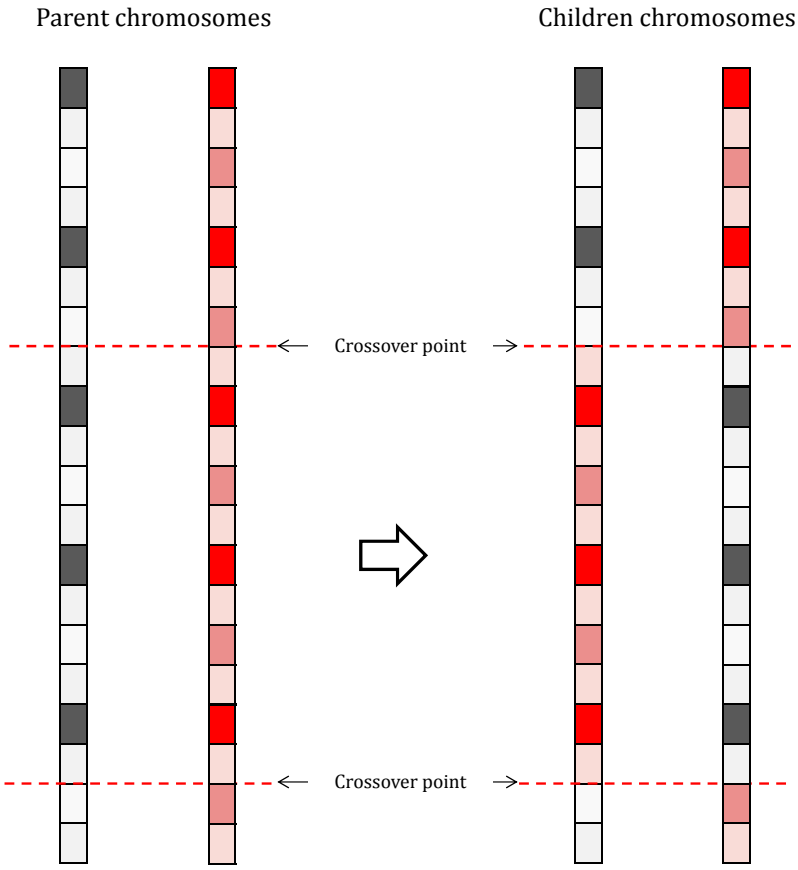


Figure 7.8: Crossover between two parent chromosomes.

#### 7.3.3.5 Genetic algorithm solution

Pseudo-code 4 provides a concise description of the implemented GA. To date, due to time constraints, we have not been able to make use of the GA. In the near future, we plan to finalize its validation and extend the research over larger network topologies and higher traffic loads.

## 7.4 Numerical results and discussion

In the following, we present results obtained via our ILP formulation. Commercial software like CPLEX [4] can be used to solve the ILP equations. Due to the complexity of our problem, we consider in our simulations the sample network shown in Figure 7.9. This network is composed of $\mathbb{N} = 6$ nodes and $\mathbb{E} = 14$ unidirectional links. Each link supports

**Pseudo-Code 4** Synopsis of the GA.

**INITIALIZATION**
**for all** $s \in \{1...Nb\}$ **do**
  x=1
  **for all** $d \in \{1...\mathbb{D}\}$ **do**
    **for all** $\epsilon \in \{1...\rho_d\}$ **do**
      $X_s[x] = rand(1...\Theta_d)$
      **for all** $a \in \{1...\mathbb{H}\}$ **do**
        $X_s[x+a] = rand(1...\mathbb{W} \times \mathbb{C})$
      **end for**
      $x+ = \mathbb{H}$
    **end for**
  **end for**
  $Population_1[s] = X_s$
  $Power[s] = Validate(X_s)$
**end for**
**PROCESSING**
**for all** $I \in \{1...Max_It\}$ **do**
  Sort the elements of $Population_1$ and $Power$ in the increasing order of $Power$.
  **if** $I == 1$ **then**
    $counter = 1$
    $Best_X = \emptyset$
  **end if**
  **if** $(Population_1[1] \in Best_X)\&\&(Population_1[2] \in Best_X)...\&\&(Population_1[N_{best}] \in Best_X)$ **then**
    $counter++$
    **if** $counter == Max_best_It$ **then**
      Return $Population_1[1]$
    **end if**
  **else**
    $counter = 1$
    **for all** $s \in \{1...N_{best}\}$ **do**
      $Best_X[s] = Population_1[s]$
    **end for**
  **end if**
  **for all** $s \in \{1...N_{survivors}\}$ **do**
    $Population_2[s] = Population_1[s]$
  **end for**
  **for all** $s \in \{1...(Nb - N_{survivors})/2\}$ (For simplification, $Nb$ and $N_{survivors}$ are considered even numbers) **do**
    $r_1 = rand(1...Nb)$
    $r_2 = rand(1...Nb)$ $(r_2 \neq r_1)$
    $X_1 = Population_1[r_1]$
    $X_2 = Population_1[r_2]$
    $Population_2[N_{survivors} + 2 \times (s-1) + 1], Population_2[N_{survivors} + 2 \times (s-1) + 2] = Crossover^1(X_1, X_2, rand(1...Max_{crossover}))$
    $Power[N_{survivors} + 2 \times (s-1) + 1] = Validate(Population_2[N_{survivors} + 2 \times (s-1) + 1])$
    $Power[N_{survivors} + 2 \times (s-1) + 2] = Validate(Population_2[N_{survivors} + 2 \times (s-1) + 2])$
  **end for**
  **for all** $I \in \{1...Max_It\}$ **do**
    $Population_1[s] = Population_2[s]$
  **end for**
**end for**
Return $Population_1[1]$

[1] The routine $Crossover(Parent_1, Parent_2, Nb_{crossover})$ produces two children chromosomes from a crossover operation between chromosomes $Parent_1$ and $Parent_2$. The crossover is operated at $Nb_{crossover}$ locations chosen randomly in the chromosomes.

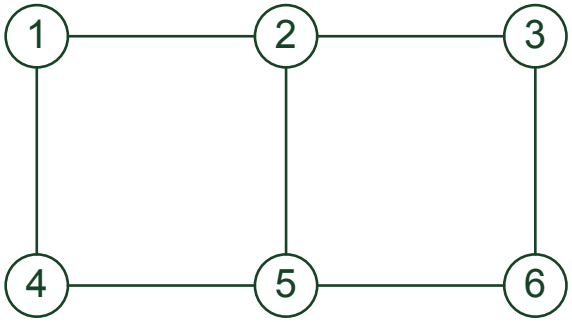


Figure 7.9: 6-node sample network.

a total of $\mathbb{W} = 20$ wavelength channels. We consider two transceiver types operating at 10Gbps and 40Gbps. Their power consumptions are 30W and 80W, respectively as given by Huawei's datasheets. As for the traffic generation, source and destination nodes are uniformly chosen among network nodes. The observation period is sampled at 10 discrete instants. The set-up of an SD is chosen uniformly in the interval [1,9] while its duration is generated according to a normal distribution $\mathcal{N}(\mu = 2, \sigma^2 = 1)$. The data rate of an SD, $\delta_d$ is a multiple of 5Gbps, generated according to a triangular distribution Tr(a, mode, b) as depicted in Figure 7.10. In our simulations, $\psi \ll \phi$. A PD is generated from an SD by extending its active duration to the whole observation period.

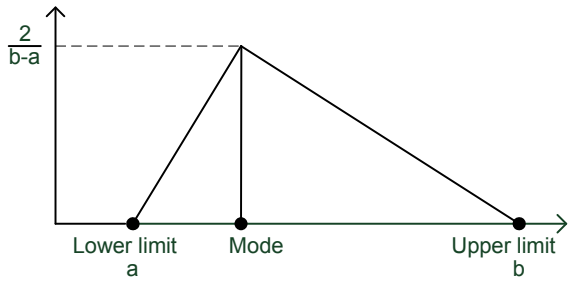


Figure 7.10: Tr(a,Mode,b): PDF of PD/SD data rates.

**7.4.0.5.1 Dimensioning scenarios** Given the aforementioned types of transceivers, we consider three dimensioning scenarios:

- 10G/40G: 10Gbps (10G) and 40Gbps (40G) transceivers are to be deployed.
- 40G: only 40G transceivers are to be deployed.
- 10G: only 10G transceivers are to be deployed.

In this part, the considered triangular function used to generate the demands' data rates ($\gamma_d$) is Tr(5,25,60).

Figure 7.11 depicts the network's power consumption for 20 and 40 demands (SDs and PDs), under the three design scenarios. The following observations can be drawn out from this figure:

- The 40G and the 10G/40G scenarios provide almost the same power consumption with a small advantage for the 10G/40G scenario. These scenarios will be compared in details in the next paragraph.

- The 10G scenario results in higher power consumption compared with the other scenarios. In the case of 40 PDs, the 10G scenario results in the rejection of 7 requests, which corresponds to a rejection ratio of 17.5%. Percentages next to dashed arrows in Figure 7.11 represent the additional power consumption in the 10G scenario, compared to 40G scenario. This difference is a consequence of the uneven energy consumption per bit sent over each of the two transceiver types ($3.10^{-6}$ J/bit for 10G transceivers vs. $2.10^{-6}$ J/bit for 40G transceivers).

- Network's power consumption is proportional to the traffic load: When the number of demands is doubled, power consumption is also almost doubled under all (non-blocking) scenarios.

- SD vs. PD: Under the 10G/40G scenario, a power gain of roughly 40% is observed for SD traffic compared to PD traffic (percentages near continuous arrows in Figure 7.11). This gain is obtained when the data volume of SDs represents 25% of that of the PDs, calculated from demand's data rates, and their set-up and tear-down times. This gain can be increased if transceivers can be temporarily switched off when they are not carrying any traffic. However, this approach is not practically possible. The use of flexible data rate transceivers can be a promising alternative but they do not yet constitute a mature technology. Such transceivers would reduce the power consumption in the whole network by automatically switching to their lowest data rate when they are not sending/receiving any traffic.

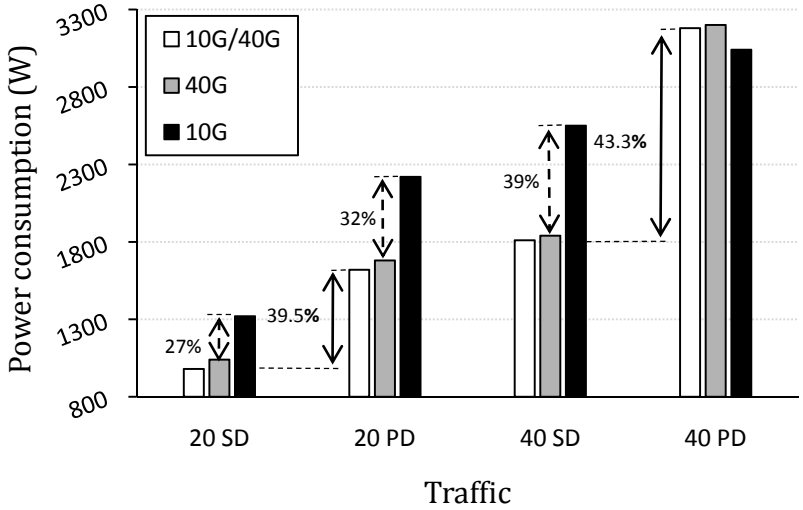


Figure 7.11: Power consumption comparison between three design scenarios: deployment of 10G and 40G transceivers, deployment of only 40G transceivers, deployment of only 10G transceivers, under different traffic loads and types.

**7.4.0.5.2 40G scenario vs. 10G/40G scenario** As shown in Figure 7.11, there is only a small gain (5,8% for 20 Demands) obtained in the 10G/40G scenario, compared to the 40G scenario. This might implicate that only few 10G transceivers are deployed, but on the contrary, this type of transceivers is effectively used in the 10G/40G scenario. Figure 7.12 depicts the percentage of 10G transceivers deployed in the network. This figure shows that the 10G/40G scenario is more adapted in terms of capacity to the traffic load than the 40G scenario. However, the small power gain is due to the fact that the ratio of the transceivers' powers ($\frac{3}{8}$) is higher than the ratio of their capacities ($\frac{1}{4}$). We notice that with the increase of the number of demands, the number of 10G cards used decreases. On one hand, the more the demands' number, the higher their time-correlation. Our approach urges the grooming of time-correlated demands over common lightpaths using low power consuming resources as much as possible. This how, and due to the difference between the power and data rate ratios of the two types of transceivers, the deployed 40G transceivers become more numerous than the 10G cards. These latter will only serve SDs of small requested capacity, beginning or ending at peak-loads as well as p-SDs carrying very low capacity. On the other hand, when the demands' number is small (*e.g.*, 20 demands), time-correlation between the demands is low. In this situation, traffic aggregation is still taking place, but resources' reutilization by uncorrelated SDs is much more appealing. This how, 10G cards are deployed at $37,5\%$ for 20 SDs.

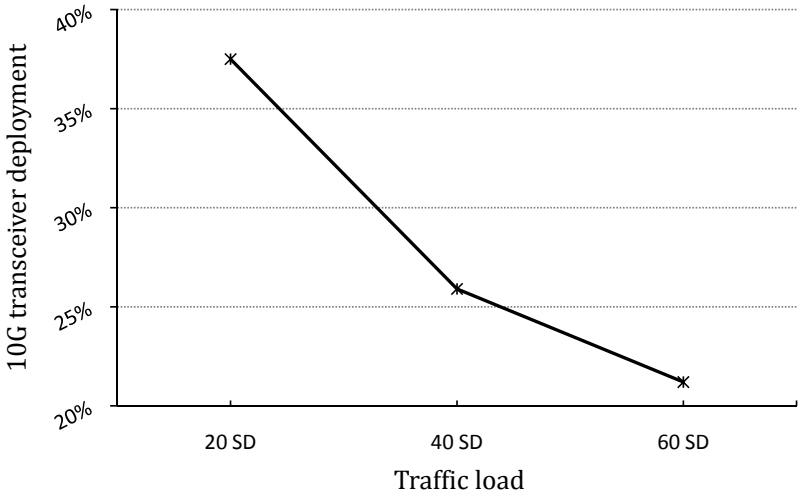


Figure 7.12: Percentage of 10G transceivers deployed in the network under the 10G/40G scenario.

Figure 7.13 depicts the network's power consumption under 40G and 10G/40G scenarios for 40 SDs. Three types of loads are considered: T10 relative to a triangular function Tr(5,10,25) for data rates generation, T25 relative to Tr(5,25,45), and T40 relative to Tr(20,40,60). The gain in power consumption between the two dimensioning scenarios is also plotted. The number of demands being constant, only the traffic load is varied with the intrinsic data rates ($\gamma_d$) of the demands. Thus the time-correlation is roughly the same for the three traffic loads. Given the load increase, p-SDs are groomed together as much

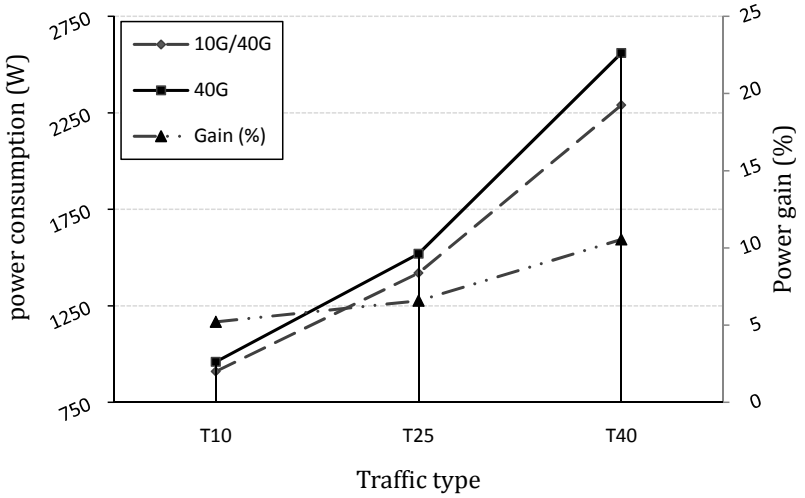


Figure 7.13: Power consumption comparison between the 40G and 10/40G design scenarios under a traffic of 40 SDs.

as possible to efficiently use the deployed resources. In this respect, few residual p-SDs with very small data rates necessitate additional cards in order to be established. In the 10G/40G scenario, 10G transceivers are deployed to serve the latter p-SDs while only more power-consuming 40G transceivers can be deployed in the 40G scenario. This explains the power gain of the 10G/40G scenario in comparison to the 40G scenario, reaching up to 10% at the highest traffic load T40.

## 7.5 Conclusion

As power consumption increases exponentially with the speed of electronics, energy savings become crucial in network design. In the context of IP-over-WDM networks, researches are carried out for the development of new power-efficient devices and systems exploiting optical technologies. In the short term, traffic rerouting and grooming strategies are promising solutions to reduce energy-related operational expenditure. To the best of our knowledge, all the proposals in this matter assume permanent connections. In this chapter, we have proposed an original approach aiming to find the ideal mapping of a set of scheduled electrical traffic demands onto a WSS-based optical infrastructure. We have formulated this problem by means of an ILP. We have considered tunable transceivers able to serve in the time domain distinct electrical connections. In coherence with existing equipment, these transceivers are distinguished by their specific data rate at 10 Gbps or 40 Gbps. We have shown that it is interesting to deploy a combination of different types of transceivers in order to reduce power consumption by means of bifurcated routing and grooming strategies. Our first objective was to compare the global power consumption of a set of SDs with the global power consumption of a set of equivalent PDs. We have assumed that each SD represents in average, a data volume equal to 25 % of the corresponding PD. The considered average activity period of an SD is 20 % of the duration of a PD (*i.e.*,

the observation period). Our numerical results show that it is possible to reduce electrical consumption by 40 %, considering the time granularity of the traffic. Given an activity of 20 % compared to the PD traffic pattern, one could expect a power gain of 80 %. The gain of 40 % obtained by our approach can be justified by the fact that transceivers are permanently active during the observation period, and temporarily under-used. The scalability of our exact approach being very limited, we have proposed a meta-heuristic approach based on a genetic algorithm, in order to extend our study to large network topologies and higher traffic loads.

# Chapter 8

# Conclusions and Perspectives

## 8.1 Conclusions

In this thesis, we have investigated two aspects of network planning, targeting, on one hand, to solve the regenerator placement problem in translucent networks environment, and on the other hand, to determine the types and numbers of transceivers at the interface between the IP and the WDM layers. Both these design problems refer to RWA and grooming problems, respectively.

Our research addresses network planning from an operator's perspective, considering the costs and the ecological footprint of the network infrastructure.

In this respect, we have first investigated QoT provisioning in core networks. We have introduced a new approach for translucent WDM network design aiming to optimize the CapEx/OpEx costs inherent to the insertion and activation of regenerators in network nodes. Considering a new regeneration site at a network node requires the installation of a pool of regenerators and its inherent powering and cooling systems. The added CapEx cost proper to regeneration is then proportional to the number of regeneration sites to be deployed. The network's OpEx costs are related to regenerator pools' supervision and maintenance. Considering supervision staff at each regeneration site implies that the fewer the sites the less the related OpEx. The proposed heuristic, COR2P, translates our CapEx/OpEx perspective incorporated in an original cost function, resulting in regenerator concentration in a few network nodes. We noticed that nodes with the higher physical degree are most favored for regeneration. We showed that a fraction of the network nodes, equipped with such pools, can offer a good performance with regard to the rejection ratio, while minimizing the network cost of regeneration. Applied to real networks such as the NSFNEet-18 backbone, about 17 % of the nodes, to be considered as regeneration sites, are sufficient to successfully establish medium to high loads. Another relevant feature of our approach is the processing order of traffic requests, the weakest requests in terms of QoT being considered in priority. This order has an important impact on regenerators'

placement, not to mention the impact of the BBF wavelength assignment strategy.

In the second part of the thesis, we addressed power consumption minimization at the WDM layer considering multi-data-rate transmission. We first identified the client cards or transceivers to be the main power-consuming components of the network infrastructure. We have then proposed to optimize their usage in order to minimize the power consumption. This investigation does not consider physical impairments at the optical layer. The essential challenge that we have addressed is considering scheduled traffic requests. The main originality of our approach consists in exploiting the space-time correlation as well as the granularity of traffic requests to optimize cards' power consumption. On the basis of this approach, we then proceed to multi-granularity traffic grooming at some of the network nodes.

We formulated our approach, based on bifurcated routing and grooming, as an ILP modeling. For small networks and/or limited number of requests, this mathematical formulation can be solved using existing dedicated software. Results showed that a combination of different types of transceivers is interesting with regard to network's overall power consumption. We also outlined the differences in power consumption between equivalent scheduled and static patterns of traffic. These two types of traffic patterns are assumed to have the same capacity specifications but the static pattern extends the activation periods of the requests to the whole observation period. We showed that it is possible to reduce electrical consumption by 40 % considering the time granularity of the traffic. Consequently, over dimensioning the core network, as it is the case nowadays, plays a great role in power waste.

## 8.2 Future work

The various fields investigated during this thesis open several perspectives:

- In the first part of the thesis, we discussed regenerator placement in the optical core network under cost considerations. It is worth noting that a regenerator consumes as much power as a transceiver having the same data rate. In this respect, the regenerator placement problem can be seen from a green perspective. In order to provide optimized power consumption under static traffic, a global optimization approach can provide a solution to the joint RWA and regenerator placement problem.

- In chapter 2, we have provided a network design road-map. With regard to the major part of this road-map, covered by our research in this thesis, we intend to investigate the QoT of established lightpaths after the RGWA operation under scheduled traffic. Future work should introduce more regenerators in order to guarantee the QoT of all-optical lightpaths resulting from the virtual topology design phase. After this operation is achieved, the whole procedure described in Figure 2.15 can then be implemented in a whole test-bed with network power consumption minimization as an objective.

- In the second part of the thesis, we were faced with the problem related to the intrinsic usage of transceivers. On-the-shelf transceivers do not present the possibility to switch to a low power consumption mode. They are always powered-on, even when serving no traffic request. This was highlighted by the fact that we obtain a gain of only 40 % between scheduled traffic and static traffic patterns, although the former's activity is about only 20 % of the the latter's. A best-effort gain of 80 % can be expected, if only transceivers can be switched On and Off, on-demand.

  Given the fact that the On/Off functionality does not constitute an applicable feature to be added in future transceivers, flexible data rate transceivers, as proposed in the literature, may have an impact on the power consumption of the network. Such transceivers can be beneficial especially under bursty traffic requests consuming high throughput and/or for scheduled traffic presenting disjoint high-correlation time intervals.

- In the end, it is crucial to finalize the genetic algorithm described in Chapter 7. Its aim is to permit extending the study of the second part of the thesis to large size networks, and higher traffic loads.

# Appendix A

# Physical layer impairments

## A.1 Linear impairments

### A.1.1 Attenuation

Attenuation in optical fiber leads to a reduction of the signal power as the signal propagates. The longer the fiber, the more attenuation the optical signal undergoes. Attenuation varies depending on the fiber type and the operating wavelength. SMFs usually operate in the 1310 nm or 1550 nm regions, where attenuation is lowest. This makes SMF the best choice for long distance communications.

Fiber attenuation is caused by scattering, absorption and bending.

- *Scattering* (often referred to as Rayleigh scattering) is the reflection of small amounts of light in all directions as it travels through the fiber. A part of the reflected light escapes out of the fiber's core, while some heads back toward the source. Some scattering is also caused by minuscule variations in the composition and density of the optical glass material. In this respect, dopants changing the refractive index of the fiber also cause more scattering.

- *Absorption* occurs when impurities, such as metal particles or moisture, are trapped in the glass. Absorption dissipates some light at specific wavelengths in the form of heat energy. Moisture occurs more naturally in fiber, and accounts for the rise in attenuation at the "water peaks" (Cf. Figure A.1).

- *Bending* is caused by fiber pinching or squeezing (micro-bends), or by fiber bending at a light radius (macro-bends). Bending results in loss of light at the caused deflections.

Figure A.1 shows the loss (attenuation coefficient) in decibels per kilometer (dB/km) by wavelength. The middle band from 1530 to 1565 nm is the conventional or C-band where WDM systems have operated using conventional erbium-doped fiber amplifiers. The band from 1565 to 1625 nm, which consists of longer wavelengths than those in the C-band, is called the L-band and is today being used in high-capacity WDM systems.

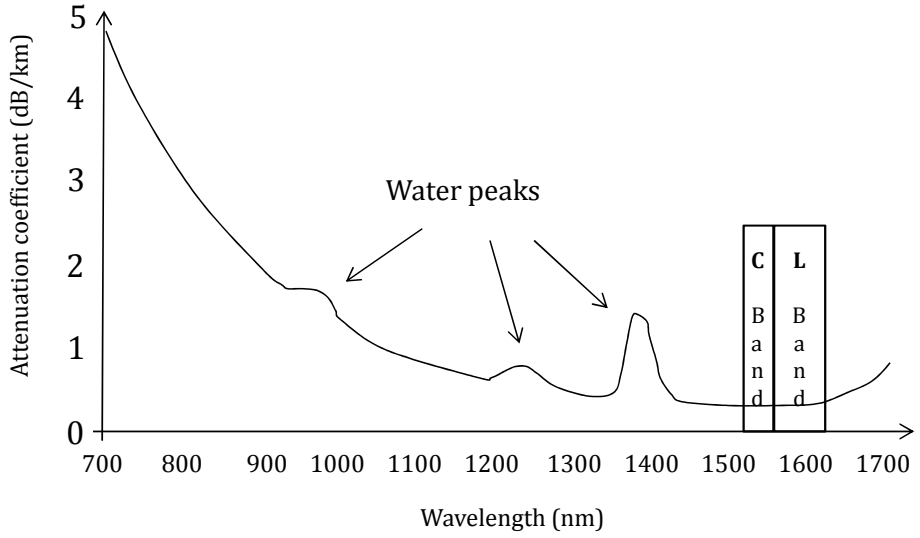


Figure A.1: Total attenuation curve.

When determining the maximum reach distance that a signal can successfully cross for a given transmitter power and a given receiver sensitivity, one must consider attenuation.

Attenuation is characterized by:

$$P_L = P_{in} e^{-\alpha L} \tag{A.1.1}$$

where $Pin$ is the optical power at the transmitter, $P_L$ be the power of the optical pulse at a distance $L$ from the transmitter and $\alpha$ the attenuation coefficient of the fiber.

For a link length of $L$ km, $P_L$ must be greater than or equal to the receiver's sensitivity $P_r$. Hence, the maximum distance between consecutive amplifiers $L_{max}$ that can be reached without re-amplification is given by:

$$L_{max} = \frac{10}{\alpha \text{ dB}} \log_{10} \frac{P_{in}}{P_r} \tag{A.1.2}$$

$L_{max}$ depends more heavily on the coefficient $\alpha$ than on the optical power $P_{in}$ injected by the transmitter. For SMF, the value of the coefficient $\alpha$ is about 0.2 dB/km in the C-band, resulting in a span length of about 80 km. New fiber optic technologies should be able of extending this length. Only standard-SMF is considered in this thesis.

### A.1.2 Amplified spontaneous emission

Due to the attenuation inherent to transmission over fiber, and in order to prevent the signal's power from reaching levels beneath the receivers' sensitivity, in-line amplifiers

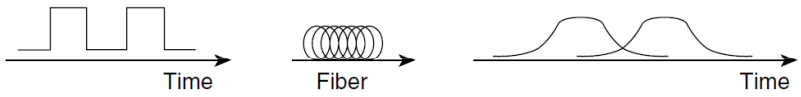


Figure A.2: Chromatic dispersion and pulse broadening.

are deployed periodically on fiber-links. As aforementioned in Section 3.2.2, an optical EDFA amplifies an incoming light signal by means of stimulated emission, but spontaneous emission also takes place. Spontaneous emission (also called noise) has a deleterious effect on the system since the next cascade of amplifiers amplifies this noise in addition to the signal resulting in the impairment called ASE. Accumulated ASE gradually degrades the OSNR along the fiber.

### A.1.3 Dispersion

As transmission systems evolved to provide longer distances and higher bit rates, dispersion became an important limiting factor. Dispersion stands for the the phenomenon where different components of the transmitted signal travel at different velocities which results in the spreading of optical pulses as they travel through the fiber. If left un-managed, pulse spreading eventually results in inter-symbol interference (ISI) when adjacent pulses overlap leading to errors in the recovery of transmitted bits. In this respect, Dispersion limits the bit rate and the maximum transmission rate on a channel. In addition, the longer the link, the greater the amount of dispersion. Intermodal dispersion, caused by the different axial speeds of different transverse modes, limits the performance of multi-mode fiber. Intermodal dispersion does not occur in a single-mode fiber. In SMF, performance is primarily limited by Polarization Mode Dispersion (PMD) and Chromatic Dispersion (CD).

**A.1.3.0.3 Chromatic Dispersion** Also called group velocity dispersion (GVD), CD occurs as a result of the wavelength-dependent silica index, as well as of the non-zero spectral width of transmitters. CD results in pulse widening since each frequency in the spectral range of a given wavelength travels in a different speed due to the varying refractive index. The more the distance traveled by a signal, the more the distortion the signal undergoes.

As shown in Figure A.2, the shape of a pulse propagating in an optical fiber is not preserved due to the presence of chromatic dispersion.

For non-dispersion-shifted fiber (standard fiber), the zero dispersion wavelength is 1310 nm. Zero-dispersion-shifted fibers zero dispersion around a specific wavelength. Figure A.3 shows dispersion for a standard fiber and a zero-dispersion-shifted fiber around 1550 nm. To compensate the accumulated CD over long-distance links, DCF presenting CD of opposite sign to that induced by the transmission fiber, are used within amplification sites (Cf. Section 3.2.2).

DCFs are deployed in double-stage amplifiers between the two EDFA amplifiers. In addition, DCM modules are deployed at the nodes in two fashions: as a pre-compensating module located just before the pre-amplifier, and as a post-compensating module, located just before the post-amplifier.

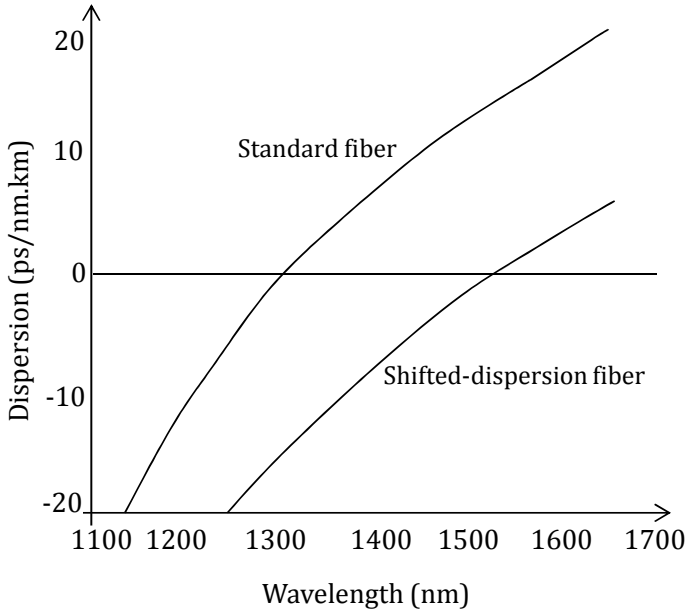


Figure A.3: Chromatic dispersion for standard and dispersion-shifted fibers.

Dispersion is never equal to zero at the reception. The presence of non-linearities impacts the dispersion influence on the transmission line [38]. Figure A.4 depicts a transmission line where double-stage in-line amplifiers are deployed at each span. The evolution of dispersion (dispersion map) is equally illustrated. Residual dispersion at the reception can be considered as a characteristic of the transmission line. Generally, receivers tolerate a certain level of dispersion.

There are more complicated CD compensating strategies deployed in mesh-networks [88]. In this thesis, we consider the strategy wherein the accumulated dispersion is reset to zero at a given wavelength with means of post-line compensation at each passage by a node.

**A.1.3.0.4 Polarization Mode Dispersion** Polarization mode dispersion (PMD) is another complex optical effect that can occur in single-mode optical fibers. Single-mode fibers support two orthogonal polarizations of the fundamental mode. If these polarization states are not maintained, an interaction between the pulses of the signal occur and the signal is smeared. PMD is the phenomenon where signal's polarizations travel with different group velocities resulting in pulse spreading. The quality of the fiber shape and external stressors cause this difference in the propagation constants of the two states. Because stress can vary over time, PMD also changes in time, unlike chromatic dispersion. PMD is proving to be a serious impediment in very high-speed systems operating at 10 Gbps bit rates and beyond.

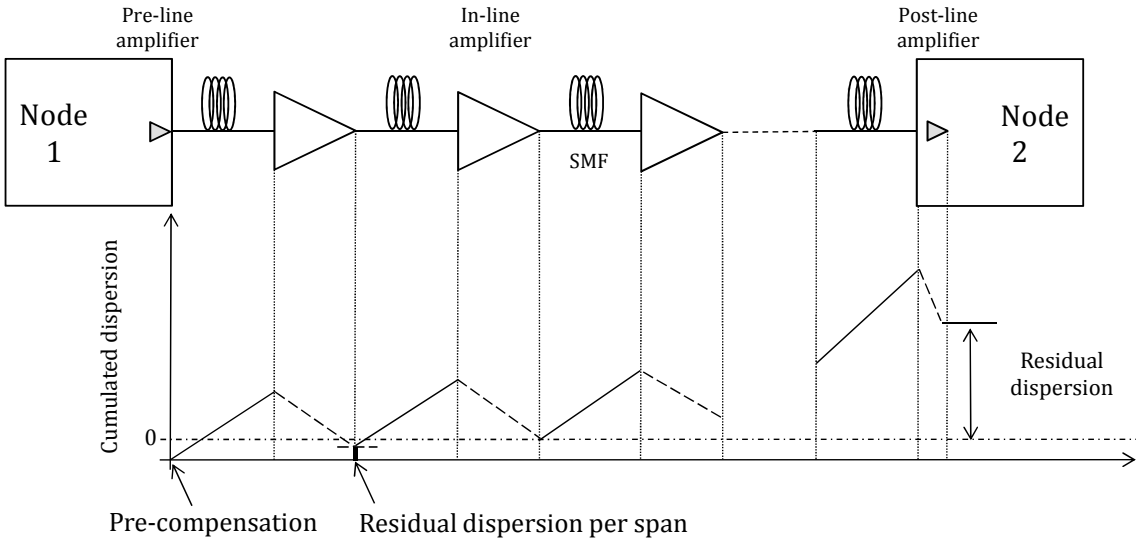


Figure A.4: Evolution of CD on a transmission line.

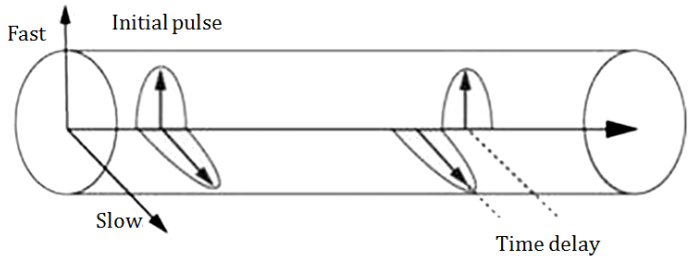


Figure A.5: Polarization mode dispersion.

Figure A.5 shows the pulse spreading due to PMD. The energy of the pulse is assumed to be split between the two orthogonally polarized modes, shown by horizontal and vertical pulses. Due to PMD, the pulse is broadened and its energy is spread over a larger time period leading to ISI. Differential group delay (DGD) stands for the time spread of the pulse due to PMD. The Differential Group Delay (DGD) representing the PMD, is accepted to have a value of no more than 10% bit time in order to conserve a good performance at the reception [5].

## A.2 Non-linear impairments

Since in DWDM long-haul transport systems we are interested in transmitting a bunch of optical channels at large distances without regeneration, high levels of optical power are deployed as aggregate power (*e.g.*, 20 dBm) and as single tributary power (*e.g.*, 3 dBm/channel) [90]. Such high power levels at the launch and at the amplifiers' outputs can give rise to non-linear interactions in the transmission fiber and amongst the transmitted channels. Non-linear impairments lead to attenuation, distortion, and cross-channel interference and impose constraints on the spacing between adjacent wavelength channels, as well as on the maximum power per channel, the maximum bit rate, and the system reach.

There are two categories of nonlinear effects in optical fibers. In the first category, the cause of non-linear effects is the molecular vibration due to the interaction between the silica medium and the light waves. The two main effects in this category are stimulated Raman scattering (SRS) and stimulated Brillouin scattering (SBS). In the second category, non-linear effect arise due to the dependence of the refractive index to the intensity of the applied electric field. The most important nonlinear effects in this category are self-phase modulation, cross-phase modulation, and four-wave mixing.

Besides, the performance of transmission components is also altered due to fatigue and aging of networking components. Performance changing can impose penalties on the OSNR of a signal at the reception.

### A.2.1 Scattering

In scattering effects, energy is transferred from one lightwave to another one called "*Stokes*" at a longer wavelength, the lost energy is absorbed by the molecular vibrations. In the case of SBS, the pump wave is the signal wave, and the Stokes wave is the unwanted wave that is generated due to the scattering process. In the case of SRS, the pump wave is a high-power wave, and the Stokes wave is the signal wave that gets amplified at the expense of the pump wave.

### A.2.2 Self-Phase Modulation

Self-phase modulation (SPM) due to the variation of the refractive index with the intensity on the same channel[1] results in variations in the phase of the signal carried by this channel. This is called "chirping" and becomes significant at high power levels.

Phase chirping results in variations of frequency around the signal's central frequency. This phenomenon enhances the pulse broadening effects of chromatic dispersion.

SPM effects are more important in systems using high transmitted powers, and can be considered the most important non-linear impairment in WDM transmission.

### A.2.3 Cross-Phase Modulation

Cross-Phase Modulation (XPM) is also a result of the Kerr effect, *i.e.*, the refraction index changing as a result of a high power inherent to neighboring channels. The narrower the channel spacing, the more important the impact of XPM. XPM is manifested through a shift in the phase of the considered signal. XPM can lead to asymmetric spectral broadening, and combined with dispersion, may also affect the pulse shape in the time domain.

### A.2.4 Four Wave Mixing

In WDM systems, Four Wave Mixing occurs when three waves at different wavelengths combine nonlinearly to generate a fourth parasitical wave at a specified wavelength as follows:

$$\omega_x = \omega_i + \omega_j - \omega_k \tag{A.2.1}$$

FWM may result in inter-channels Xtalk. In contrast with SPM and XPM, which are significant mainly in high-bit rate systems, the FWM effect is independent of the bit rate but is critically dependent on the channel spacing.

### A.2.5 Out-band Crosstalk

Out-band Xtalk, also known as inter-channel Xtalk and incoherent Xtalk, is the superposition of generated signals from different channels than the considered channel, over this last channel. Inter-channel crosstalk may be present in demultiplexers and spectral filters. This incoherent effect is weaker than the coherent one considered previously.

[1]The changing of the refractive index with the intensity of an applied electric field is called "Kerr effect".

## A.3 Summary

Chromatic dispersion and Kerr effect (SPM, XPM) are the major impairments induced by transmission over fiber. Although CD is the most important phenomenon limiting the performance of optical systems operating at moderate bit rates, non-linear effects become important at higher bit rates. The non-linear phase-shift induced by the Kerr effect will be noted $\Phi_{nl}$, in the following sections.

# List of Publications

## Journal publications

- "**Translucent network design from a CapEx/OpEx perspective**", Mayssa Youssef, Sawsan Al-Zahr, Maurice Gagnaire, Photonic Network Communications journal, Springer.

## Conference proceedings

- "**Power-Aware Multi-Rate WDM Network Design under Static/Dynamic Traffic**", Mayssa Youssef, Elias A. Doumith, Maurice Gagnaire, IEEE Global Communications 2011 (IEEE GlobeCom 2011).
- "**Traffic-Driven vs. Topology-Driven Strategies for Regeneration Sites Placement**", Mayssa Youssef, Sawsan Al-Zahr, Maurice Gagnaire, IEEE ICC, 2010.
- "**Cross-Optimization for RWA and Regenerator Placement in Translucent WDM networks**", Mayssa Youssef, Sawsan Al-Zahr, Maurice Gagnaire, IFIP/IEEE ONDM, 2010.

# Bibliography


[1] *ADVA optical networking*, http://www.advaoptical.com/.

[2] *Energy efficient ethernet study group*, http://ieee802.org/3/az/.

[3] *Huawei*, http://www.huawei.com/.

[4] *ILOG CPLEX*, www.ibm.com/software/integration/optimization/cplex-optimizer.

[5] *ITU-T Recommendation G.69, Optical interface for single channel STM and other SDH systemswith optical amplifiers*, 2003.

[6] *Amsterdam internet exchange*, 2011, http://www.ams-ix.net/.

[7] A. Lord, *The economic benefits of all-optical core networks around europe*, International Workshop on the Future of Optical Networking (FON) (2006).

[8] D.M. Marom, D.T. Neilson, D.S. Greywall, C. S. Pai , N.R. Basavanhally, V.A. Aksyuk, D.O. Lopez, F. Pardo, M.E. Simon, Y. Low, P. Kolodner, and C.A. Bolle, *Wavelength-selective 1×K switches using free-space optics and MEMS micromirrors: theory, design, and implementation*, IEEE Journal of Lightwave Technology **23** (2005), no. 4, 1620–1630.

[9] I. Chlamtac, A. Farago, and T. Zhang, *Lightpath (wavelength) routing in large wdm networks*, IEEE Journal on Selected Areas in Communications **14** (1996), no. 5, 909 – 913.

[10] A. Bianzino, C. Chaudet, F. Larroca, D. Rossi and J.-L. Rougier, *Energy-aware routing: a reality check*, IEEE GlobeCom Workshop on Green Communications (GreenCom'10), 2010.

[11] A. Gumaste, T. Antony, *DWDM Network Designs and Engineering Solutions*, Cisco Press, Indianapolis, USA, 2003.

[12] A. Saleh, *Island of transparency: An emerging reality in multiwavelegnth optical networking*, IEEE/LEOS Summer Topical Meeting on Broadband Optical Networks and Technologies (1998).

[13] S. Al Zahr, E.A. Doumith, and M. Gagnaire, *An exact approach for translucent wdm network design considering scheduled lightpath demands*, Telecommunications (ICT), 2011 18th International Conference on, may 2011, pp. 450 –457.

[14] D. Allan, N. Bragg, A. McGuire, and A. Reid, *Ethernet as carrier transport infrastructure*, Communications Magazine, IEEE **44** (2006), no. 2, 95 – 101.

[15] Annalisa Morea, *Contribution à l'étude des réseaux optiques translucides : évaluation de leur faisabilité technique et de leur intérêt économique*, Ph.D. thesis, Ecole nationale supérieure des télécommunications, Telecom Paris, 2006.

[16] B. Bathula and J. Elmirghani, *Green networks: Energy efficient design for optical networks*, WOCN'09, 2009.

[17] B. P. Keyworth, *ROADM subsystems & technologies*, Optical Fiber Communication Conference (2005).

[18] B. Ramamurthy, D. Datta, H. Feng, J. P. Heritage, and B. Mukherjee, *Transparent vs. opaque vs. translucent wavelength-routed optical networks*, Optical Fiber Communication Conference, 1999.

[19] A. Birman, *Computing approximate blocking probabilities for a class of all-optical networks*, Selected Areas in Communications, IEEE Journal on **14** (1996), no. 5, 852 –857.

[20] Biswanath Mukherjee, *Optical WDM networks*, Springer, 2006.

[21] R. Bolla, R. Bruschi, F. Davoli, and F. Cucchietti, *Energy efficiency in the future internet: A survey of existing approaches and trends in energy-aware fixed network infrastructures*, Communications Surveys Tutorials, IEEE **13** (2011), no. 2, 223 –244.

[22] C. Dorize, A. Morea, O. Rival and B. Berde, *An energy-efficient node interface for optical core networks*, ICTON'10, 2010.

[23] L. Ceuppens, A. Sardella, and D. Kharitonov, *Power saving strategies and technologies in network equipment opportunities and challenges, risk and rewards*, Applications and the Internet, 2008. SAINT 2008. International Symposium on, 2008.

[24] J. Chabarek, J. Sommers, P. Barford, C. Estan, D. Tsiang, and S. Wright, *Power awareness in network design and routing*, INFOCOM 2008. The 27th Conference on Computer Communications. IEEE, april 2008.

[25] G. Charlet, *QPSK with coherent detection over ultra-long distance improved by nonlinearity mitigation*, IEEE/LEOS Summer Topical Meetings, 2007 Digest of the, july 2007, pp. 43 –44.

[26] L. Chiaraviglio and I. Matta, *GreenCoop: Cooperative green routing with energy-efficient servers*, e-Energy, 2010.

[27] L. Chiaraviglio, M. Mellia, and F. Neri, *Energy-aware networks: Reducing power consumption by switching off network elements*, Citeseer, 2008.

[28] ———, *Energy-aware backbone networks: A case study*, Communications Workshops, 2009. ICC Workshops 2009. IEEE International Conference on, june 2009.

[29] ———, *Reducing power consumption in backbone networks*, Communications, 2009. ICC '09. IEEE International Conference on, june 2009.

[30] P.B. Chu, Shi-Sheng Lee, and Sangtae Park, *Mems: the path to large optical cross-connects*, Communications Magazine, IEEE **40** (2002), no. 3, 80 –87.

[31] A. Coiro, M. Listanti, A. Valenti, and F. Matera, *Reducing power consumption in wavelength routed networks by selective switch off of optical links*, Selected Topics in Quantum Electronics, IEEE Journal of **17** (2011), no. 2, 428 –436.

[32] D. Eppstein, *Finding the K shortest paths*, SIAM Journal of Computing **28** (1998), no. 2, 652–673.

[33] M. De Groote, K. Manousakis, P. Kokkinos, D. Colle, and *et al.* Pickavet, *Cost comparison of different translucent optical network architectures*, Telecommunications Internet and Media Techno Economics (CTTE), 2010 9th Conference on, 2010.

[34] E.A. Doumith, S. Al Zahr, and M. Gagnaire, *Mutual impact of traffic correlation and regenerator concentration in translucent wdm networks*, Communications (ICC), 2011 IEEE International Conference on, june 2011.

[35] E. Karasan, M. Arisoylu, *Design of translucent optical networks: Partitioning and restoration*, Photonic Network Communications **8** (2004), no. 2, 209–221.

[36] E. Yetginer, G. Rouskas, *Power efficient traffic grooming in optical WDM networks*, GLOBECOM'09, 2009.

[37] E.L. Goldstein, J. Nagel, J.Strand, R.Tkach, *National-scale networks likely to be opaque*, Lightwave Xtra! (1998), 92–97.

[38] Y. Frignac and S. Bigo, *Numerical optimization of residual dispersion in dispersion-managed systems at 40 Gbit/s*, Optical Fiber Communication Conference, 2000, vol. 1, 2000, pp. 48–50.

[39] G. Gavioli, P. Bayvel, *Multichannel all-optical 3R regenerative wavelength conversion using an integrated semiconductor optical amplifier array*, Lasers and Electro-Optics Society, 2003.

[40] G. P. Agrawal, *Fiber-optic communication systems*, John Wiley and Sons, 2002.

[41] G. Prasanna, B.S. Kishore, G.K. Omprasad, K.S. Raju, R. Gowrishankar, K. Venkataramaniah, R. Johnson, and P. Voruganti, *Versatility of a colorless and directionless WSS-based ROADM architecture*, 2009.

[42] G. Shen and R. Tucker, *Energy-minimized design for IP over WDM networks*, Journal of Optical communications networks, vol. 1, 2009.

[43] G. Shen, W. Grover, T.Cheng, S. Bose, *Sparsely placement of electronic switching nodes for low blocking in translucent optical networks*, OSA Journal of Optical Networking **1** (2002), no. 12, 424–441.

[44] M. Gagnaire, E.A. Doumith, and S. Al Zahr, *A novel exact approach for translucent wdm network design under traffic uncertainty*, Optical Network Design and Modeling (ONDM), 2011 15th International Conference on, 2011.

[45] B. Garcia-Manrubia, P. Pavon-Marino, R. Aparicio-Pardo, M. Klinkowski, and D. Careglio, *Offline impairment-aware rwa and regenerator placement in translucent optical networks*, Lightwave Technology, Journal of **29** (2011), no. 3, 265 –277.

[46] S.S. Gorshe and T. Wilson, *Transparent generic framing procedure (GFP): a protocol for efficient transport of block-coded data through SONET/SDH networks*, Communications Magazine, IEEE **40** (2002), no. 5, 88 –95.

[47] C. Gunaratne and K. Christensen, *Ethernet adaptive link rate: System design and performance evaluation*, Local Computer Networks, Proceedings 2006 31st IEEE Conference on, 2006.

[48] C. Gunaratne, K. Christensen, B. Nordman, and S. Suen, *Reducing the energy consumption of ethernet with adaptive link rate (alr)*, Computers, IEEE Transactions on **57** (2008), no. 4, 448 –461.

[49] C. Gunaratne, K. Christensen, and S.W. Suen, *Ngl02-2: Ethernet adaptive link rate (alr): Analysis of a buffer threshold policy*, Global Telecommunications Conference, 2006. GLOBECOM '06. IEEE, 2006.

[50] S. Han, *Moore's law and energy and operations savings in the evolution of optical transport platforms*, Communications Magazine, IEEE **48** (2010), no. 2, 66–69.

[51] D. Hillerkuss, R. Schmogrow, M. Hübner, M. Winter, B. Nebendahl, J. Becker, W. Freude, and J. Leuthold, *Software-defined multi-format transmitter with real-time signal processing for up to 160 Gbit/s*, Signal Processing in Photonic Communications, Optical Society of America, 2010.

[52] F. Idzikowski, S. Orlowski, C. Raack, H. Woesner, and A. Wolisz, *Saving energy in ip-over-wdm networks by switching off line cards in low-demand scenarios*, Optical Network Design and Modeling (ONDM), 2010 14th Conference on, february 2010.

[53] N. Iiyama, H. Kimura, and H. Hadama, *A novel wdm-based optical access network with high energy efficiency using Elastic OLT*, Optical Network Design and Modeling (ONDM), 2010 14th Conference on, 2010.

[54] ITU-T recommendations G709, *Interfaces of the optical transport network (OTN)*, 2003.

[55] Russo J., *Network technology energy efficiency*, Berkeley Symposium on Energy Efficient Electronic Systems (2009).

[56] J. Leuthold, C.H. Joyner, B. Mikkelsen, G. Raybon, J.L. Pleumeekers, B.I. Miller, K. Dreyer and C.A. Burrus, *100 Gbit/s all-optical wavelength conversion with integrated SOA delayed-interference configuration*, Electronics letters, June 2000.

[57] J. Restrepo, c. Gruber and C. Mas Machuca, *Energy profile aware routing*, ICC'09, 2009.

[58] K. H. Liu, *IP over WDM*, John Wiley & Sons, 2002.

[59] C. Laperle, B. Villeneuve, Zhuhong Zhang, D. McGhan, Han Sun, and M. O'Sullivan, *WDM Performance and PMD Tolerance of a Coherent 40-Gbit/s Dual-Polarization QPSK Transceiver*, Lightwave Technology, Journal of **26** (2008), no. 1, 168 –175.

[60] M. Gagnaire, S. Al Zahr, *Impairment aware routing and wavelength assignment in translucent networks: State of the art*, IEEE Communications Magazine **47** (2009), no. 5, 55–61.

[61] M. Gupta and M. Thorup, *Greening of the internet*, Proc. ACM SIGCOMM'03, 2003.

[62] M. Xia *et al.*, *Greening the optical backbone network: a traffic engineering approach*, ICC'10, 2010.

[63] M.A. Ezzahdi, S. Al Zahr, M. Koubàa, N. Puech, M. Gagnaire, *LERP: a quality of transmission dependent heuristic for routing and wavelength assignment in hybrid WDM networks*, Proc. IEEE ICCCN'06, 2006, pp. 125–130.

[64] K. Manousakis, K. Christodoulopoulos, E. Kamitsas, I. Tomkos, and E.A. Varvarigos, *Offline impairment-aware routing and wavelength assignment algorithms in translucent wdm optical networks*, Lightwave Technology, Journal of **27** (2009), no. 12, 1866 –1877.

[65] M. Matsumoto, *Performance analysis and comparison of optical 3R regenerators utilizing self-phase modulation in fibers*, Lightwave Technology, Journal of **22** (2004), no. 6, 1472 – 1482.

[66] M. Mizukami, J. Yamaguchi, N. Nemoto, Y. Kawajiri, H. Hirata, S. Uchiyama, M. Makihara, T. Sakata, N. Shimoyama, H. Ishii, and F. Shimokawa, *128×128 3D-MEMS optical switch module with simultaneous optical paths connection for optical cross-connect systems*, Photonics in Switching. PS '09. International Conference on, sept. 2009.

[67] A. Morea, N. Brogard, F. Leplingard, J.-C. Antona, T. Zami, B. Lavigne, and D. Bayart, *QoT function and A∗ routing: an optimized combination for connection search in translucent networks*, J. Opt. Netw. **7** (2008), no. 1, 42–61.

[68] A. Morea, F. Leplingard, J.-C. Antona, P. Henri, T. Zami, and D. Kilper, *Advanced test-beds to validate physical estimators in heterogeneous long haul transparent optical networks*, Journal of Networks **5** (2010), no. 11.

[69] Zhaoyi Pan, B. Chatelain, D.V. Plant, F. Gagnon, C. Tremblay, and E. Bernier, *Tabu search optimization in translucent network regenerator allocation*, Broadband Communications, Networks and Systems, 2008. BROADNETS 2008. 5th International Conference on, 2008, pp. 627 –631.

[70] O.B. Pardo, J. Renaudier, H. Mardoyan, P. Tran, G. Charlet, and S. Bigo, *Investigation of design options for overlaying 40Gb/s coherent PDM-QPSK channels over a 10Gb/s system infrastructure*, Optical Fiber communication/National Fiber Optic Engineers Conference, 2008. OFC/NFOEC 2008. Conference on, feb. 2008.

[71] A.N. Patel, Chengyi Gao, J.P. Jue, Xi Wang, Qiong Zhang, P. Palacharla, and T. Naito, *Traffic grooming and regenerator placement in impairment-aware optical wdm networks*, Optical Network Design and Modeling (ONDM), 2010 14th Conference on, feb. 2010.

[72] R. Giles, K. Kumaran, D. Mitra, C. Nuzman, and I. Saniee, *Selective transparency in optical networks*, Proc. IEEE MILCOM02, 2002.

[73] B. Ramamurthy, S. Yaragorla, and Xi Yang, *Translucent optical wdm networks for the next-generation backbone networks*, Global Telecommunications Conference, 2001. GLOBECOM '01. IEEE, 2001.

[74] J. Renaudier, G. Charlet, M. Salsi, O.B. Pardo, H. Mardoyan, P. Tran, and S. Bigo, *Linear fiber impairments mitigation of 40-gbit/s polarization-multiplexed qpsk by digital processing in a coherent receiver*, Lightwave Technology, Journal of **26** (2008), no. 1, 36 –42.

[75] O. Rival, A. Morea, and J.-C. Antona, *Optical network planning with rate-tunable NRZ transponders*, Optical Communication, 2009. ECOC '09. 35th European Conference on, 2009.

[76] M. Rochette, Libin Fu, V. Ta'eed, D.J. Moss, and B.J. Eggleton, *2R optical regeneration: an all-optical solution for BER improvement*, Selected Topics in Quantum Electronics, IEEE Journal of **12** (2006), no. 4, 736 –744.

[77] P. Roorda and B. Collings, *Evolution to Colorless and Directionless ROADM Architectures*, Optical Fiber communication/National Fiber Optic Engineers Conference, 2008. OFC/NFOEC 2008. Conference on, feb. 2008.

[78] S. Rumley and C. Gaumier, *Cost aware design of translucent wdm transport networks*, Transparent Optical Networks, 2009. ICTON '09. 11th International Conference on, 28 2009-july 2 2009.

[79] S. Al Zahr, M. Gagnaire, and N. Puech, *Impact of wavelength assignment strategies on hybrid WDM network planning*, Proc. DRCN'07, 2007.

[80] S. Al Zahr, M. Gagnaire, N. Puech, M. Koubàa, *Physical layer impairments in WDM core networks: a comparison between a north-American backbone and a pan-European backbone*, Proc. IEEE Broadnets'05, 2005, pp. 335–340.

[81] S. Chen, S. Raghavan, *Regenerator location problem*, INFORMS Telecommunication Conference (2006).

[82] S. Dixit, *IP over WDM: Building the Next-Generation Optical Internet*, John Wiley and Sons, 2003.

[83] S. L. Jansen *et al.*, *Mixed data rate and format transmission by mid-link spectral inversion*, OSA/SPPCom, 2004.

[84] S. Mechels, L. Muller, G. D. Morley, and D. Tillett, *1D MEMS-Based Wavelength Switching Subsystem*, IEEE Communications Magazine **41** (2003), no. 3, 88–94.

[85] S. Pachnicke, T. Paschenda, P. Krummrich, *Assessment of a constraint-based routing algorithm for translucent 10 Gbits/s DWDM networks considering fiber nonlinearities*, Journal of Optical Networking **7** (2008), no. 4, 365–377.

[86] ———, *Physical impairment based regenerator placement and routing in translucent optical networks*, IEEE OFC/NFOEC'08 (2008), 1–3.

[87] A.A.M. Saleh, *Transparent optical networking in backbone networks*, Optical Fiber Communication Conference, 2000, vol. 3, 2000, pp. 62 –64.

[88] Sawsan Al Zahr, *Planification de réseaux wdm translucides avec qualité de transmission garantie*, Ph.D. thesis, Ecole nationale supérieure des télécommunications, Telecom Paris, 2007.

[89] R. Schmogrow, D. Hillerkuss, M. Dreschmann, M. Huebner, M. Winter, J. Meyer, B. Nebendahl, C. Koos, J. Becker, W. Freude, and J. Leuthold, *Real-time software-defined multiformat transmitter generating 64QAM at 28 GBd*, Photonics Technology Letters, IEEE **22** (2010), no. 21, 1601 –1603.

[90] Alexandros Stavdas, *Core and metro networks*, John Wiley and Sons, 2010.

[91] J. Suzuki, T. Tanemura, and K. Kikuchi, *All-optical regeneration of 40-Gb/s low-Q signal using XPM-induced wavelength shift in highly-nonlinear fiber*, Optical Communication, 2005. ECOC 2005. 31st European Conference on, vol. 2, sept. 2005, pp. 199 – 200.

[92] B. Teipen, K. Grobe, M. Eiselt, and J.-P. Elbers, *Adaptive optical transmission for dynamic optical networks*, Transparent Optical Networks (ICTON), 2010 12th International Conference on, 2010.

[93] R.S. Tucker, R. Parthiban, J. Baliga, K. Hinton, R.W.A. Ayre, and W.V. Sorin, *Evolution of WDM Optical IP Networks: A Cost and Energy Perspective*, Lightwave Technology, Journal of **27** (2009), no. 3, 243 –252.

[94] V. P. Kaminow and Tingye Li , *Optical fiber telecommunications*, vol. IV-B, 2002.

[95] W. Shen, Y. Tsukishima, K. Yamada and M. Jinno, *Power-efficient multi-layer networking: design and evaluation*, ONDM, 2010.

[96] X. Yang, B. Ramamurthy, *Sparse regeneration in translucent wavelength-routed optical networks: architecture, network design and wavelength routing*, Photonic Network Communications **10** (2005), no. 1, 39–50.

[97] Y. Huang, J. P. Heritage, and B. Mukherjee, *Connection provisioning with transmission impairment consideration in optical WDM networks with high-speed channels*, IEEE/OSA Journal on Lightwave Technology **23** (2005), no. 3, 982–993.

[98] Y. Wu, L. Chiaraviglio, M. Mellia and F. Neri, *Power-aware routing and wavelength assignment in optical networks*, ECOC'09, 2009.

[99] Xi Yang and B. Ramamurthy, *Dynamic routing in translucent wdm optical networks: the intradomain case*, Lightwave Technology, Journal of **23** (2005), no. 3, 955 – 971.

[100] T.T. Ye, L. Benini, and G. De Micheli, *Analysis of power consumption on switch fabrics in network routers*, Design Automation Conference, 2002. Proceedings. 39th, 2002.

[101] M. Youssef, S. Al Zahr, and M. Gagnaire, *Cross optimization for RWA and regenerator placement in translucent WDM networks*, (2010).

[102] ———, *Traffic-driven vs. topology-driven strategies for regeneration sites placement*, Communications (ICC), 2010 IEEE International Conference on, may 2010.

[103] Mayssa Youssef, Sawsan Al Zahr, and Maurice Gagnaire, *Translucent network design from a CapEx/OpEx perspective*, Photonic Network Communications **22**, 85–97.

[104] T. Zami, A. Morea, F. Leplingard, N. Brogard, D. Bayart, S. Bigo, and J.-P. Faure, *Driving technologies addressing the future dynamic transparent core networks*, Transparent Optical Networks, 2008. ICTON 2008. 10th Anniversary International Conference on, vol. 2, june 2008.

[105] X. Zhao, L. Wang, D. Lu, C. Lou, Y. Sun, L. Zhao, and W. Wang, *40-Gb/s all-optical 3R regeneration with semiconductor devices*, Wireless and Optical Communications Conference (WOCC), 2010 19th Annual, may 2010.